IMPLICATIONS OF THE INNATE IMMUNE RESPONSE IN TUBERCULOSIS AND CARDIAC ALLOGRAFT VASCULOPATHY

by

Jill Alexandra Moore

Submitted in partial fulfilment of the requirements
for the degree of Master of Science

at

Dalhousie University
Halifax, Nova Scotia
June 2014

For Pat

TABLE OF CONTENTS

LIST OF TABLES

LIST OF FIGURES

ABSTRACT

Reactivation of latent tuberculosis (TB) in HIV-infected individuals has arisen as a major contributor to early death in areas where TB and HIV overlap. $CD4^+$ T cells are the targets of HIV, leading to insufficient IFN-γ to control disease. In the first section of this thesis I tested natural extracts to synergize with IFN-γ to control *Mtb* growth. Infected macrophages were treated with the extracts and IFN-γ. Although the extracts showed no synergy with IFN-γ, this model of *ex vivo* infection could provide a template for future study.

The second section investigated the contribution of pre-existing atherosclerosis to the development of allograft vasculopathy (AV). Aortas from ApoEKO mice bearing an atherosclerotic lesion were transplanted into fully disparate recipients, treated with Cyclosporin A and changes in size and structure were analyzed. The results support our hypothesis that by 7d changes in the atherosclerotic lesion post-transplant set the stage for AV.

LIST OF ABBREVIATIONS AND SYMBOLS USED

α	Alpha
Ab	Antibody
Abx	Antibiotics
AFB	Acid-Fast Bacilli
AHS	Autologous Human Serum
AIDS	Acquired Immune Deficiency Syndrome
ANOVA	Analysis of Variance
APC	Antigen Presenting Cell
ApoE	Apolipoprotein E
ApoEKO	Apolipoprotein Knockout
β	Beta
BAL	Bronchalveolar Lavage
BCG	Bacillus Calmette–Guérin
CAV	Cardiac Allograft Vasculopathy
CD	Cluster of Differentiation
CFU	Colony Forming Units
CNI	Calcineurin Inhibitor
Cs	*Cordyceps sinensis*
CyA	Cyclosporin A
d	Day
DAMPs	Damage-Associated Molecular Pattern molecules
DC	Dendritic Cell
DMEM	Dulbecco's Modified Eagle Medium
DOTS	Directly Observed Treatment, Short-course
DTH	Delayed-Type Hypersensitivity
EC	Endothelial Cell
ECM	Extracellular Matrix
EDTA	Ethylenediaminetetraacetic acid
EEL	External Elastic Lamina
Ep	*Echinacea purpurea*
FBS	Fetal Bovine Serum
FGF	Fibroblastic Growth Factor
γ	Gamma
h	Hour
H&E	Haematoxylin and Eosin
HAART	Highly Active Anti-Retroviral Therapy
HBSS	Hank's Balanced Salt Solution
HDL	High Density Lipoprotein
HIV	Human Immunodeficiency Virus
HLA	Human Leukocyte Antigen
Hm	*Heracleum maximum*
IEL	Internal Elastic Lamina
IFN	Interferon
IGRA	Interferon Gamma Release Assay

INH	Isoniazid
IL	Interleukin
IVUS	Intravascular Ultrasound
i.p.	Intraperitoneal
LAM	Lipoarabinomannan
LDL	Low Density Lipoprotein
LPS	Lipopolysaccharide
ManLAM	Mannose-capped Lipoarabinomannan
MDR-TB	Multi-Drug Resistant Tuberculosis
MGIT	Mycobacterial Growth Indicator Tube
MHC	Major Histocompatibility Complex
MIC	Minimum Inhibitory Concentration
MID	Minimum Infectious Dose
min	Minute
ml	Milliliter
µl	Microlitre
MOI	Multiplicity of Infection
Mtb	*Mycobacterium tuberculosis*
NaOH	Sodium Hydroxide
NK	Natural Killer
NMS	Normal Mouse Serum
NO	Nitric Oxide
PAMPs	Pathogen-Associated Molecular Pattern molecules
PANTA	Polymyxin B, Amphotericin B, Nalidixic Acid, Trimethoprin, Azlocillin
PBMC	Peripheral Blood Mononuclear Cell
PBS	Phosphate Buffered Saline
PPD	Purified Protein Derivative
PRR	Pattern Recognition Receptor
RIF	Rifampicin
RNS	Reactive Nitrogen Species
ROS	Reactive Oxygen Species
RPMI	Roswell Park Memorial Institute
s.c.	Subcutaneous
sf-RPMI	Serum-free RPMI
SMC	Smooth Muscle Cell
TB	Tuberculosis
TEM	Tranmission Electron Microscopy
TGF	Transforming Growth Factor
Th	T Helper Cell
TLR	Toll-Like Receptor
TNF	Tumor Necrosis Factor
TST	Tuberculin Skin Test
VEGF	Vascular Endothelial Growth Factor
WHO	World Health Organization
wk	Week
XDR-TB	Extensively Drug-Resistant Tuberculosis

ACKNOWLEDGEMENTS

Thank you to my supervisor, Dr. Tim Lee, for being incredibly supportive and encouraging. I've learned so much over the years, and could not have completed this degree without your guidance, patience, and good humour. Many thanks to my committee members Dr. Laurette Geldenhuys and Dr. Greg Hirsch, and to Dr. Andrew Stadnyk for agreeing to be my external examiner. I owe much to the staff of the Pathology Department, especially to the graduate co-ordinator Dr. Wenda Greer, who was attentive, involved, and always looking out for my best interests.

The tuberculosis project was complicated and required a lot of staff involvement for me to perform experiments in the hospital Level III facilities. Thank you to Dr. David Haldane and to the Level III laboratory technicians for their time and assistance, both here at the QEII and the SJRH in New Brunswick. I consider it incredible timing that I had the chance to work with Dr. Duncan Webster. His enthusiasm and affection for his work and the people that surround him was, quite aptly, infectious!

Our laboratory's microsurgeon, Brenda Ross, was instrumental in the completion of the atherosclerosis project, from the challenging surgeries to technical assistance at the bench. We both experienced blood, sweat, and tears to see this project's end. I am grateful to Julie Jordan, who first introduced me to this phenomenal lab. Thank you for having the inkling that I might be a good fit. A gigantic hug to all of my amazing labmates that I have worked with over the past ten years. You are an incredibly bright, talented, supportive bunch of friends. Thank you for all of your help and making this time so memorable. I wish you all great success in life, professional and otherwise.

Lastly, this is for my family. Thank you to my parents for your unwavering support, I hope I have made you proud. To my husband, thank you for being my backbone. You have devoted yourself to wrangling children day and night; you've sacrificed vacation time, RRSP contributions and home improvement; you've given up countless hours of your time to give me *my* time, never once believing it wasn't the right thing to do, even when I was floundering. And to my boys, Duncan and Nathan, you are my heart and soul. You weren't aware at the time, but you were and always will be my motivators to do my best and to finish what I've started.

CHAPTER 1. INTRODUCTION

1.1. Project 1. Implications of the Innate Immune Response in TB

1.2. Background

Tuberculosis (TB), caused by the bacterium *Mycobacterium tuberculosis* (*Mtb*), is one of the oldest known human diseases. There were close to 10 million people with TB in 2011[1] and this is a substantial rise from 1990 when the number was estimated to be 5.2 million.[1] Notwithstanding this growth in the number of TB affected individuals, the most recent data from the World Health Organization show that there is considerable progress toward a global target (the Millennium Development Goal) of 50% reduction in new cases by 2015. Despite this progress toward the 50% global reduction, TB continues to be a significant problem.

Almost 1.5 million people die from TB annually, making it the world's most deadly bacterial pathogen and one of the world's most serious infectious diseases.[2] The majority of the cases and deaths occur in developing countries. Even with widespread use of protective vaccination (the Bacille Calmette–Guérin [BCG] vaccine), TB continues to spread uncontrollably in areas of the world burdened by poor sanitation, malnutrition, and poverty.

It would be a mistake to think that TB is restricted to the developing world. It is a treatable and mostly curable disease, yet in developed countries like Canada, TB still persists, and the majority of TB cases occur in marginalized populations. In Canada, for example, an overwhelming proportion of TB cases occur in Aboriginal and foreign-born Canadians. Aboriginals are particularly overrepresented in TB prevalence and have a 20 fold greater chance of developing TB than non-Aboriginal Canadians.[3]

The *Mycobacterium tuberculosis* bacterium is the causative agent in TB. The disease has many manifestations but is primarily a pulmonary disease, due to its mode of transmission via aerosol droplet nuclei. Sneezing, coughing, talking, or laughing can propel the bacilli into the air. Bacilli can remain in these droplets for several hours, and the minimum infectious dose (MID) for *Mtb* is only 3 organisms.[4] Once inhaled, the larger droplet nuclei become lodged in the upper respiratory tract, but the smaller droplets migrate further into the lung, eventually residing in the alveolar spaces. If left untreated, an infected individual can subsequently infect 10-15 others every year.[1]

1.3. Current diagnostics

The most commonly used test to assess for TB exposure is the TST, or Mantoux, test. In this test small amounts of purified protein derivative (PPD) from *Mtb* are injected intradermally. A positive TST is the result of uptake of the PPD by local macrophages and presentation of this antigen to local memory T cells (Tm).[5] The presence of *Mtb* antigen-specific Tm cells is an indication of prior exposure. Induration results from the activation of these Tm in the skin, leading to the release of IFN-γ and a subsequent influx of macrophages through a delayed type hypersensitivity (DTH)-type response.[5] Macrophage influx into the local site initiates focal inflammation and the reaction is read by measuring the diameter of the induration between 48 and 72h after injection.

There are limitations with the TST test. The first is that false positives may arise from previous exposure to the BCG vaccine.[6] This is an important limitation as most areas with high prevalence of TB are also areas where the BCG vaccine is widely used.[7,8] Moreover,

the test will not detect infection in someone who has been recently infected with TB, or in those with compromised immune systems. Given the fact that a significant percentage of individuals in sub-Saharan Africa, a region rife with TB infection, are HIV positive (low $CD4^+$ T cell counts) this represents a significant limitation to the TST.[5] New diagnostic tools seek to overcome some of these limitations by using more specific immunodiagnostic tools, and one example is the interferon-gamma (IFN-γ) release assay (IGRA).[9] Rather than looking at the focal inflammatory response due to macrophage activation and accumulation by IFN-γ, IGRAs measure the upstream event of IFN-γ production in the Tm cells.[10,11] These assays measure the release of IFN-γ in whole blood samples incubated *in vitro* with PPD, and exposure of *Mtb*-specific Tm cells to PPD causes quick release of IFN-γ in the blood that is markedly above baseline.[9,12] Though more specific than the TST, the IGRA still has limited reliability in HIV-infected individuals.[12,13]

The oldest diagnostic tool for TB exposure is the chest radiograph (x-ray). Currently chest x-rays are used primarily as a confirmation of infection and to confirm the extent of lung involvement in patients with prior infection.[14] Active disease can still be confirmed by evidence of live acid-fast bacteria (AFB) in the sputum.[15] Sputum smear microscopy is the most widely-used, definitive diagnostic measure but it may have low sensitivity in HIV positive individuals, and is also unable to detect drug resistance.[16,17] There is an urgent need for faster and less expensive tests to confirm TB cases in resource-poor settings. As such, TB management based on clinical observations is essential, and often begins before test results are available. Those include fatigue, fever, unexplained weight loss, night sweats, productive cough, chest pain, and hemoptysis (coughing up blood).[18]

This clinical presentation, along with the patient medical history, usually leads to a potential diagnosis of TB infection.

1.4. Antibiotics and Antibiotic Resistance

The most important advance in TB treatment came with the introduction of rifampicin (RIF) in 1963, and there have been no new classes of TB drugs since.[19] Currently, RIF and isoniazid (INH) are considered the two most powerful anti-TB drugs and they are used alongside ethambutol, pyrazinamide, and streptomycin as the first line of defense against TB.[20] When administered daily for six months, this cocktail of antibiotics has proved to be effective in most cases. But mutant strains of *Mtb* have emerged that are resistant to these first-line drugs. The development of resistance is primarily due to inconsistent or partial treatment, resulting from complex dosing schedules, longer treatment times, and patient non-compliance.[19] Not surprisingly, the most affected by cost are those in the poorest regions of the world where TB is rampant. Transmission rates soar when the infection cannot be well controlled, and the emergence of multi-drug resistant *Mtb* to both RIF and INH (MDR-TB) is cause for great concern.[19]

MDR-TB results from either primary infection with resistant bacteria, or may develop during the course of treatment.[21,22] Measures taken to prevent the patient acquiring resistant mutations during their treatment would dramatically reduce the incidence of MDR-TB.[23] The Directly Observed Therapy Short-Course (DOTS) Strategy was employed by the WHO to help combat MDR-TB and provides supervision and patient support to avoid non-compliance.[24] Ideally it ensures that a patient takes the

recommended drugs necessary for the entire treatment period.[25] The DOTS strategy also works to increase case detection, ensure drug availability and to keep associated costs low, and pushes for greater international political financial commitments for the eradication of TB.[24] Of greater concern is the emergence of extensively drug-resistant *Mtb* (XDR-TB) that are resistant to INH and RIF as well as any fluoroquinolone and any of the second-line anti-TB injectable agents (amikacin, kanamycin and/or capreomycin).[23] XDR-TB do not respond to the six-month treatment with first-line drugs and can take two years or more to treat with drugs that are less potent, more toxic and much more expensive.[26,27] These developments would suggest that TB could spread unchecked in the next several years.

There is currently reason to have new hope for TB control. For the first time in 50 years, 2012 marked the development of a new drug (bedaquiline) to be registered to combat DR-TB.[28,29] In 2013 delamanid became the second.[30] The long-term activity against XDR-TB of these drugs is unknown, but it is possible that resistance will develop against these antibiotics as well. One particular concern with respect to XDR-TB is that it has recently emerged in areas heavily affected by HIV.[27] This presents a massive challenge to global TB control since control of TB infection in HIV-infected individuals is already a significant problem.

1.5. HIV and TB Co-infection

HIV is the most potent risk factor for reactivation of latent tuberculosis, and TB is currently the leading cause of death in HIV-infected individuals.[31] Those with HIV/TB co-infection are burdened with an accelerated progression of both diseases, and it is

believed that there are now over 14 million people worldwide who are dually infected.[32,33] TB deaths account for over 25% of all AIDS-related deaths, and 99% of those deaths are in developing countres.[1,34]

The synergy between HIV and TB has serious consequences. First, there is extensive literature on how an *Mtb* infection increases HIV load in the lung.[35,36] The immune response to TB and the excessive production of TNF increases the replication of the HIV in the local sites of *Mtb* infection, shown *in vitro* using monocytic cell lines such as THP-1.[37] Many other *in vivo* studies, sampling PBMC-derived monocytes from serum[38], bronchoalveolar lavage (BAL)[39], or pleural fluid, convincing show that TB provides the perfect milieu of continuous cell activation and dysfunction in the production of cytokines, chemokines, and their receptors for enhanced systemic HIV replication.[40,41]

Second, co-infected individuals are 30 times more likely to develop active TB than HIV-uninfected persons and an elevated risk of death or another severe, life threatening opportunistic disease other than active TB due to their compromised immune systems.[33,41] The reduction in $CD4^+$ T cells, the target of HIV, potentiates more than 20 systemic opportunistic infections aside from tuberculosis.[35] And, perhaps most importantly, the relationship between HIV infection, immunodeficiency and reactivated TB infection hinges on the importance of the $CD4^+$ T cell/ IFN-γ axis.[42] The imbalance of $CD4^+$ T cell number and function due to HIV reduces the elaboration of the IFN-γ that, as described below, is critical for the maintenance of the granuloma that encapsulates the active bacilli in latent TB.[36,43] IFN-γ is also essential for effective immunity to newly acquired TB.[44] Reduction in $CD4^+$ T cell numbers by HIV thus limits the very arm of the

immune response required to fight off newly acquired TB disease and to control latent infection.[38] One of the mechanisms that facilitates this is via the upregulation of *Mtb* receptors on macrophages[40] and manipulation of the TNF-mediated macrophage responses to *Mtb*, which is reduced upon HIV infection.[45] Patel *et al* demonstrated the reduction of TNF and subsequent macrophage apoptosis both *in vitro* and *ex vivo* once cells are infected with HIV.[45] When macrophage responses fail, control of latent TB disease fails, and there is fulminant infection and death.[38] Poverty, overcrowding, malnutrition, and difficult access to care impede all efforts aimed at controlling both HIV and TB.

When latent TB is detected in an HIV-positive person, a course of chemoprophylaxis is given, usually either INH or RIF for a few months.[46] Treatment of a co-infected patient is exacerbated by the fact that while immunocompromised, they need a therapeutic regimen of 18 months to control the TB infection, rather than the 6-9 month regimen of antibiotic treatment for patients with robust immune systems.[46] This is difficult to achieve in areas of poorly funded health care and widespread poverty. Highly active anti-retroviral therapy (HAART) is the aggressive treatment regimen used to suppress active viral replication.[47] HAART substantially improves HIV prognosis by helping restore the immune system, but can be jeopardized by side effects.[48] This means being combined with other drugs to fight various other opportunistic infections. Access to HAART to prevent immune system collapse would greatly reduce the number of people who become ill and die from TB. It is crucial to start HAART early after HIV diagnosis to prevent reactivation of latent TB.[49] But adequate measures to control TB are still not implemented in most settings that provide treatment to HIV/AIDS patients. Delayed

treatment means that many of those co-infected have severe immunodeficiency and high plasma viral load.[48] These patients will usually die from disseminated TB fairly quickly.

1.6. Immune Response to *Mtb*

1.6.1. Innate Immunity

Macrophages are one of the most important cells in innate defence, and through evolution, macrophages have developed methods of recognizing bacterial carbohydrates, lipids, and other pathogen-derived components.[50] These components are often referred to as pathogen associated molecular patterns (PAMPs) and are recognized through the cell's pattern recognition receptors (PRRs).[51] Immediate recognition and engagement with bacterial PAMPs by PRRs can stimulate macrophages, NK cells, dendritic cells (DCs), T cells, and B cells, and allow for very rapid innate immune responses but also facilitate the activation of adaptive immunity.[52,53] Stimulation of PRRs promotes macrophages and dendritic cells to express higher levels of Class II MHC and co-stimulatory molecules, and this enables them to efficiently act as antigen presenting cells (APC) to T cells and initiate the adaptive arm of immunity.[54] The most important PRRs in macrophages that are involved in anti-TB immunity are mannose receptors, Toll-like receptors, DC-SIGN, NOD-like receptors, and Dectin-1.[55] After recognition of *Mtb* with these receptors, intracellular signaling cascades are activated which eventually will lead to the activation of NF-κB, transcription of pro-inflammatory cytokines and cell activation.[56]

The macrophage mannose receptor binds bacterial carbohydrate, and is one of the most important factors in anti-TB immunity. It is a cell bound C-type (calcium dependent) lectin that binds polysaccharide structures of bacteria and viruses, including HIV, and is

highly expressed on alveolar macrophages.[55] The mannose receptor on macrophages functions as an activator of phagocytosis once it binds to LAM and other *Mtb* cell wall components.[57]

The Toll-like receptors (TLRs), are a large family of transmembrane receptors that engage PAMPs and DAMPs (damage associated molecular patterns) and bind bacterial lipoproteins.[50] TLRs are signaling receptors, expressed on the cell surface but also intracellularly in cells such as macrophages and dendritic cells.[58] The PAMPs on *Mtb* are recognized primarily by TLR2, leading to a signaling cascade in which the adaptor molecule MyD88 plays an important role.[59] The activation of both the NF-κB pathway and the MAPK pathway leads to induction of inflammatory genes and the production of inflammatory cytokines such as TNF, IL-1ß, and IL-12.[60] In early infection, TLRs, especially TLR-2, connect the innate and adaptive immune response that are fundamental in keeping *Mtb* growth under control.[61,62]

DC-SIGN (Dendritic Cell-Specific Intercellular adhesion molecule-3-Grabbing Non-integrin) plays important role in macrophage-DC interactions and subsequent DC migration and interaction with T cells.[63] DC-SIGN recognizes LAM, a glycolipid that is shed by *Mtb* during phagocytosis that modifies the phagosome membrane to prevent the formation of the phagolysosome.[64]

NODs (nucleotide-binding oligomerzation domain) are surveillance proteins in the cytosol that are routinely exposed to bacteria, and share binding features of surface bound TLRs.[65,66] NODs recognize microbial products released into the cytosol, in particular bacterial cell wall proteoglycans, and subsequently activate the NF-κB pathway.[51] NOD2 in particular plays a critical role in the type 1 IFN-γ response in *Mtb* infection.[67]

Phagocytosis of *Mtb* also involves scavenger receptors, complement receptors and Dectin-1. Dectin-1 is present on macrophages and dendritic cells and recognizes ß-glucans.[68] The precise *Mtb* PAMP that leads to recognition through Dectin-1 is not completely known, but Dectin-1 is understood to function alongside TLR2 and is involved in the production of cytokines and ROS.[57]

1.6.2. Macrophage activation

TLR2 signaling after engagement with *Mtb* PAMPs recruits the adaptor molecule MyD88 and the downstream events that take place involve phosphorylation of a number of kinases (Figure 1.1).[50] After IRAK (IL-1 receptor associated kinase) 1 and 4 have been phosphorylated they dissociate from MyD88 and interact with TRAF (TNF receptor associated factor) 6.[54,56] TRAF6 is phosphorylated and recruited to IRAK to activate the NF-κB pathway as well as the MAPK pathway (not shown). Additional kinase TAK1 and its binding proteins phosphorylate the IKK complex, which is the converging point for NF-κB activation.[69] The IKK proteins phosphorylate IκB, which then becomes susceptible to ubiquination and targets it for degradation by the proteasome.[70] The NF-κB dimer is released and translocates to the nucleus, regulating the transcription of genes involved in inflammatory responses.[70] A regulatory mechanism for NF-κB signaling is necessary to control inflammation. Once NF-κB translocates to the nucleus it promotes the transcription of a large number of genes. One of these genes is IκB alpha, which modulates cell signaling by exporting NF-κB back out of the nucleus.[71]

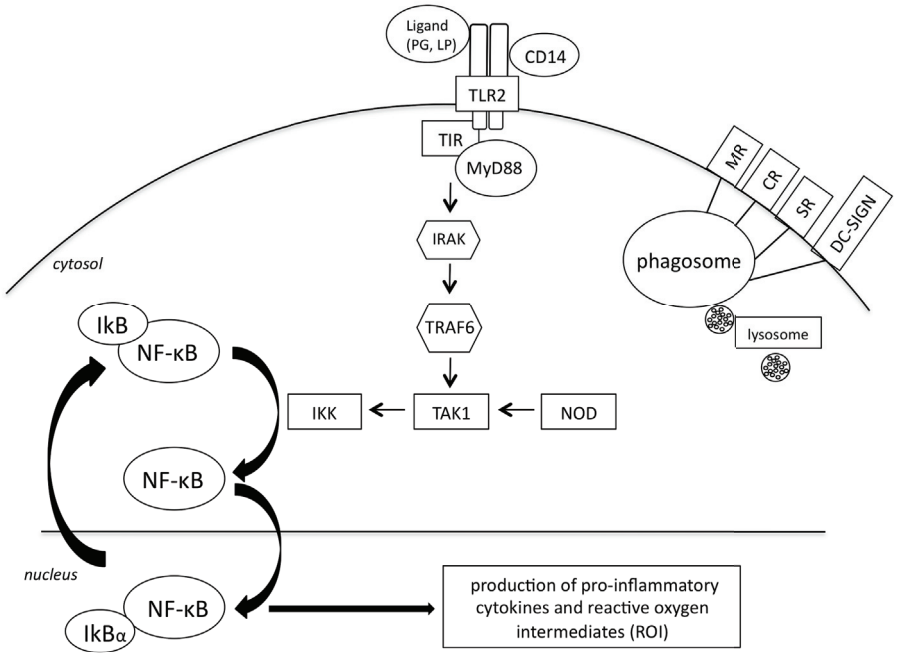

Figure 1.1. Pattern recognition receptors in macrophages*. The innate recognition and intracellular signaling occurs immediately after Mtb makes contact with the macrophage. TLR2 and other Mtb-specific receptors trigger a signaling cascade via a MyD88-dependent pathway that eventually leads to translocation of NF-κB to the nucleus and the transcription of genes involved in the inflammatory response, including pro-inflammatory cytokines and ROS. PG= proteoglycan. LP= bacterial lipoprotein. MR=mannose receptor. CR=complement receptor 1. SR=scavenger receptor. DC-SIGN= dendritic cell-specific intercellular adhesion molecule-3-grabbing non-integrin. NOD= nucleotide-binding oligomerization domain protein.*

The binding of bacteria and subsequent activation of macrophages initiates phagocytosis and uptake into phagosomes. This is followed by vesicle acidification and fusion of the phagosome with lysosomes.[55] Phagolysosome fusion results in the production of reactive oxygen species and reactive nitrogen species as well as the release of antimicrobial peptides and lysosomal enzymes.[72] The primary oxygen-derived products (ROS) are superoxide, hydrogen peroxide and hydroxyl radicals, and the most important nitrogen intermediate is the short lived but potent molecule nitric oxide.[73–75]

1.6.3. *Mtb* survival strategies in macrophages

Mtb bacilli have evolved ways to survive and replicate in the phagosomal compartment of macrophages via a number of complex mechanisms, altering lysosome activity and phagosomal acidification, enhancing its ability to persist inside the cell.[76,77] The cell wall of *Mtb* is unique in that it is comprised of over 60% lipid.[78] There are also mycolic acids, cord factor, wax-D, and lipoglycans including LAM or, in the case of slow growing, more virulent *Mtb,* mannose capped LAM (ManLAM). These components increase *Mtb* resistance to many antibiotics, to osmotic lysis by activated complement, resistance to macrophage bactericidal products, and overall virulence.[79]

In most cases, *Mtb* remain in the phagosome that is now a protected environment for replication. An example of this is the decreased production of IL-10 by DCs and macrophages after binding with LAM.[80] Under normal circumstances it is sensible that the secretion of IL-10 is involved as a regulatory mechanism that limits tissue damage from the initial inflammatory response. But in the case of *Mtb* infection, LAM and

ManLAM contribute to *Mtb* survival by protecting infected macrophages from apoptosis.[81,82] Thus, LAM is a major determinant of *Mtb* virulence.

Finally, the function of a 19kDa lipoprotein on *Mtb* that binds TLR2 is unknown, but it is understood to have a role in cell death and manipulation of bactericidal mechanisms in macrophages.[83] Of particular interest is that it promotes the inhibition of IFN-γ mediated signaling and limits the upregulation of class II MHC.[84]

1.6.4. Adaptive Immunity

Adaptive immunity to *Mtb* is primarily a Type 1 $CD4^+$ T cell (Th1) response, known as a delayed type hypersensitivity (DTH) response that induces a large influx of macrophages to the site of infection.[85] The Th1 cells are crucial to the T cell/IFN-γ/TNF axis that controls TB. In an otherwise healthy individual, a significant percentage of *Mtb* bacilli are killed, and the *Mtb* elements are killed and taken up by local DCs, already activated by PAMPs resulting from the infection.[85] DCs that have processed *Mtb* antigens migrate to local lymph nodes and present Ag to $CD4^+$ T cells.[86] $CD4^+$ T cell activation results in proliferation and differentiation into IFN-γ producing Th1 cells.[87,88] B cell activation and antibody production to intracellular bacteria like *Mtb* is present but limited.[33] Th1 cells then leave the lymph nodes and transit by the circulation to the site of infection, and it is there that the Th1 effectors secrete large amounts of IFN-γ.[89] As a result macrophage activation is increased, resulting in greater killing and an increase in class II MHC molecules, recruiting more T cells, perpetuating the DTH response. This positive feedback loop is dependent on IFN-γ production.[90,91] Th1-derived IFN-γ fulfils two important functions. First, IFN-γ activates local macrophages to increase phagocytosis and killing by increasing TLR expression.[85] Downstream, IFN-γ can increase TLR

signaling by enhancing intracellular pathways, such as increasing MyD88 expression.[92] Macrophages and alveolar epithelial cells produce NO in the initial response to *Mtb* once it reaches the lung, and IFN-γ greatly elaborates NO and increases the macrophage oxidative burst, critical to the killing of the majority of bacilli upon early infection (Figure 1.2).[75]

When IFN-γ binds to its receptor, the receptor undergoes a conformational change, so that inactive JAK2 autophosphorylates, and subsequently JAK 1 is phosphorylated.[93] This initiates the formation of a paired set of STAT docking sites recruited by the receptor, at which time they associate with two STAT molecules.[93,94] They are brought in close proximity to JAK1 and 2, and STAT 1 is phosphorylated in this process. Phosphorylated STAT1 homodimers travel to the nucleus and bind to an IFN-γ activation site (GAS) element, initiating the activation of IFN-γ regulated genes. Negative regulation of IFN-γ signaling is due to a number of factors, including ligand degradation once the receptor is recycled at the cell surface, and dephosphorylation of JAKs due to protein tyrosine phosphatases (PTPs) in the cytosol and the nucleus.[94]

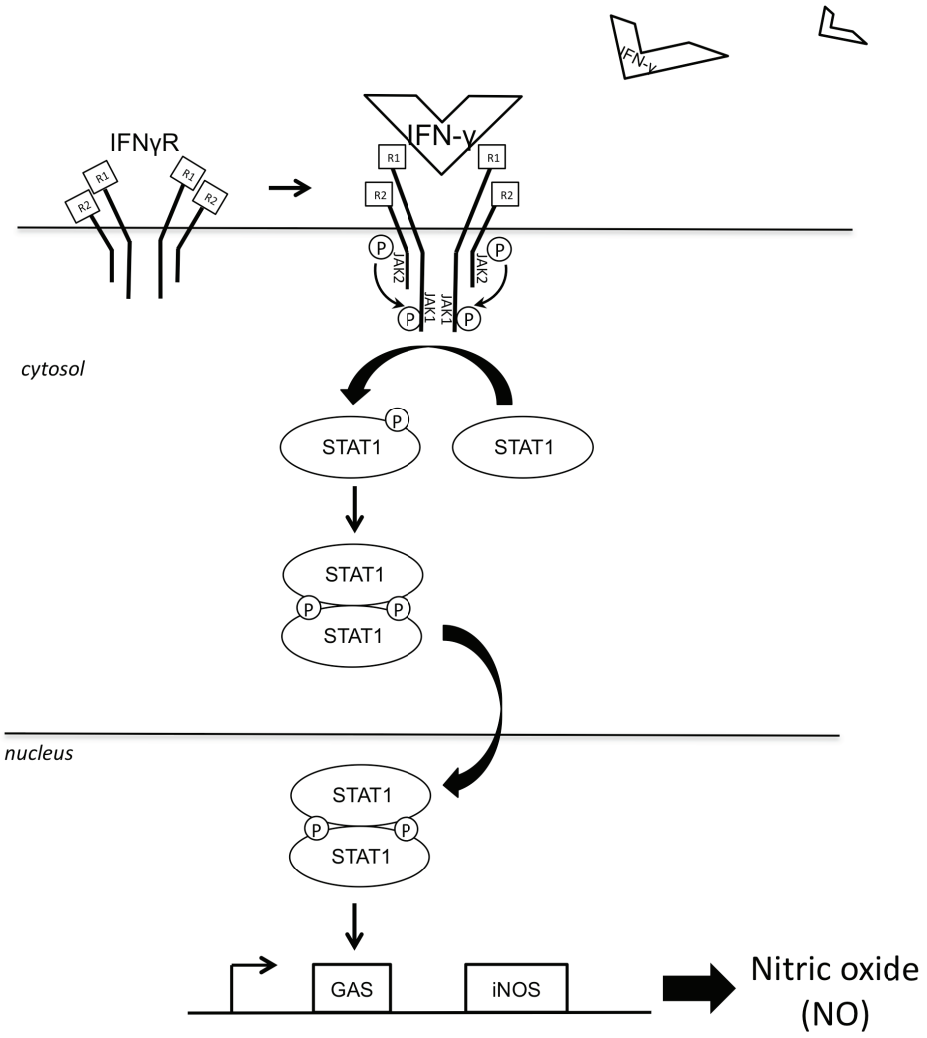

Figure 1.2. IFN-γ signaling. *IFN-γ signaling via the JAK/STAT pathway for the production of the reactive nitrogen species nitric oxide (NO), resulting in NO-induced apoptosis in infected macrophages. NO production is dependent on the activation of inducible nitric oxide synthase (iNOS). Transcription of iNOS requires IFN-γ engagement with Mtb cell surface receptors and subsequent intracellular signaling.*

Even though IFN-γ is capable of enhancing the killing response of infected macrophages, it is not effective enough to allow for complete clearance of *Mtb* from the lung. But macrophages stimulated with IFN-γ release large amounts of tumor necrosis factor (TNF) to produce a strong granulomatous response.[95] TNF serves to recruit large numbers of macrophages from the circulation to the site of infection. This, along with increased Th1 cell recruitment, allows for the containment of the *Mtb* in a granuloma or tubercle.[96]

The innermost section of the granuloma contains the infected macrophages and free *Mtb*, which forms the caseous necrotic core. The outer layer of the granuloma is composed of macrophages and the Th1 cells that are responsible for the IFN-γ that sustains it.[97] Continuous activation of macrophages here allows for ingestion and destruction of any *Mtb* escaping from the edge of the caseum.[98] In a healthy individual, TB infection can remain in a latent state within the granuloma, often for the lifetime of the person affected.[99] Loss of either IFN-γ production from Th1 cells or subsequent loss of TNF production from macrophages causes failure of this ongoing containment that characterizes latent TB.[95]

The central role played by $CD4^+$ T cells in the containment of *Mtb* bacilli means that any factors affecting T cell number or function would adversely affect control of TB.[99] If a person's $CD4^+$ T cell count falls for any reason, although the most obvious being HIV infection, the granuloma fails.[100] It is because of this that the infection develops into fulimant disease. The failure of the granuloma is associated with the emptying of caseous material and the formation of a lung cavity.[101] Here the new oxygen-rich environment allows for explosive growth of the bacilli, and the bacilli are very easily discharged into the bronchi and other parts of the lung and outer environment. The exact mechanisms

involved in reactivation of TB at this stage are unclear and there is evidence that at this point the bacilli can multiply extracellularly for the first time.[102] The pathology associated with this infection, and the cell-mediated immune response mounted to try to clear it, is often fatal.

1.7. Immune enhancement to control *Mtb* infection

1.7.1. Rationale

The standard drug regimen for TB is now over 50 years old (when rifampin was first used). This has allowed plenty of time for *Mtb* to develop resistance to current therapeutic agents. Two new anti-TB drugs have recently appeared (bedaquiline (2012) and delamanid (2013)).[28,30] However, antibiotic resistance in *Mtb* is rampant, and will most likely develop in these drugs in the future. It is a particularly acute problem in infected individuals that are immunocompromised (either naturally or acquired).[103] An alternate strategy to antibiotic therapy is to boost the immune response in these immunocompromised patients allowing them to control TB infection more efficiently. This strategy could work when combined with standard antibiotic therapy and might slow the rate of development of resistance to novel antibiotic treatments.

World-wide, traditional medicine has a long history of treatment of infectious diseases, including the industrialized world where novel pharmaceuticals from plants, fungi, and animal based holistic treatments have played and continue to play a major role in primary health care as they do in many developing countries.[104–107] The proposal here is that the use of traditional medicinal agents with reported immune enhancement functions could boost type 1 immune responses. This would include enhancing phagocytosis, killing

ability and TNF production by macrophages. All three of these elements would allow for a better response to TB and contribute to the stability of the granuloma in immunocompromised patients with latent TB.

1.7.2 Selected treatment agents

1.7.2.1. *Echinacea purpurea*

There are many species of *Echinacea*, a group of perennial prairie wildflowers of the family Asteraceae. Of these, *Echinacea purpurea* (purple coneflower), is the most popular cultivar throughout Canada, the United States, and Europe not only as a showy flowering perennial, but also for its widely reported medicinal uses.[108] It is reported to be the most common neutraceutical in North America, and approximately 40% of individuals using it to combat the common cold on a regular basis.[109] For clarity, all references to *Echinacea* in this thesis refer to *Echinacea purpurea*.

The studies investigating *Echinacea* species are widespread and diverse, including effects on wound damage, inflammation, and tumour growth.[110] But the majority of *Echinacea* research has been devoted to prevention of upper respiratory tract infections. It has been the focus of a limited number of clinical trials, testing its efficacy against a number of viruses including rhinovirus, coronavirus, adenovirus, and influenza.[111] In particular, the clinical trial conducted by Goel and colleagues (2004) showed that after the onset of cold symptoms in an *Echinacea*-dosed group versus a placebo, a 23% reduction in cold symptoms was seen at the end of the 7d treatment period. Shah (2007) and colleagues performed a meta-analysis evaluating the effect of *Echinacea* preparations on the incidence and duration of the common cold in randomized placebo-controlled studies.

The summary of study data showed that *Echinacea* decreased risk of a patient contracting a cold by 58%. It was also found to decrease the duration of colds slightly.[109] Jawad *et al* conducted the largest clinical trial using *Echinacea* for respiratory infections to date. They showed that compliant prophylactic intake of *Echinacea* over a 4-month period appeared to provide a "positive risk to benefit ratio", with significant reductions being observed in the number of episode days, co-medicated episodes, and recurring infection during treatment compared to a placebo.[111]

There are certainly studies that oppose the effectiveness of *Echinacea* preparations in combating the common cold. A limitation to studies in terms of immunomodulatory activity is the fact that no two treatment agents are exactly alike.[112] Moreover, there is often no indication of the level of proposed active agent in the treatment used in the study.[108] Since *Echinacea* was first examined there have been many active ingredients identified. These include caffeic acid derivatives, chicoric acid (phenolic), essential oils, polyacetylenes, echinacin, echinacoside, flavonoids, polysaccharides, and alkylamides.[113] The phytochemical variability in different preparations is influenced by many intrinsic and extrinsic factors. Intrinsic factors include the growing conditions, harvest techniques, and storage, and extrinsic factors include aspects of the preparation and storage of the extract.[110,114] Some manufacturers control batch-to-batch variation. Factors R&D in Vancouver, BC, extract particular elements and recombine them at specific concentrations to ensure batch to batch homogeneity in certain phytochemical elements.[115] Another consideration is the risk of endotoxin contamination, which is substantial during the extraction process. This can lead to false positives in those cases

when endotoxin concentration is not monitored.[108] This is an especially acute problem in studies with innate immune activity where it is crucial to control for endotoxin.[116]

1.7.2.2. *Echinacea* and Macrophage Activation

The majority of the data coming from studies using *Echinacea* provide evidence of a mechanism of immunomodulatory action involving the activation of innate immune cells. The most convincing data demonstrate the effects of purified *Echinacea* polysaccharide preparations on macrophage activation. We, and others, have shown that it is a potent activator of macrophages *in vitro* and *in vivo* in a murine model.[117–120] Others have demonstrated similar effects in human macrophages.[115,119,121] Importantly, *Echinacea* polysaccharide has been shown to increase *in vitro* production of TNF, IL-1, and IL-6.[110,117,122]

Of particular relevance to this project is the data that links *Echinacea* polysaccharide to enhanced macrophage activity in a model of intracellular bacterial infection. *Listeria monocytogenes* is an intracellular bacterium that causes the human disease Listeriosis. Like *Mtb*, *Listeria* resides in macrophages. In a seminal study, Steinmuller (1993) used immunocompromised mice to determine if *Echinacea* could enhance innate immune responses to *Listeria* infection. CyA was administered to ablate $CD4^+$ T cell activity. Their results confirmed that macrophages, not lymphocytes, were required for the reduction in bacterial burden that was observed. Sullivan also showed this effect in an in vivo study using *Listeria*-infected mice, where *Echinacea* polysaccharide was delivered orally for 2d before and 1d after infection. *Echinacea* polysaccharide significantly

reduced bacterial burden and suggests that it has the ability to decrease the severity of intracellular infection.

1.7.2.3. *Cordyceps sinensis*

Cordyceps sinensis (caterpillar fungus) is a parasitic fungus that primarily invades the larvae of a particular species of moth (*Hepialus armoricanus*).[123] Once the larval moth has been infected, the fungus germinates and fills the larvae with the mycelium containing many hyphae, and then sprouts a fruiting body.[124] Due to the protruding fruiting body above ground, the mycelium can be harvested. Dried *Cordyceps* mycelium has had a long history of use in traditional Chinese medicine for a variety of ailments, including for asthma, bronchitis, cancer, chemoprotection, enhanced exercise performance, hepatitis, hyperlipidemia, immunosuppression, and chronic renal failure.[125] In the last decade, due to increased popularity, demand and the scarcity of wild *Cordyceps*, the price of the fungal mycelium has risen 20% annually.[126,127] Cultivated *Cordyceps* mycelium is an alternative to wild-harvested *Cordyceps*, and is typically by growth of pure mycelia in culture.[127]

1.7.2.4. *Cordyceps* and Macrophage Activation

The active ingredients in *Cordyceps* mycelium have still not been clearly determined, but studies have shown the active components in a whole *Cordyceps* extract to include cordycepin and cordycepic acid, ergosterol, polysaccharides, nucleosides, and peptides.[123,128] The polysaccharide component is well documented as a major active ingredient of *Cordyceps* ranging from 3 to 8% of its total dry weight.[125] The majority of current data *in vitro* and in murine models indicate that the polysaccharide fraction of

Cordyceps is the most important in the activation of macrophages for enhanced secretion of cytokines.[128–132] Importantly for this study, Zhang (2008) demonstrated that an "exopolysaccharide" fraction enhanced TNF activity in peritoneal macrophages isolated from tumor bearing mice, and increased IFN-γ mRNA expression in the splenic lymphocytes.[133]

Our laboratory demonstrated that an aqueous *Cordyceps* extract activates macrophages to produce pro-inflammatory cytokines in the setting of intracellular bacterial infection. It was observed that *Cordyceps*-stimulated macrophages *in vitro* produce IL-6 and TNF, as well as increase production of NO in the presence of IFN-γ.[134] In an *in vivo* study of intracellular infection, *Cs* was able to decrease bacterial load in mice infected with *Listeria monocytogenes*. [134]

1.7.2.5. *Heracleum maximum*

Heracleum maximum (cow parsnip) is a member of the Apiaceae family and is native to Canada and parts of U.S.[135] Apiaceae is a large family of plants, with *Heracleum* species alone comprising approximately 120 species.[136] The Apiaceae family contains many plants that have varying biological properties that are used in traditional medicine. Common for this group of plants is the presence of bioactive secondary metabolites such as essential oils, phenolics, alkamides, and coumarins.[136] It is highly antimicrobial and is phototoxic, but these compounds can be removed to test for other active ingredients. [137]

1.7.2.6. *Heracleum* and Macrophage Activation

Studies have been performed on *Heracleum* species in the past, mostly as an antifungal agent.[138,139] There is less data on the immunostimulatory properties of *Heracleum*.

Webster et al originally investigated the immunostimulatory effects of an aqueous extract of *Heracleum* on mouse peritoneal macrophages.[140] The extract showed to have enhanced IL-6 activity compared to a control. Previous to these studies, in an *in vitro* study using isoniazid as a positive control, a sterile aqueous extract of prepared ground *Heracleum maximum* root demonstrated complete inhibition of the growth of both *Mycobacterium tuberculosis* and *Mycobacterium avium*.[141] Webster et al followed this study using a sterile aqueous *Heracleum maximum* extract, derived from the roots, as a treatment agent against mycobacteria and demonstrated significant antimycobacterial activity against a rifampicin control. More recently their laboratory was able to identify key antimycobacterial components in the extract.[142]

1.8. Objectives

The objectives of this study are to examine whether our selected agents activate type-1 immunity in a manner that would suggest they could be used to treat TB disease.

The specific objectives are:

(1) To establish an *ex vivo* human model to mimic, as closely as possible, human TB infection using a virulent strain of *Mtb* (H37Rv) and freshly isolated human macrophages.

(2) To assess three aqueous extracts made from natural products for their ability to boost macrophage responses in combination with IFN-γ to resist intracellular infection by *Mycobacterium tuberculosis*.

1.9. Project 2. Implications of the Innate Immune Response in Cardiac Allograft Vasculopathy (CAV)

1.10. Background

In industrialized countries, cardiovascular diseases are top killers of men and women, and, in Canada alone, responsible for over 20% of all fatalities.[150] The global epidemic in obesity and subsequent increase in Type II diabetes has exacerbated this situation since both are major risk factors for hypertension, atherosclerosis and cardiac failure.[151,152] Transplantation remains the treatment of choice for improving the quality of life and increasing the lifespan of patients with end-stage heart failure.[153,154]

The first heart transplants were performed in South Africa in the late 1960s, before the etiology of graft rejection was understood.[155] In these early days before modern immunosuppressive regimens, recipients of organ transplantation died within the first year because of human leukocyte antigen (HLA) incompatibility.[156] HLA antigens are the vehicles that present peptides to the cell surface and instigate appropriate immune responses through HLA/T cell receptor interactions.[157] The disparity in HLA between donor and recipient creates an environment for immune activation and tissue destruction.[158] There are two classes of HLA antigens of significant importance in transplantation, class I (HLA- A, B, and C) and class II (HLA- DR, DQ, DP).[159] There are two genes for each HLA loci resulting in up to 12 different HLA molecules on the cell surface. The three most important loci to match for transplantation are HLA-A, HLA-B, and HLA-DR, a so-called six-point match.[160] There is agreement among the transplant

community that there is a direct relationship between the long term survival of the graft and the number of HLA-A, B, and DR mismatches.[158,161,162] Kidney transplantation is routinely performed after matching HLA antigens, and thus has better long-term outcomes than hearts.[158] Practical considerations for the lack of HLA matching in hearts include size matching, availability of donors, and the necessity for much shorter cold ischemia times, which prevent heart transplant teams from achieving the level of HLA matching that is currently standard in kidney transplantation.[159,163]

1.11. Acute Allograft Rejection

Every transplanted organ is subject to some degree of acute rejection. Acute rejection is considered to be predominantly a T cell-mediated process.[164] According to the International Grading System for categorizing transplant rejection, severe acute cellular rejection (ACR) in transplanted hearts is defined as having diffuse, aggressive cellular infiltrates, along with edema, haemorrhage, and vasculitis.[165] There is also obvious and sometimes widespread destruction of myocytes. Varying degrees of acute cellular rejection have been shown to occur within days to months after transplantation, and within one year of transplantation, between 20-40% of heart transplant recipients experience at least one acute rejection episode.[165] Acute antibody-mediated rejection (AMR) has been suggested to be much less common than ACR, occurring in only approximately 10% of patients.[166] Recent data is pointing to a potential revision upward of the estimated frequency of AMR, as AMR becomes a more popular area of research.[167–169]

1.11.1. Innate Responses in Graft Rejection

An allogeneic graft provides a strong immunological stimulus, and as such, all arms of the immune response are engaged in the development of acute rejection.[170] Many studies have shown a primary role for T cells in both ACR and AMR, but the activation of T cells requires the appropriate engagement of the innate immune compartment. [171,172] Thus, post-transplant inflammation is critical to the activation of adaptive immunity. The elaboration of pro-inflammatory mediators due to tissue injury is independent of the adaptive immune response, and critical to its development.[173] Organ procurement, cold storage, and surgical trauma are key components associated with graft injury.[174] Oxygen deprivation in the graft, and subsequent reperfusion with whole blood, results in a phenomenon known as ischemia/reperfusion injury (IRI) where neutrophils play a key role.[175] Immediately post-transplant, there is a release of reactive oxygen species (ROS) and pro-inflammatory cytokines that activate vascular endothelial cells, degrade pathogens, and recruit neutrophils within minutes of reperfusion.[175] Neutrophil recruitment initiates a cascade of events that include breakdown of extracellular matrix and cell death (both necrosis and apoptosis).[176] Additionally there is dendritic cell activation, activation of tissue macrophages and recruitment of further neutrophils and circulating monocytes.[177] The initiation of IRI occurs through damage associated molecular patterns (DAMPs). The engagement of DAMPs with complement receptors and TLRs on macrophages and dendritic cells in the donor tissue promote pro-inflammatory cytokine release and DC maturation.[171] The inflammation and cell destruction created by IRI leads to the egress of donor dendritic cells that can activate recipient adaptive immune responses by so called "direct presentation" of foreign

HLA.[178] Direct cell destruction also leads to the release of HLA molecules from donor cells into the extracellular space.[179] This leads to uptake and processing of foreign HLA molecules by recipient DCs for presentation of foreign HLA peptides in the context of Class II MHC as well as in the context of Class I MHC (through cross presentation).[179] Presentation of donor antigens in self MHC is referred to as indirect presentation, and both will lead to the activation of adaptive immunity against the graft.[173,180]

1.11.2. Adaptive Responses in Graft Rejection

Following the response to tissue injury and inflammation discussed above, antigen presenting cells (APCs) from the graft migrate to recipient lymph organs where they will encounter T cells.[181] Activation of T helper (Th) cells is pivotal to the initiation of acute rejection events, and they are activated by a multi-signal pathway.[173] The first signal occurs via the stimulation of the T cell receptor (TCR) when presented with an allo-peptide in the groove of Class II MHC on the surface of an APC.[182] This first signal activates a number of intracellular kinases, a discussion of which is outside the scope of this thesis research. One important end result of the activation of this kinase cascade is the liberation of intracellular stores of Ca^{++}.[183] One of the most important activities of this intracellular Ca^{++} is the activation of calcineurin and subsequent de-phosphorylation of nuclear factor of activated T cells (NFAT). NFAT translocates to the nucleus and acts as a transcription factor for new gene expression.[184] Additional to the interaction of the TCR with the APC, a second signal is required to activate the T cells. This second signal is provided by the interaction of the B7 molecule on the surface of the APC with its receptor on the surface of the T cell (CD28).[182] This second signal also activates through intracellular kinases and leads to the translocation of another set of transcription factors

that work in tandem with NFAT to initiate the expression of the IL-2 gene and the IL-2R gene.[185] The expression of IL-2 and IL-2R leads to the engagement of IL-2 with its receptor on the surface of the T cells.[186] This engagement of IL-2 with its receptor represents the third signal of T cell activation, initiating cell proliferation through a series of events involving the mammalian target of rapamycin (mTOR) pathway.[187,188] Upon activation, T cells orchestrate both ACR and AMR through secretion of cytokines (such as IFN-γ, IL-2, IL-4, IL-6 and IL-12), resulting in three main immune defenses.[189] The first is that $CD8^+$ T cells become activated to kill donor cells, and over time this destroys parenchymal structures and initiates fibrosis. Secondly, once activated, T cell interactions with B cells cause maturation of B cells, which provide defense via the secretion of antibodies. Finally, Th1 cells orchestrate the effector response that results from active secretion of IFN-γ, mobilizing and activating tissue macrophages and other immune cells, other lymphocytes, and endothelial cells.[189] The continuous influx of Th1 effectors to the site of graft damage allows acute rejection events to persist.

With the high probability of mismatch within populations, the inevitable tissue damage and inflammation due to ischemic events, and the innate and adaptive immune processes that are initiated, there will always be acute rejection events. This highlights the vital role of immunosuppression to control and treat allorecognition and rejection.

1.12. CNI Immunosuppression

The understanding of the three signaling events for effective T cell function has guided the development of immunosuppressive therapy in transplant recipients.[190] A cocktail of immunosuppressive drugs is administered post-transplant to block these events.[191]

Decades ago calcineurin inhibitor (CNI) immunosuppressive drugs emerged as the mainstay of post-transplant immunosuppression.[192] In cardiac transplantation the majority of studies have reinforced the view that CNI immunosuppression is critical for long-term graft survival. The two dominant CNI immunosuppressive drugs are cyclosporine and tacrolimus, and their primary mode of action is to prevent the dephosphorylation of phosphorylated NFAT by calcineurin.[193,194] Phosphorylated NFAT cannot translocate from the cytoplasm to the nucleus and thus, in the presence of CNI, IL-2 transcription and subsequent T cell activity are shut down.[195] Thus cyclosporine and tacrolimus interfere with the activation of $CD4^+$ T cells, a crucial step in the prevention of acute cell-mediated allograft rejection.[194]

There are many complications with using CNI such as cyclosporine. One of the most serious complications of long-term use is chronic nephrotoxicity, which is augmented when in combination with other immunosuppressive drugs (sirolimus).[196] There are other major morbidities associated with its use, including hypertension, hyperlipidemia, and increased risk of opportunistic infections and certain malignancies.[192] Ultimately, it is important to realize that while CNI ablates the majority of $CD4^+$ T cell activity, it is less able to reduce $CD8^+$ T cell activity. We, and others, have suggested that the progression to late cardiac graft rejection is due primarily to the activities of $CD8^+$ T cell- mediated killing, leading to late graft rejection.[197–200] This could explain why current CNI based immunosuppressive regimens do not limit the development of late graft rejection.

1.13. Late Graft Rejection and CAV

Since the inception of CNI, there has been dramatic improvement in early graft survival,

and currently the data for graft survival one year post-transplant is near 90%.[201] Despite these excellent short-term outcomes, CNI and other immunosuppressive agents are still unable to prevent the development of chronic rejection responses. The survival of transplanted hearts 10 years post transplant still averages only approximately 50% and this number is not improving as years go by and new immunosuppressive drugs are used.[201] Chronic rejection of cardiac transplants is a multifactorial pathological vascular remodeling process, often referred to as cardiac allograft vasculopathy (CAV). Approximately 50% of recipients at one year post-transplant and 75% by three years post-transplant have diagnosable CAV.[202] In the coronary epicardial vessels CAV is characterized by an inward expansion of the intimal layer.[203] It is generally regarded that the intimal expansion in the is the most important aspect of CAV with respect to organ survival.[202,204] The immunological risk factors including HLA mismatches, severity of IRI, and number of acute rejection episodes predict more severe CAV, but there are also non-immunological risk factors such as donor and recipient age, graft ischemic time, and bacterial or viral infections, that are known to be associated with CAV.[202,205]

1.14. Etiology of CAV (in Humans and Rodents)

Part of the complexity in developing novel treatments for CAV relates to the discrepancy in the expression of CAV in animals and humans. This is most profoundly seen in the intimal lesion in the epicardial coronary arteries. Until recently, our understanding was based primarily on a widely accepted paradigm using rodent models of CAV.[205,206] In rodents, the internal elastic lamina (IEL) serves as a base for a single-layer of endothelial cells that sits on a thin basement membrane (Figure 5.1). In humans the structure of the intimal layer is more complex. All human donor epicardial CA possess a SMC-rich

diffuse intimal layer from birth. It has been observed as adaptive intimal thickening, non-atherosclerotic intimal thickening, or diffuse intimal thickening.[207,208] Our laboratory has referred to this intimal cushion as benign intimal thickening (BIT), and for clarity, BIT will be used for the remainder of this thesis. By early adulthood, the BIT layer is at least as thick as the media (usually 200-300μm).[208] BIT does not obstruct the lumen, and is thought to represent adaptation to cardiac mechanical forces.[209] This BIT layer, with few exceptions, is generally absent in laboratory animals. It has been shown that the prevalence of an intimal cushion in a variety of species is negligible.[208,210]

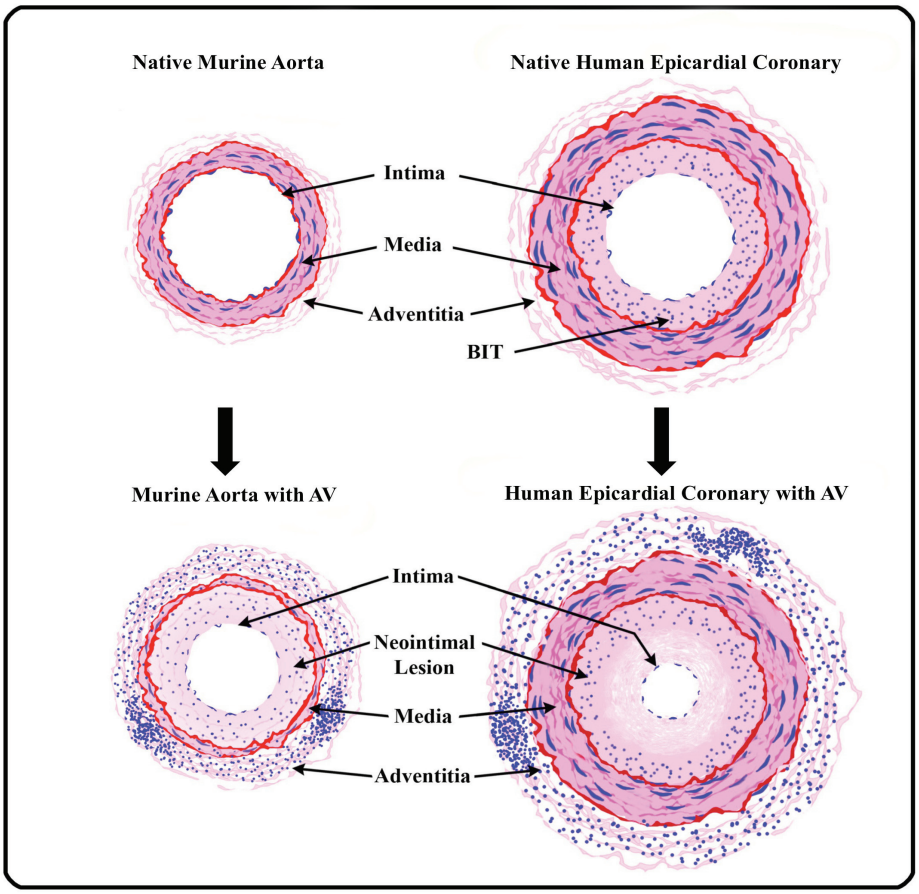

Figure 1.3. Human versus mouse native aorta *(courtesy Dr. M. Hart-Matyas). The top left panel shows a normal murine aorta with three distinct layers, including the intima, media, and adventitia. The bottom left panel shows a mouse aorta with AV. There is a loss of SMCs from the media accompanied by the development of an intimal lesion, composed of proliferating cells characteristic of smooth muscle cells, as well as lymphocytes and macrophages. In the top right panel, a normal human coronary artery is also comprised of three layers, but the innermost layer is made up of a diffuse intimal cushion known as benign intimal thickening (BIT). In human CAV (bottom right), the difference lies within two contiguous layers of the BIT and the post-transplant neointima.*

The original paradigm of how CAV developed in human epicardial CA was based entirely on older studies using rodent vessels. Because the neointima in the rodent vessels consist entirely of SMC it was originally thought that after transplant, donor SMC in the media migrate across the IEL into the subendothelial intimal space and develop into a homogeneous neointimal lesion.[211,212] Later evidence demonstrated that the cells that populated the *de novo* neointimal AV lesion in rodents are all recipient, not donor, in origin.[213,214] This led to a modified hypothesis that recipient myofibroblasts migrate from the bloodstream into the intima, drawn in by inflammatory signals from the injured endothelium.[215]

The rodent data has now been shown to be inconsistent with the observations of human CAV. In fact, lesions in humans are almost entirely donor in origin.[216,217] The other striking difference is that human CAV presents itself as two distinct layers. The layer that lies adjacent to the media is SMC-rich and macrophage poor, which our laboratory and others believe to be the BIT layer that has been transferred over from the donor.[218,219] Our laboratory has demonstrated with a mechanical injury model in rats that the BIT survives transplantation.[220] Moreover, we have found that human cardiac transplants harvested at 1, 4 or 10 days post transplant all show an intact BIT layer, thus proving that the BIT layers survives clinical transplantation.[220] Thus, the starting point while studying the mechanisms of CAV between human and rodent is very structurally different. The implications of carry-over BIT to the expression of human CAV have not been fully recognized to date. The more luminal layer of the human CAV lesion is lipid and macrophage rich, less cellular than the deeper medial layer, and contains more fibrotic factors like TGF-β.[221]

It also appears more eccentric in nature than the BIT layer. This layer contains a high proportion of macrophages and lipid, and is suggestive of an atherosclerotic-like lesion.[221] If the most luminal area of the lesion resembles atherosclerosis, this presents the possibility that *de novo* lesion growth post-transplant is a result of an accelerated atherogenesis. This could be due to ischemia reperfusion injury and subsequent inflammatory responses to donor elements after transplant.[222] The high lipid environment created by CNI immunosuppression post-transplant could accelerate this process.[223] One could speculate that this lesion progression is intensified if donor atherosclerosis is already present, and have very significant impact on graft survival after transplantation.

1.15. Atherosclerosis

Atherosclerosis may begin in early childhood. 50% of infants have small collections of macrophages with lipid droplets in the coronary arteries, which dissipate in childhood but return at puberty in larger accumulations.[207] The initiating events in atherosclerosis are difficult to elucidate, because early atheroma development often occurs in conjunction with BIT.[224] In addition, both are usually found within the epicardial coronary arteries and the more proximal regions of the aorta. Williams and Tabas (1995) first proposed the response to retention hypothesis for atheroma development, where lipoproteins are retained in the intima by binding to extracellular proteoglycans from established BIT.[225]

The most recent evidence by Nakashima (2007) supports this. Nakashima has shown that extracellular matrix (ECM) lipid deposition in the deeper region of the more luminal BIT layer precedes macrophage accumulation, and colocalizes with intimal proteoglycans.[222] The proteoglycan-lipoprotein complexes increase the lipoprotein susceptibility to

oxidation, leading to inflammatory signals that promote macrophage activation, uptake of lipid, and formation of foam cells.[226,227] Other studies show early events in atherosclerosis may be stimulated by the increased expression of HLA-DR molecules in the more luminal layer of BIT.[228] The Bobryshev group showed a positive correlation between HLA-DR with extracellular lipid accumulation.[229] It is believed that this is a source for inflammatory cell recruitment and Ag presentation, creating "microsites" for atherogenesis.[229]

While the earliest events in atherosclerosis are still not clearly defined, the literature characterizes it as an archetype of chronic inflammation that begins with endothelial damage.[219,225,230–232] Normal endothelium, in general, does not attract leucocytes until the endothelial cells have met with an inflammatory insult, like mechanical stress or alterations in blood flow.[230] Augmented wall stress may promote the production of proteoglycans by SMC.[221] These proteoglycans bind lipoprotein components and retain LDL in the intima, facilitating their oxidative modification.[221,226] This would support the observations that the first visible fatty streaks tend to be in the branches of the BIT layer in muscular arteries like the coronary arteries and the aorta.[222] It would also provide insight into why there is modification of LDL particles before being taken up by macrophages.[222,226] Once in the intima bound to proteoglycan, LDL is prone to oxidation by innate inflammatory enzymatic attack.[228] The oxidized LDL (oxLDL), along with the simultaneous changes in blood flow at branch points, can lead to the expression of adhesion molecules like E-selectin and VCAM-1.[233] These act in synergy with MCP-1, CCL5 (RANTES), CXCL10 (IP-10), and CX3CL1 (fractaline) to attract monocytes, DCs, T cells, and NK cells.[234,235] Recruited monocyte-derived macrophages increase their

expression of a number of TLRs and scavenger receptors that leads to ingestion of the oxLDL and intracellular accumulation of cholesterol.[236]

With the understanding that the arterial intima of a mouse is structurally different than the human, there should be fundamental differences in how LDL binds and accumulates in the sub-endothelial space. In the mouse, early signs of inflammation happen simultaneously with lipid accumulation.[230] Previous reports suggest that in animal models there is increased expression of VCAM-1 in arterial branches when mice are subjected to an atherogenic diet, and this response has been observed to be sufficient to initiate atheroma development.[230,237]

Immunity to atherosclerosis is primarily a Th1 response, and is strikingly similar to the DTH response in an *Mtb* infection. In this case, the Th1 cells drive the T cell/IFN-γ/TNF axis that strongly influences the growth of the atherosclerotic lesion.[233] After antigen presentation, $CD4^+$ activation and subsequent macrophage activation (as described above) leads to larger numbers of foam cells and increased extracellular lipid.[238,239] Matrix metalloproteases (MMPs) secreted from activated macrophages degrade collagen and break down elastin.[240,241] MMPs may also be involved in the proliferation and migration of SMCs.[240] When there is release of inflammatory mediators and growth factors (TGF-β, CTGF, FGF, VEGF) from macrophages, SMC from the media are also activated and transition from a fairly stable contractile phenotype to a more macrophage-like phenotype.[242] Once active, they can also imbibe lipid and proliferate.[243] While proliferating, SMC also increase production of proteoglycan with high binding affinity for LDL.[244] If there is migration to the intima, the intermixing of SMCs and inflammatory cells form a more advanced, intermediate lesion.[245] The robust adaptive response and the

activation of SMCs continues uninhibited, thus results in an advanced plaque containing immune cells, a lipid core, apoptotic cells, cholesterol, new extracellular matrix components, calcification, and a fibrous cap.[242,243,246]

1.16. Donor-Derived Atherosclerosis and Contribution to CAV

Understanding the impact of donor-derived atherosclerosis on CAV should be of great concern. More than ever before, patient waiting lists are getting longer for a very limited pool of donor hearts. As a result, the criteria for suitable donors have been expanded to the point where older donor hearts are being transplanted.[247] The importance of this is that not only can the development of atherosclerosis begin early in life, but the incidence of atherosclerosis increases significantly with age.[248] In the earlier days of heart transplantation, the upper limit for donor age was 35. Now, almost 50 years later, hearts are routinely being used from donors over 40 and occasionally over 50 years old.[249] In Canada alone, the average age of deceased organ donors is 48 years old.[150] The ISHLT guidelines for care of heart transplant recipients (2010) indicate that donor age is an independent, yet, the most consistent risk factor for the onset of atherosclerosis. This compounds the influence of other risk factors, like body mass index (BMI), hypertension, or smoking, for earlier graft failure or death from other causes after transplant.[250,251]

If evidence indicates that the majority of the normal human population has some degree of atherosclerosis in at least one of their major coronary epicardial vessels, then there is an assumption that the majority of donor hearts are being transplanted with a certain amount of atherosclerosis.[204,248] It has also been shown that this atherosclerosis is being transferred to the recipient.[252] An angiographic study in transplant recipients by Gao et al.

described the appearance of AV lesions in the coronary arteries and observed two distinct types.[253] With ethics approval, our laboratory gained access to the Capital District Health Authority (CDHA) heart tissue at the QEII Health Sciences Centre in Halifax to examine tissue from a normal human population. Coronary arteries from 10 patients who died for reasons other than heart failure were examined. Dr. Greg Hirsch assessed the potential donor status of this group of hearts based on medical records. We used the standard pathological criteria for defining arterial stenosis (courtesy Dr. Mathieu Castonguay). In this sample group, 2/10 had mild or no arterial stenosis, 4/10 had moderate stenosis, and 4/10 had severe stenosis (Figure 1.4). All of these individuals met the donor criteria for transplantation. The level of arterial stenosis in the human coronary artery tissue that was examined agrees with that in the literature, indicating that the majority of donors have some degree of stenosis in at least one coronary artery. If it is present in a majority of donors, naturally occurring atherosclerosis is a prominent component of human heart transplant vessels. The combination of a pre-existing atherosclerotic lesion and the growth of the neointimal lesion post-transplant may have significant consequences on long-term graft survival. For this project, a mouse model of transplanted atherosclerosis was incorporated to mimic the clinical setting as closely as possible.

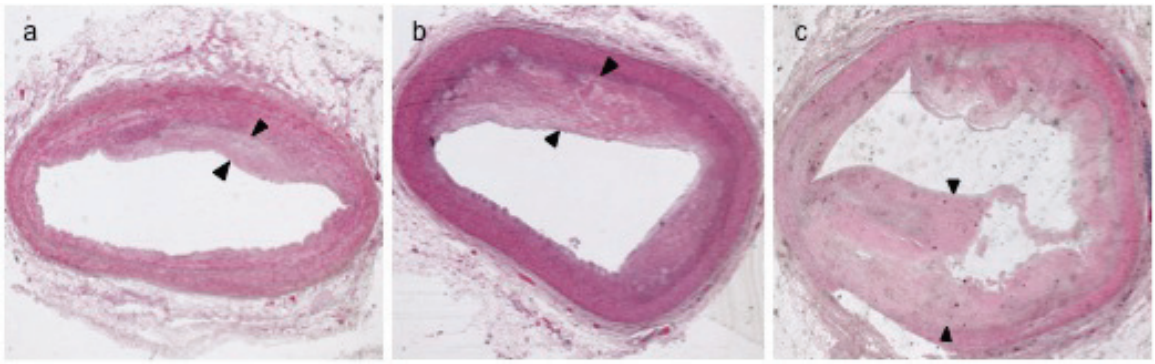

Figure 1.4. Representative images from human epicardial vessels at autopsy. *Panel a, b, and c represent mild, moderate, and severe arterial stenosis, respectively. This group of patients examined (n=10) had died for reasons other than heart failure, and met all donor criteria for transplant. Arrowheads demarcate the inner and outermost edges of the atherosclerotic lesion. Original magnification 2.5x.*

1.17. Apolipoprotein E Knockout Mouse Model of Atherosclerosis

The apolipoprotein E knockout mouse model is well established in the study of atherosclerosis.[254–258] Mice as a species are highly resistant to atherosclerosis development, and induced mutations are necessary for examining atherosclerosis development that is similar to humans.[259] Apolipoproteins in plasma are involved in lipoprotein metabolism. Apolipoprotein E (ApoE) is synthesized primarily in the liver, and is specifically involved in degrading particles rich in cholesterol and triglycerides.[260] It also acts as a ligand for receptors in the liver that clear chylomicrons and VLDL.[260] Due to rapid hepatic LDL clearance, wild-type mice have a completely different lipid profile than humans, with total cholesterol around 85mg/dL, comprised of mostly HDL.[259] Apolipoprotein E knockout (ApoEKO) refers to the targeted ApoE gene inactivation in the mouse that impairs the clearance of lipoproteins in plasma, and renders the mouse hyperlipidemic and hypercholesterolemic.[254] When maintained on a normal chow diet, ApoEKO mice have total plasma cholesterol level of 400mg/dL or greater, facilitating the development of spontaneous atherosclerosis.[261]

An extensive review by Daugherty (2002) compared several transgenic and gene-targeted mice for their similarities to human atherosclerosis development. The ApoEKO mouse has proved to be the most comparable to human in lesion characteristics, cellular components and progression.[262] They also have a similar predilection of site in the aortic tree as the lesions develop. A direct relationship exists between early atherosclerotic lesions that develop in the proximal aorta and lesions that develop in the distal aorta as the mouse ages.[263] Our laboratory confirmed this progression of lesion development throughout the aortic tree over time (between 12-32 weeks) (A. Zaki, unpublished). My

transplant model requires lesion growth in the abdominal aorta, highlighting the significance of using older mice. The second important factor in using older mice is the composition of the lesion. Advanced plaques in mice at 28 weeks of age and beyond have the characteristics most similar to established lesions in human atherosclerosis in size and complexity.[262]

1.18. Hypothesis/Objectives

It is not fully understood whether transmission of donor atherosclerosis will impact patient survival after transplantation. My hypothesis is that donor-derived atherosclerosis contributes to the growing neointimal lesion of AV, and the post-transplant vasculopathy is a combination of donor and recipient elements that creates an inflammatory state of "accelerated" atherosclerosis. The specific objectives of my project are to analyze the morphological changes in the structure of the atherosclerotic lesion at early time points after it is transplanted, and how these early changes might relate to the development of AV. Of particular interest are the changes in atherosclerotic lesion size and composition. The changes observed could provide significant insight into the mechanisms for retention of donor-derived atherosclerosis and the influence it may have on the initiation of AV after transplantation.

CHAPTER 2. MATERIALS AND METHODS

2.1. Aqueous extracts of *Echinacea purpurea*, *Cordyceps sinensis*, and *Heracleum maximum*

An extract comprised of *Echinacea purpurea* aerial parts and roots was prepared and supplied by Factors R&D Inc. (Vancouver, BC). The alkamides, cichoric acid and polysaccharides in this extract were obtained by water/ethanol extraction of various parts of freshly harvested *Echinacea purpurea* plants. Purity of these extracts (>95%) was determined by high-pressure liquid chromatography and UV-visible spectral analysis through published methods. The polysaccharides were precipitated from the extract to create a polysaccharide-enriched aqueous solution via ethanol (EtOH) extraction. Briefly, 5ml of *Echinacea* solution was diluted in 45ml 95% EtOH in a 50ml centrifuge tube. It was mixed vigorously by hand, followed by centrifugation at 500 x g. The eluant was decanted and the pellet was resuspended in 45ml 95% EtOH. This was considered the first wash, and the pellet was washed three times in total. For the last wash the suspension was moved to a pre-weighed petri dish and left to air dry in the laminar flow hood (Labconco, Kansas City, MO). Once the EtOH evaporated, it was weighed again, then resuspended in 5ml ddH_20 and stored at 4°C until use. The total weight of dry polysaccharide in each tube was based on total mg of crude herb in the 50ml bottle. At the time of experimentation, the solution was diluted in sterile RPMI 1640 (ICN Biomedicals; Irvine, CA) supplemented with 100U/ml penicillin, 100µg/ml streptomycin, 10% fetal bovine serum (FBS) (Gibco, Grand Island, NY), and 2g/L sodium bicarbonate

and filter sterilized using 0.22µm filters (Millipore; Bedford, MA) before use. The final working concentrations were 5.6 and 2.8mg/ml.

Our laboratory obtained *Cordyceps sinensis* dried mycelium from Yantai Ruidong Science and Technology Developing Co., Ltd. (China). A sterile aqueous solution was prepared by first grinding 7g of *Cordyceps* to a fine powder using a mortar and pestle. The powder was added to 100ml of sterile, distilled, deionized water (ddH_20) and boiled for 1h. Once the mixture was cooled it was homogenized using a Polytron tissue homogenizer. The homogenate was centrifuged at 200 x g for 15 min at room temperature (RT) to remove course particulates, then further centrifuged at 15000 x g for 10min at 4ºC to remove fine particulates. The remaining homogenate was freeze-dried in pre-weighed 50ml centrifuge tubes. Once completely freeze-dried it was re-weighed and then stored at -20ºC until use. It was reconstituted and diluted in sterile RPMI supplemented with 10% FBS and filter sterilized using 0.22µm filters (Millipore) before use. Final working concentrations were 4 and 6mg/ml.

Hercleum maximum was collected by our collaborator, Dr. Duncan Webster, Dept. of Infectious Disease and Medical Microbiology, Saint John Regional Hospital, Saint John, N.B. and prepared as previously described.[143] Freshly harvested plant roots were air-dried and ground using a Waring commercial blender. Approximately 10g of ground root sample was placed in distilled H_2O (200 ml) and brought to a boil and allowed to simmer for 1.5h. The supernatant was removed and centrifuged at 200 x g for 10min to remove particulates. Ratio for preparation of sample was 1g ground root: 10ml ddH_2O. All samples were filtered sterilized using 0.22µm filters. Each filtrate was divided into 1ml

aliquots and stored at 4ºC until use. Samples were diluted in 10% RPMI and the working concentrations were 1:20, 1:40, and 1:80 of the original aqueous sample.

2.2. Macrophage isolation and culture

Human macrophages were cultured from isolated peripheral blood monocytes. Approximately 100ml of venous blood was collected in heparinized vaccutainers from healthy, tuberculin-negative volunteers by a registered phlebotomist. Blood was diluted with an equal volume of Hank's Buffered Saline Solution (HBSS) (Gibco) containing 2% FBS. Dilute blood was layered on a Ficoll-Paque gradient (Ficoll-Paque Plus, Stem Cell Technologies, Vancouver, BC) and centrifuged at room temperature at 400 x g for 30min with no brake. Peripheral blood mononuclear cells (PBMCs) were collected from the plasma-Ficoll interface layer following centrifugation. The PBMCs were washed three times in HBSS and 2% FBS to remove excess Ficoll, then prepared for the isolation in HBSS containing 2% FBS and 1mM EDTA. Monocytes were isolated from PBMCs by negative selection using a human monocyte enrichment cocktail and magnetic microparticles (EasySep CD14 Human Monocyte Enrichment Kit (StemCell Technologies, Vancouver, B.C.). Cocktail and microbeads were added at a concentration of 50µl per 1ml cells. Isolated monocytes were resuspended in RPMI media with 5% FBS. They were plated in 48-well Nunclon® polypropylene plates (Sigma-Aldrich, St. Louis, MO) at a concentration of $3x10^5$ cells in 500µl per well for 7d. 24h before infection with *Mycobacterium tuberculosis* (*Mtb*), cells were gently washed and wells were filled with antibiotic (Abx)-free RPMI media with 1% FBS in 500µl volume per well. Plates were transferred to the Level III laboratory and incubated for 24h.

2.3. Flow cytometry

Detection and purity of $CD14^+$ monocytes was assessed by flow cytometry, or FACS™ (fluorescence-activated cell sorting). Briefly, cells were resuspended in 5ml polystyrene tubes in staining buffer (PBS containing 1% FBS and 0.09% sodium azide). Non-specific binding was blocked with FITC (fluorescein isothiocyanate)- conjugated mouse IgG2a antibodies (BD Biosciences, Franklin Lakes, NJ) on ice for 10min. Mouse anti-human CD14 antibody (Mo-P9; Stem Cell Technologies, Vancouver, BC) was added to the PBMC and the enriched monocytes for 30min on ice. Cells were then washed and resuspended in PBS containing 1% FBS and 1% formalin for fixation and subsequent analysis on the flow cytometer (BD FACScalibur). Analysis of the cell population was done using CellQuest Software (BD Biosciences).

2.4. Cytospin

Using a Shandon Cytospin 4 cytocentrifuge, (Thermo Scientific, Waltham, MA), pre-labeled silinated slides were inserted into centrifuge funnels. The funnels were prepared for the addition of cells using 20µl cushion of PBS. $1x10^6$/ml monocytes were collected after enrichment and resuspended in a total volume of 1ml sterile PBS. A total volume of 75µl of cells was added to each funnel. Once the spin cycle was complete, the slides were removed from the funnels and left to air dry. The cells were then fixed with Giemsa solution (Sigma-Aldrich Co., Saint Louis, MI) and visualized for nuclear morphology.

2.5. *Ex vivo* intracellular infection

The intracellular bacteria *Mtb* H37Rv (ATCC) stock culture was kindly provided by Dr. David Haldane, Director of Bacteriology and Special Pathogens, QEII Health Sciences Centre, Halifax, N.S. The stock culture of *Mtb* H37Ra was provided by Dr. Webster at the Saint John Regional Hospital. Stocks of *Mtb* were stored at -70°C, and at the time of the experiment, a 7ml Mycobacterial Growth Indicator Tube (MGIT) Becton Dickinson Biosciences, Cockeysville, MD) containing Middlebrook 7H9 broth (VWR, Radnor, PA) was supplemented with 800µl PANTA (BD Biosciences) and 0.05% Tween 80 (Biorad Laboratories, Hercules, CA). A heavy suspension of *Mtb* H37Ra or H37Rv was added to the tube and incubated until the culture had grown to mid-exponential phase, with a viable count of approximately $3x10^7$- $5x10^7$ *Mtb*/ml, approximately 7d.[144] For inoculation of human macrophages, a 0.5 McFarland was attained (10^7-10^8 *Mtb* per ml) on the nephlometer (ATB 1500, Biomérieux, Marcy L'Étoile, France) after the MGIT reached mid-exponential growth phase. On Day 0 the MGIT was centrifuged at 300 x g for 10min. The *Mtb* suspension was transferred to a snap-cap tube and then sonicated for 30sec and placed in the nephlometer. Here either more suspension or more MGIT broth was added to reach a final concentration of 0.5 McFarland. 4ml of the 0.5 McFarland suspension was added to 16ml RPMI supplemented with 0.05% Tween80 and PANTA to dilute to 1:5. This achieved a working concentration of 10^6-10^7 *Mtb*/ml. The final multiplicity of infection (MOI) was between 13-16 for the duration of the experiments.

Existing media was carefully removed from the plate wells and 800µl of inoculum was added. The plates were returned to the incubator for 6h to allow for incorporation of *Mtb* into the cells.[145] After 6h the wells were washed two times with RPMI-10. *Cordyceps*, *Echinacea*, or *Heracleum* treatments were added to the wells with 2U/ml interferon

gamma (IFN-γ) (recombinant human IFN-γ (Sigma-Aldrich Co.). Negative control wells contained media alone, and positive control wells contained 2U/ml IFN-γ. Plates were returned to incubator. After 7d incubation, wells were washed with serum-free, antibiotic-free RPMI. After the third wash the media was removed and the cells were lysed with 100µl of 0.25M NaOH for 15min. A 10µl loop of lysate was plated on Middlebrook 7H9 agar plates. The plates were incubated for 3wk at 37°C. After 3wk the colony forming units (CFU) were counted and recorded for analysis.

2.6. Statistics

This experiment was performed a total of seven times. The data shown are the results of three successful experiments. Statistical significance was determined by the Kruskal-Wallis analysis of variance by ranks for non-parametric data using GraphPad Prism 5 statistical software (GraphPad Software Inc., La Jolla, CA). The Dunn's post-test was applied for multiple comparisons. P values of <0.05 were considered to be significant.

2.7. Animals

Male 30-32wk old Apolipoprotein E knockout mice on a C57BL/6 background (B6.129P2-^{Apoetm1Unc}/J (B6 ApoEKO; H-2^{b}) with naturally occurring atherosclerotic lesions were used as donors. Male 8-10wk old C3H/HeJ mice were used as recipients. All mice were purchased from Jackson Laboratories (Bar Harbour, ME) and maintained in the Carleton Animal Care Facility at the Sir Charles Tupper Medical Building at Dalhousie University in a specific pathogen free environment. Mice were fed a standard chow diet and water *ad libitum*. All animal experiments were performed in compliance with the guidelines of the Canadian Council on Animal Care.

2.8. Aortic transplantation

Abdominal aortic segments were transplanted as our laboratory has previously described.[264] Briefly, B6 ApoEKO aortic segments were examined by an operating microscope (Zeiss). Those identified as containing a single, focal, eccentric atherosclerotic lesion were used for transplantation. A section containing a suitable lesion was harvested and flushed with saline for transplant into the recipient. The 1mm section was kept in cold saline until transplant, with a cold ischemic time of 20min or less. The recipient (C3H) infrarenal abdominal aorta was isolated and, after clamping of the proximal and distal areas, the recipient aorta was transacted. The donor aorta with lesion was then interposed with end-to-end anastamoses using an 11-0 suture in an interrupted fashion. The clamps were removed and blood flow was re-established.

2.9. Immunosuppression

Cyclosporine (CyA; Sandimmune i.v.^{TM}) was purchased from the QEII Health Sciences Centre Pharmacy, Halifax, NS and diluted in 0.9% sterile saline to obtain the desired concentration. Aortic allograft recipient mice were treated subcutaneously with 50mg/kg/day CyA for the duration of each experiment. This dose has previously been shown to be sufficient to ablate acute cardiac rejection.

2.10. Histology

Aortas were harvested at 1d, 4d, and 7d post-transplantation, and there were 4 animals per group. Aortic graft segments were flushed with heparinised saline and fixed in 10% formalin at 4ºC for 18-24h. Grafts were subsequently transferred to phosphate buffered saline (PBS) for 1-2h and then transferred into 70% ethanol (EtOH) until processing.

Samples were embedded in paraffin and 5µm cross-sections were sectioned with a Leica microtome (Wetzlar, Germany). Sections were deparaffinxed in xylene, hydrated through an ethanol series, and stained with Harris' Hematoxylin and 0.5% Eosin (H&E) for general histology and digital assisted morphometric analysis.

2.11. Calculation of lesion area /volume

Atherosclerotic lesions were measured *in situ* with a Pelco micro-ruler (Redding, CA). Once the outer lesion area was measured the lesions were excised and fixed for sectioning. The paraffin embedded lesions were sectioned on a Leica microtome. Serial 5µm sections of the entire lesion were prepared and processed for H&E, as above. Every 5^{th} section of the lesion was measured for area using the Microbrightfield Stereo Investigator, Neurolucida Software Version 7, MBF Bioscience (Williston, VT) and an Olympus BMAX microscope. Images of histological sections were captured using a Zeiss Axiocam camera (Zeiss, Thornwood, NY).

2.12. Immunohistochemistry

To visualize alpha-actin positive SMC, paraffin sections were deparaffinised in xylene, hydrated through an EtOH series, washed in 0.1M PBS and antigen retrieval was performed. Endogenous peroxidase was quenched with a 20min incubation in 3% hydrogen peroxide in 0.1M PBS. Non-specific blocking was performed with horse serum specific to the secondary antibody used (Vector Laboratories, Burlingame, CA). The primary antibody was a monoclonal anti-mouse alpha-SMA (1:2000, Sigma; Saint Louis, MO). Primary antibody was detected with the appropriate biotinylated secondary antibody (horse anti-mouse BA-2001, Vector Labs Inc). Sections were then washed in

PBS and incubated with a peroxidase avidin/biotin complex kit (Vector Labs Inc). One drop of 3,3'-diaminobenzidine (DAB; Dako, Mississauga, ON) in 1ml of substrate buffer was used as the chromogen. Sections were counterstained with Mayer's Hematoxylin, dehydrated and coverslipped with mounting media Cytoseal 60 (Thermo Scientific).

2.13. Transmission Electron Microscopy (TEM)

Aortic graft segments were fixed with 2.5% glutaraldehyde in 0.1M sodium cacodylate buffer and post-fixed with 1% osmium tetroxide. After washing, the segments were incubated in 0.25-0.5% uranyl acetate, rinsed and dehydrated through acetone. Segments were embedded in epon-araldite resin and sectioned using an ultramictrotome (Reichert Jung Ultracut E) with a diamond knife. Sections were stained with lead citrate and uranyl acetate before examination on a JOEL 1230 transmission electron microscope at an accelerating voltage of 80kV. Digital images were captured using a CCD digital camera.

CHAPTER 3. RESULTS

3.1. Natural health products for enhancement of innate immunity against intracellular infection (Project 1)

Mycobacterium tuberculosis (*Mtb*) is an intracellular pathogen that resides within macrophages. Upon cell activation, cytokines and antimicrobial mediators such as TNF, NO, and SO^- are able to control most of the infection until adaptive immunity is triggered and there is a sustained DTH reaction. In healthy persons, the production of IFN-γ by Th1 cells is critical for the macrophage response that contains *Mtb*-infected cells in a granuloma. However, the Th1-IFN-γ-TNF axis is interrupted when an individual is immunocompromised, especially in the case of HIV co-infection, leading to reactivation and fulminant TB infection.

In this pilot project aqueous extracts of *Echinacea purpurea (Ep), Cordyceps sinensis (Cs)*, or *Heracleum maximum (Hm)*, were examined to see if they could enhance the activity of IFN-γ-driven responses in *Mtb*-infected human macrophages. Monocytes were first isolated from whole blood using a human $CD14^+$ monocyte enrichment kit. The kit contained antibodies directed against CD2, CD3, CD16, CD19, CD20, CD56, CD66b, and CD123, and the resulting monocyte population was preserved. To determine the purity of the isolated cell population, flow cytometry was performed (Figure 3.1). FITC-labeled mouse anti-human IgG2a antibodies were used for the isotype control. FITC-labeled mouse anti-human CD14 antibody was added to the PBMC before and after enrichment. Figure 3.1 shows 11.6% of the PBMC were positive for CD14 before enrichment. After enrichment, we achieved monocyte purity between 73% (shown) and

91% over the course of experimentation (purity increased over the duration of the experimentation). A cytospin was performed on the isolated cells (Figure 3.2) to confirm the enrichment of the monocyte population from the initial the PBMC. The contaminating population was primarily lymphocytes and neutrophils.

3.1.1. *Echinacea purpurea* does not limit or reduce *Mtb* colonies *ex vivo*

Freshly isolated human monocytes were grown and plated in media for 7d. The transitioned macrophages were then infected with *Mtb* H37Rv. They were treated 6h later with IFN-γ (2U/ml) alone, or with IFN-γ as well as an aqueous extract of *Ep* at two different dilutions. After 7d the cells were lysed and the lysates were plated and incubated a further 3wk. Figure 3.3 shows the CFU from the lysates of the *Mtb*-infected macrophages after treatment. The cultures that received no treatment with IFN-γ or test agent showed CFU ranging from 12-110. This was our control for bacterial growth without the addition of IFN-γ. This data reveal that there is a wide variation in CFU using this technique and that this variation is likely to negatively affect statistical analysis of future results. The cultures that received IFN-γ alone showed CFU ranging from 0-3 over the six plates that were counted. This data shows that, at this dose, *Mtb* growth was completely ablated. Surprisingly, when aqueous extracts of *Ep* were added along with the IFN-γ bacterial growth was restored to a certain extent ($p<0.05$). At a concentration of 5.6mg/ml, CFU ranging range between 0-180 CFU were observed. At an *Ep* concentration of 2.8mg/ml a similar effect was seen. Thus, the addition of *Ep* at 5.6 or 2.8mg/ml to the IFN-γ treatment reduced the bactericidal effect of the IFN-γ rather than enhancing it, as had been expected.

3.1.2. *Cordyceps sinensis* does not limit or reduce *Mtb* colony growth *ex vivo*

The second agent to be tested was *Cs*. Macrophages were infected as described above. At 6h post-infection they were treated with two concentrations of an aqueous extract of *Cs*, at 6mg or 4mg/ml, again with the addition of the standard dose of IFN-γ at 2U/ml. Insufficient numbers of human monocytes were obtained from the purification to include a no treatment control group in this pilot experiment. CFU were counted 3wk after infection and treatment. The results are shown in Figure 3.4. As with *Ep*, treatment with *Cs* appeared to restore bacterial growth. As above, cultures treated with IFN-γ alone showed nearly completely abated growth. In contrast, the addition of *Cs* to the IFN-γ treatment resulted in substantial bacterial growth in the cultures, suggesting it was inhibiting the bactericidal effect of IFN-γ.

3.1.3. *Heracleum maximum* does not limit or reduce *Mtb* colonies *ex vivo*

The third agent to be tested was *Hm*. Macrophages were infected as described above. At 6h post-infection IFN-γ (2U/ml) alone, or along with an aqueous extract of *Hm* was added to infected macrophages. As noted in the *Cs* experiment above, there were an insufficient number of purified monocytes available to include a no treatment group in this pilot experiment. CFU were counted 3wk after infection and treatment. The results are shown in Figure 3.5. As seen in the earlier figures, IFN-γ was effective at limiting bacterial growth. The data arising from the *Hm* treated groups (all with IFN-γ as well) were surprising. At the highest concentration of the extract, bacterial growth was seen to be limited at least as much as with the IFN-γ alone. Although the data for this group shows a mean CFU that is lower than the IFN-γ alone, this did not reach statistical

significance. In contrast, at lower concentrations (higher dilutions) CFU counts were significantly ($p<0.05$) higher than CFU resulting from cultures of IFN-γ alone. Both 1:40 and 1:80 dilutions showed this effect with the 1:80 dilution being the most marked.

3.2. Changes in the atherosclerotic lesion after transplantation

3.2.1. Quantification of change in atherosclerotic lesion volume after transplant is not possible based on outer lesion area before transplant.

In our assessment of the fate of the atherosclerotic lesion after transplant, we first examined whether the gross size of the lesion increased, stayed the same or decreased after transplantation. Since we could not measure the internal volume of the lesion directly we assessed whether a readily available parameter could be used as a correlate for lesion size. Since lesions can be visualized from the outer layer of the aortic segment we examined whether the lesion area visible at the outer surface could be used as a surrogate for the internal lesion volume.

To find out whether this was possible we first started with 10 control ApoEKO mice with advanced atherosclerotic lesions. In this control group of non-transplanted lesions, the outer lesion area of the aortic lesions were measured *in situ* with a micro-ruler (Figure 7.1). These dimensions were used to determine outer lesion area, assuming a basic ellipse shape (area of ellipse= pi* ½ a^2*b^2). The same group of lesions were then removed, formalin fixed, embedded in paraffin, and processed for histology. Once processed they were serial sectioned which allowed for calculation of area for each 5μm section. Using the area measurements from all of the serial sections morphometric analysis was

performed to determine the **actual volume** of the control lesions (using Neurolucida image analysis software). Subsequently, a ratio was calculated between the outer lesion area and the actual volume (Neurolucida data). The average of these ratios was multiplied by outer lesion area to produce a **predicted volume** (Table 7.1).

The data in Table 3.1 clearly illustrate there is enormous variability in the ratio between outer lesion area and actual volume. The ratio, which was hoped to be relatively constant, varied between 27:1 and 113:1. Thus, when the average ratio is used to calculate a predicted internal lesion volume, the calculated volume is highly variable. Figure 3.7 shows the actual volume versus predicted volume compared to an ideal correlation line. In this figure error bars were artificially added that represent a 30% threshold (above and below the measured data) because we predicted that a variation up to 30% in the fit to the correlation line might be acceptable for the purposes of this study. Even with this assessment predicted and actual volume were within the threshold for only 3/10 lesions.

Further examination of the sections showed that the reason for this large variation is that the shape of the internal lesions varied dramatically among samples. A roughly elliptical shape was predicted for the internal lesion along the length of the involved area. As shown in Figure 3.8, this was not the case. The shape of the internal lesions in these samples (as determined by their accumulated volume over length by the software) varied widely. In this figure, CL4 and CL5 show roughly elliptical lesion shapes over the length of the lesion as we had hoped, but CL1 and CL3 show two peaks of lesion, indicating that the lesion in these samples is uneven.

Based on the predicted versus actual volume in this group of control ApoEKO lesions, it was determined that it is not possible to establish a correlate between predicted volume and actual volume based on this method of calculating lesion area. This meant that we had no way of measuring a reduction in volume over time post transplant in these lesions.

3.2.2. Atherosclerotic lesion remodeling is initiated early, but not immediately, post-transplant.

3.2.2.1. control "pre-transplant" atherosclerotic lesion

To examine the fate of the lesions in a direct way, we examined the atherosclerotic lesions at various times after transplantation for evidence of morphological changes. We accomplished this by standard histology, by immunohistochemistry and by TEM. Initially we characterized native C3H aortas by histology and TEM as controls. Figure 3.9 shows representative H&E cross sections showing the three layers of the normal, non-lesioned aorta. The intima is the innermost layer to the lumen that includes the internal elastic lamina (IEL) and a single layer of endothelial cells. The media (M) contains several layers of elastin and is populated by smooth muscle cells. The adventitia (A) is the outermost layer and is mostly comprised of connective tissue. The TEM micrograph shows the IEL and underlying elastic layers, with very closely associated SMC nuclei and SMC bodies, endothelial cell nuclei and cell bodies, and surrounding ground substance.

The lesioned aortas were examined next. The atherosclerotic lesion in an ApoEKO mouse closely resembles that of a human lesion, in both composition and complexity. In Figure 3.10 the micrographs represent what was observed in the untransplanted ApoEKO control group (n=4). The H&E sections show the contrast between the involved and uninvolved

area. In the uninvolved area, all three layers of the aorta look similar to the normal aorta in Figure 3.9. The endothelial cell nuclei are visible in the intima and there are layers of elastin heavily populated with SMC. In the involved area, there are pockets of foam cells and possibly lipid-laden SMC. The extracellular lipid resides in the more luminal areas of the lesion, while the cholesterol clefts are found in the deeper layers. The elastin layers in the media are often fractured accompanied by more disrupted areas of SMC. The adventitia consistently shows cellular infiltration, indicating an immune contribution to the atherosclerotic lesion formation. Panel (c) of this figure shows an alpha-SMA stain of the same control lesion and the distribution of the SMC, indicating that this lesion is at an advanced stage where the fibrous cap has already formed. It also shows the presence of SMC in the intima as well. The TEM micrograph of the control lesion (d) clearly demonstrates lipid droplets in the foamy macrophages in the lesions and a distinct layer of endothelial cells overlaying the atherosclerotic lesion. The IEL is not present in this micrograph since the foamy macrophages overlay the IEL to such an extent that it is not visible. In the TEM, a distinct IEL could be visualized below the atherosclerotic lesion (data not shown), but for the most part the lesions were too large to capture in their entirety. Note in this micrograph that the lipid bearing cells appear to be quite homogeneous and appear to have a particular orientation. There are varying degrees of electron density in the lipid at this point.

3.2.2.2. 1 day post-transplant

By 1d post transplant there are significant changes to this pre-transplant picture. Figure 3.11 (a-f) shows representative histological images from the 1d group of animals post-transplant. There is complete loss of endothelium at this time point (a-b). This is not

unexpected given earlier data from us, and others, that IRI severely damages the endothelial layer. IRI has also initiated as significant neutrophil response as evidenced by the significant influx of neutrophils and mononuclear leukocytes into the adventitia. In these samples we saw neutrophils in the adventitia of all sections and a varying degree of neutrophils in the media (c). In the areas of the media where there is neutrophil influx, there is accompanying loss of SMC (d-e). The most unexpected observation at this point is that there is no neutrophil influx or neutrophil accumulation in the lesion (f). It is worth noting that at the suture sites there is some compression of the elastic layers and SMC loss in those areas, but it is still possible to observe the composition of the aorta independent of those areas.

The distribution of alpha-SMA positive cells in and around the lesion is shown in Figure 3.12. As expected, the media remains positively stained but not the lipid core. The darkly stained outer rim of the lesion, indicating the presence of a fibrous cap characteristic of an advanced lesion, would further suggest that the lesion remains intact at 1d despite the insult of IRI. Figure 3.13 shows representative images of the 1d group at high magnification (TEM). Here the endothelium is very clearly gone, and there is significant platelet deposition (a-b). Foam cells appear to comprise the outermost areas of the lesion and line up in an orientation very similar to that seen in the pre-transplant sample (c). The lipid-bearing cells compared to the control look normal, and again, there is no cellular infiltration, which corresponds with what was seen in the histology images at this time point (d).

3.2.2.3. 4 days post-transplant

Figure 3.14 shows by 4 days post transplant it is clear that there is continued loss of SMC from the media (a). The predominance of neutrophil accumulation has given way to an influx of macrophages by 4d post-transplant, and numerous neutrophils can now only be seen in small clusters around the sutures in a typical suture reaction response (b). The higher magnification of the lesion and the SMC-actin staining reveals a loss of positively-stained cells around the cap region of the lesion, but the lesion itself still appears very cellular with numerous SMCs and macrophages (c-d). The media is still very positively stained in the uninvolved area. Most importantly, the lesion looks similarly unaffected as it did at 1d post-transplant.

The TEM images (Figure 3.15 a-f) reveal a more complete story of what is happening to these lesions, as it would seem at this point the changes are too subtle to be easily recognized by standard histology. The TEM images reveal that platelet deposition is still present (a-b). Lipid bearing macrophages can still be easily identified within the lesion but they look dissimilar from the lipid-bearing macrophages seen at 1d or in the control animals. The cells have lost the characteristic orientation that was seen in the control lesions and the lesions at 1d post transplant (c-d). There appears to be more ground substance between the cells and the lesion is, in general becoming disorganized. These data suggest that at 4d post-transplant the lesion is beginning to suffer negative effects of transplantation. Note that although these subtle changes can be seen, there is still no

neutrophil or mononuclear cell infiltration of the lesion. The lesion at this point seems to be protected from infiltration.

3.2.2.4. 7 days post-transplant

By 7d post transplant there is evidence of a inflammatory response in the adventitia, indicated by the heavy presence of macrophages, lymphocytes, and in some areas, eosinophils (Figure 3.16). The media is now being aggressively attacked by a second wave of neutrophils (a) and potentially migrating toward the intima. A fibrotic response has begun in the adventitia as well, indicated by the presence of oriented fibroblastic cells. The H&E also reveals some evidence of apoptosis in the media and adventitia. Endothelial cell replacement has further progressed. Surprisingly, even in this second wave of inflammatory cell infiltrate, the atherosclerotic lesion still appears minimally affected. Lipid bearing macrophages still appear to constitute the majority of the lesion (b). The alpha-SMA stain appears consistent with the H&E images, and clearly shows the presence of the fibrous cap that remains even 7d later.

Again, examination by TEM shows subtle changes are ongoing in the lesion that are morphologically unrelated to the changes going on around it (Figure 3.17). The TEM micrograph reveals that re-endothelialization has not fully taken place and there are still large areas covered in platelets (a). In the cases where lipid is seen in the cells, the droplet size appears much smaller (b). The phenotype of the cells in the atherosclerotic lesion have changed to such an extent that they are barely recognizable as the cells that were in the lesion in the first place, or may very well be not the same cells (c). They have lost the original orientation, they no longer appear to have cell-to-cell communication, there are

very large areas of intercellular ground substance, and few have intracellular lipid remaining. The cellular infiltrate in the adventitia, consisting of a large number of neutrophils, is shown in (d). Of interest is that the lesion is still populated with cells and does not show extensive areas of cell death. This suggests that the cell phenotype has either changed or the cells have been replaced. Infiltration of neutrophils and inflammatory mononuclear cells in the lesion does not seem to have occurred on a large scale. This suggests again that the processes ongoing in the lesion are dramatic but are different than the processes ongoing in the rest of the vessel. A flow chart depicting the summary of events that are occurring in the first 7d are displayed in Figure 3.18.

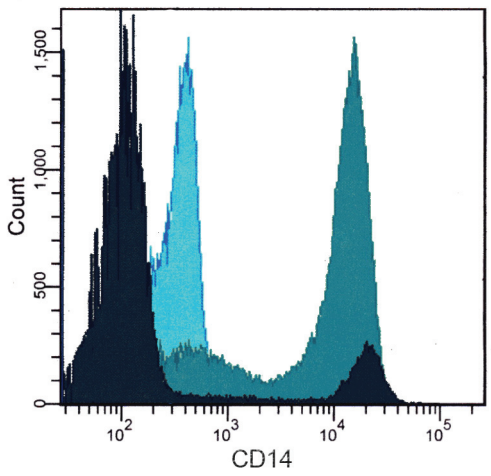

Figure 3.1. Characterization of CD14$^+$ monocytes by flow cytometry from freshly isolated peripheral blood mononuclear cells (PBMC). This figure shows composite histogram of fluorescence intensity in the isotype control (in blue) (FITC-labeled mouse anti-human IgG) and the PBMC population before enrichment (in black) with the addition of FITC-labeled CD14$^+$ antibody. The fluorescence of the CD14$^+$ monocyte population after enrichment is shown in dark green.

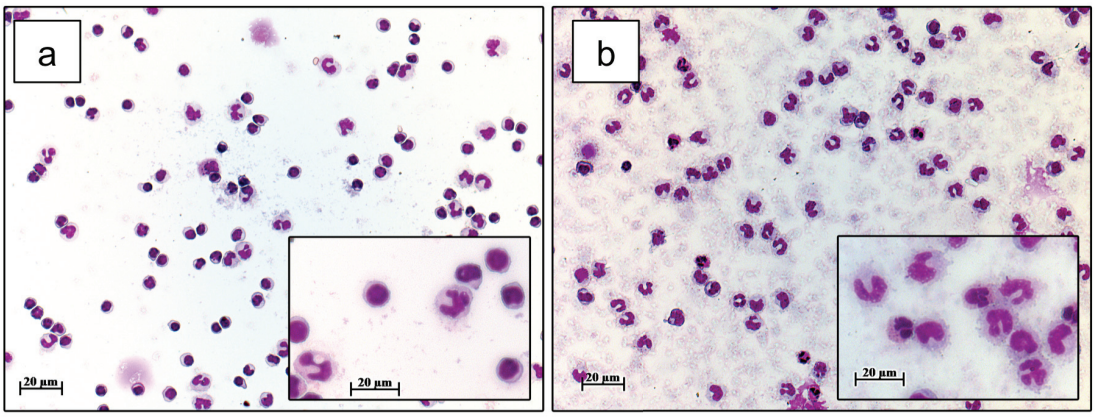

Figure 3.2. Monocyte purity before (a) and after (b) $CD14^+$ enrichment via negative selection. Cells were visualized after being fixed with Giemsa solution. The panel on the left shows PBMCs before negative selection. The right panel shows monocytes visualized after enrichment (Giemsa stain; 75,000 cells/ml).

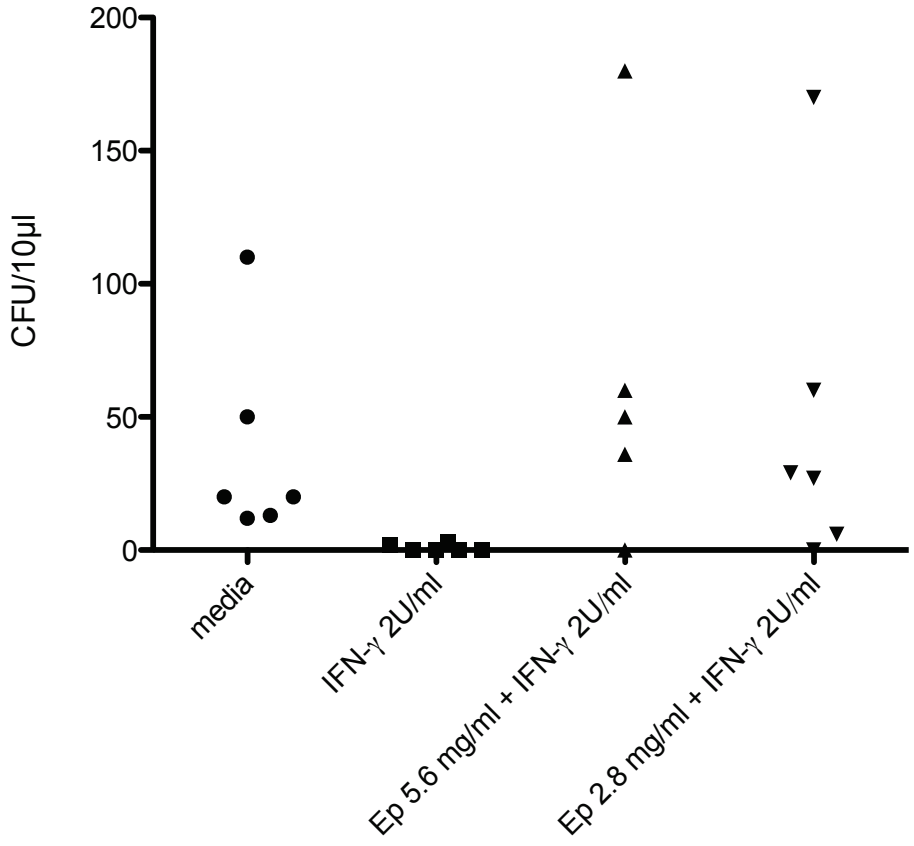

Figure 3.3. Treatment of *Mtb*-infected human macrophages with *Echinacea purpurea (Ep)* + low level IFN-γ did not limit colony growth compared to the media control. Human macrophages were infected with *Mtb* H37Rv (MOI= 13.3) and treated with media, media+ 2U/ml IFN-γ, 5.6mg/ml or 2.8mg/ml *Ep* and 2U/ml IFN-γ. Shown are the colony forming units (CFU)/10µl 3wk after cell lysis.

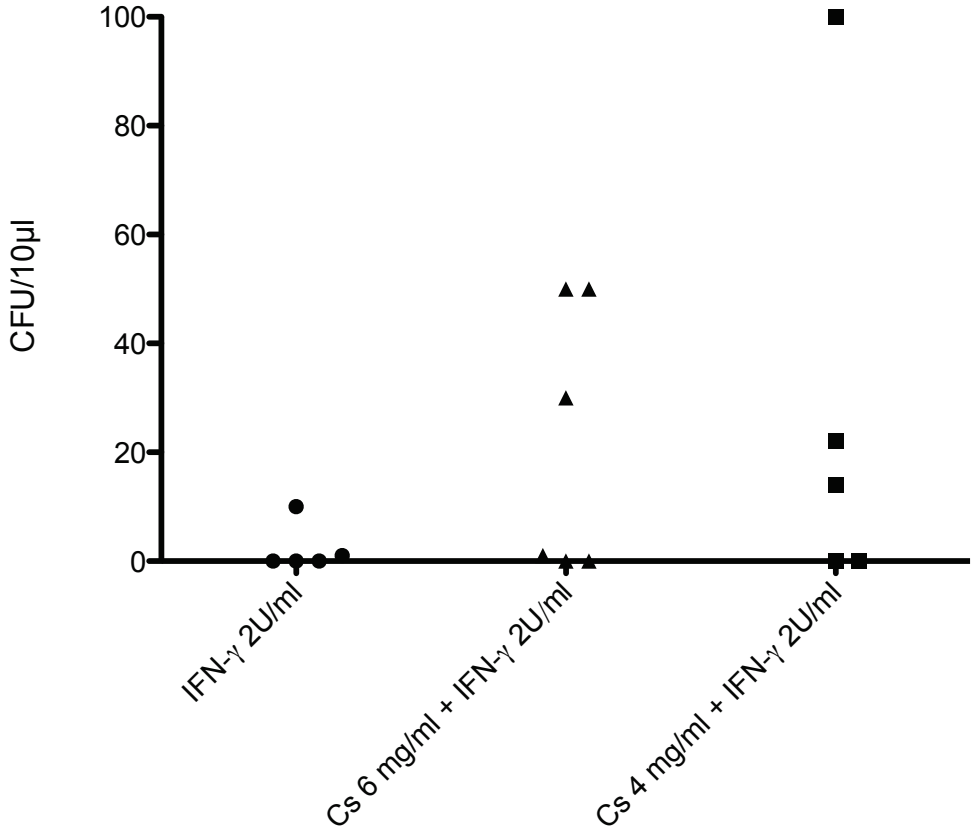

Figure 3.4. Treatment with *Cordyceps sinensis (Cs)* + low level IFN-γ did not limit colony growth in *Mtb*-infected human macrophages compared to the IFN-γ control. Human macrophages were infected with *Mtb* H37Ra (MOI=16) and after 6h treated with 2U/ml IFN-γ and 4 or 6mg/ml *Cs* with 2U/ml IFN-γ. Shown are CFU/10µl 3 weeks after cell lysis.

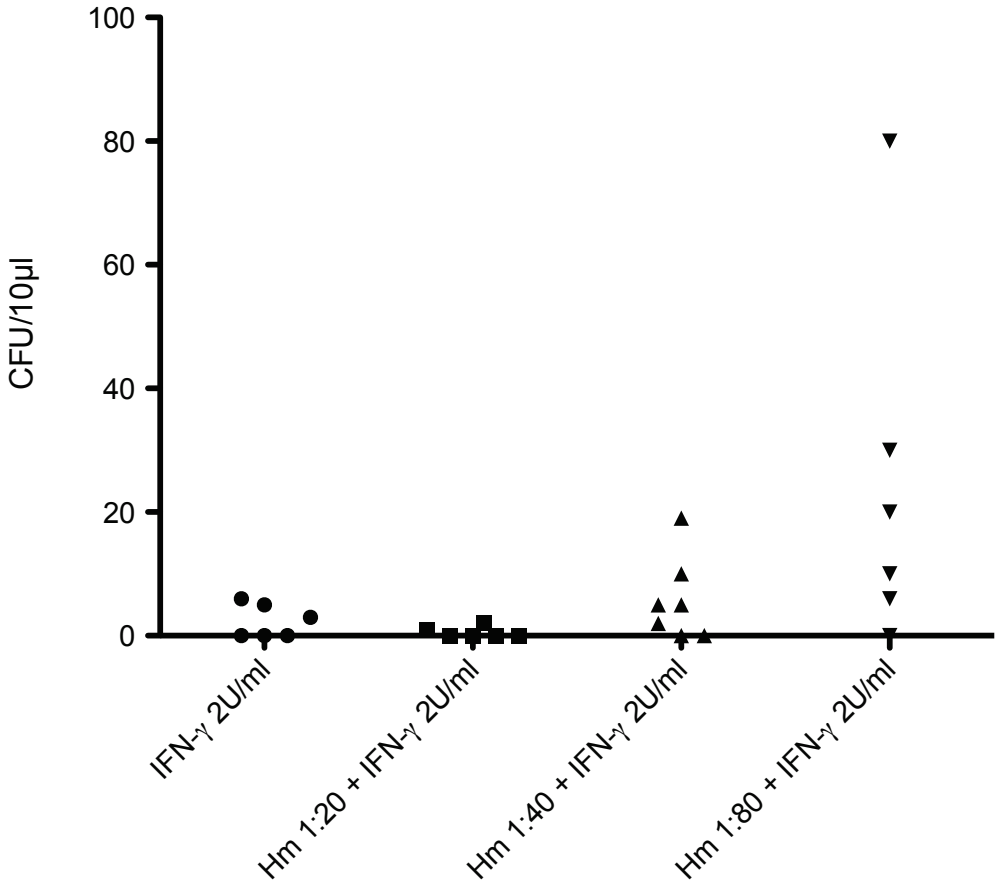

Figure 3.5. Treatment of human macrophages with *Heracleum maximum (Hm)* + low level IFN-γ did not limit colony growth compared to the IFN-γ control. Human macrophages infected with *Mtb* H37Ra (MOI=13.3) were treated with doubling dilutions of *Hm*. Shown are the CFU/10µl 3wk after cell lysis.

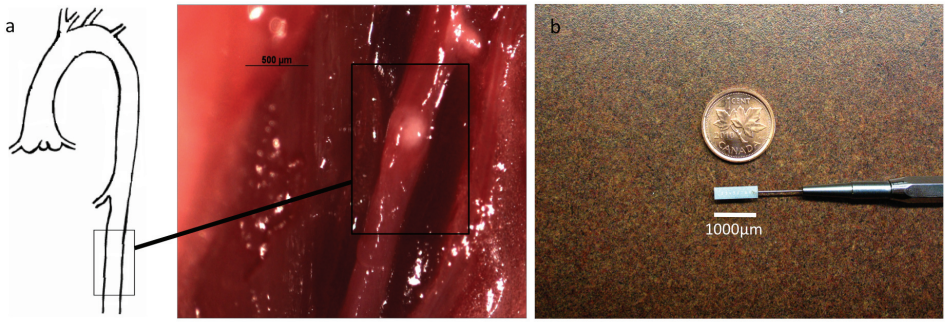

Figure 3.6. Abdominal aorta from ApoEKO mouse bearing a lesion suitable for transplant (a). Lesions were measured *in situ* with a micro-ruler (seen in panel (b) compared to the size of a penny) before harvesting. The micro-ruler was able to measure the outer lesion area under the view of the light microscope to the nearest 50µm.

ID	*Ruler LD (um)*	*Ruler SD (um)*	*Outer Lesion Area (um2)*	*Actual V (um3)*	*Ratio (Actual V: outer lesion area)*	*Predicted V (um3)*
CL1	550	500	215984.5	6,234,030	28.9	12,307,056
CL2	700	700	384845.1	31,703,700	82.4	24,121,830
CL3	500	400	157079.6	11,686,600	74.4	9,845,645
CL4	400	300	94247.8	2,934,530	31.1	5,907,387
CL5	500	300	117809.7	10,757,900	91.3	7,384,234
CL6	550	450	194386.0	8,220,960	42.3	12,183,986
CL7	800	450	282743.3	18,407,600	65.1	17,722,161
CL8	700	450	247400.4	27,973,700	113.1	15,506,891
CL9	300	200	47123.9	1,279,460	27.2	2,953,694
CL10	550	500	215984.5	14,729,000	68.2	13,537,762
					62.4	

Table 3.1. Predicted volume versus actual volume of aortic segments from Apolipoprotein E knockout mouse (ApoEKO) mice bearing an atherosclerotic lesion (n=10). CL= control lesion. LD= long diameter. SD= short diameter. V= volume. The average ratio (62.4) was multiplied by the outer lesion area to calculate a predicted volume for each lesion.

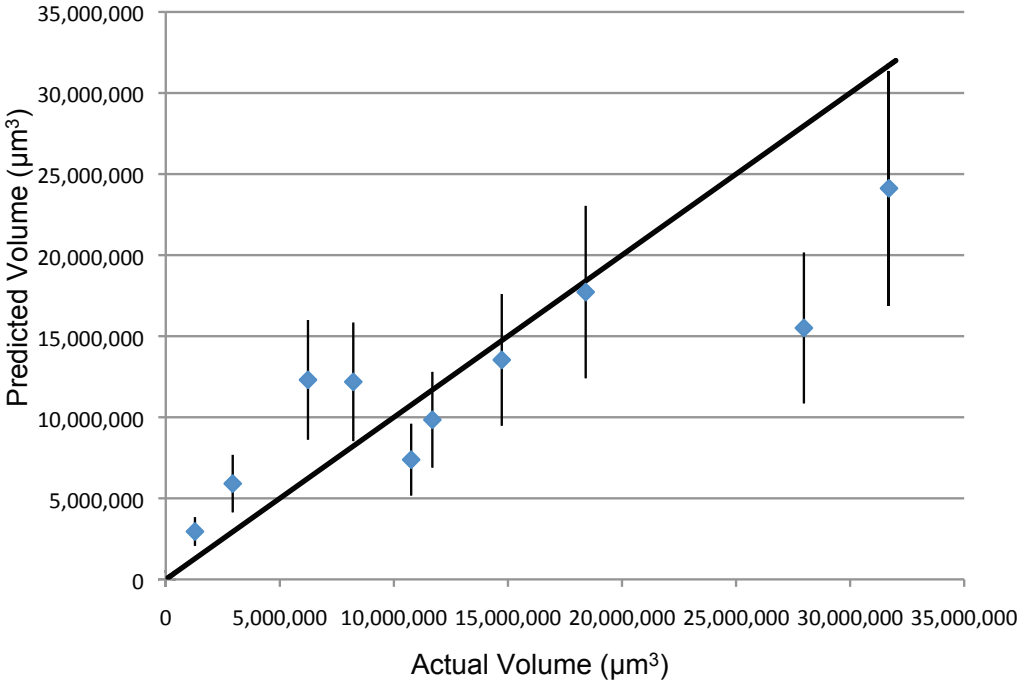

Figure 3.7. Correlation between predicted volume and actual volume using the calculations shown in Table 7.1. The correlation was plotted for each animal and compared to an ideal fit line. Data are accompanied by an artificial 30% threshold to see whether the data lies within a 30% variation of the ideal fit. Only 3/10 of the control atherosclerotic lesions crossed the ideal fit line even with this 30% threshold added (n=10).

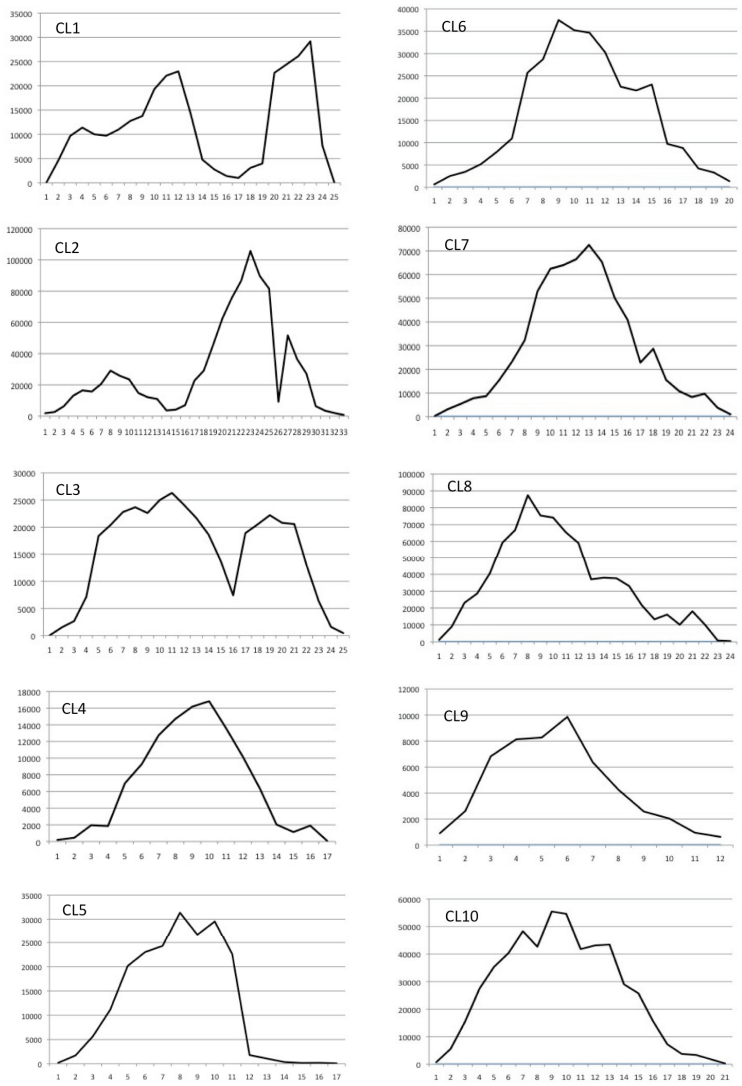

Figure 3.8. ApoEKO assessment of internal lesion shape by Neurolucida. These images were built from the volumes of the individual serial sections. Internal lesion volume was calculated from the area of each serial section x 5µm section. X axis=serial section from which a contour was measured (from the beginning to end of each lesion). Y axis= area (μm^2). CL= control lesion. Note scale and area vary between each lesion, so they are not relative in size to one another.

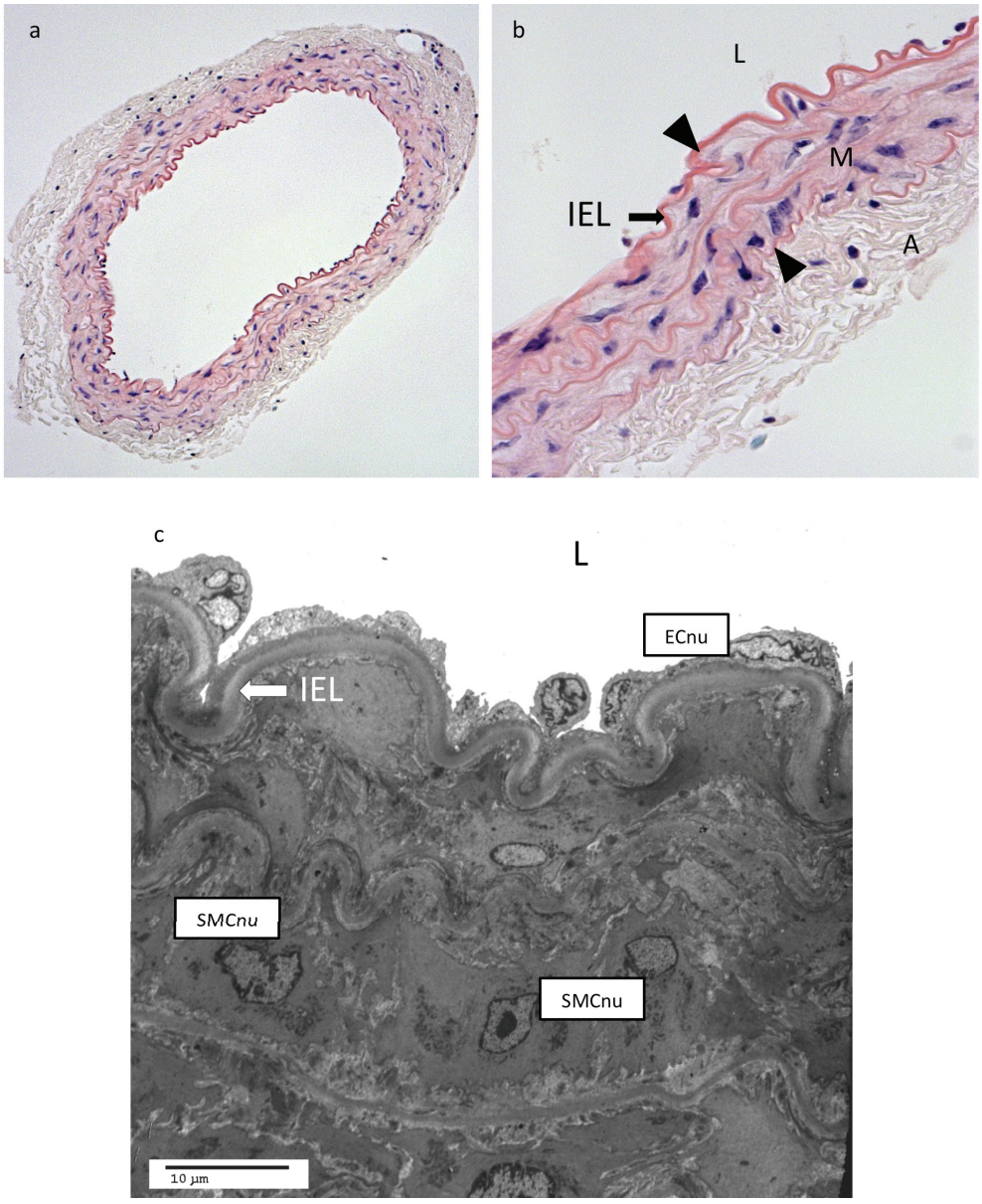

Figure 3.9. Representative cross sections of native C3H mouse aorta. Panel a and b show histological examination. In panel b the media (M) is demarcated by arrowheads. A=adventitia. IEL= internal elastic lamina. L=lumen. Panel c shows similar C3H aorta by TEM. SMCnu= smooth muscle cell nucleus. ECnu= endothelial cell nucleus.

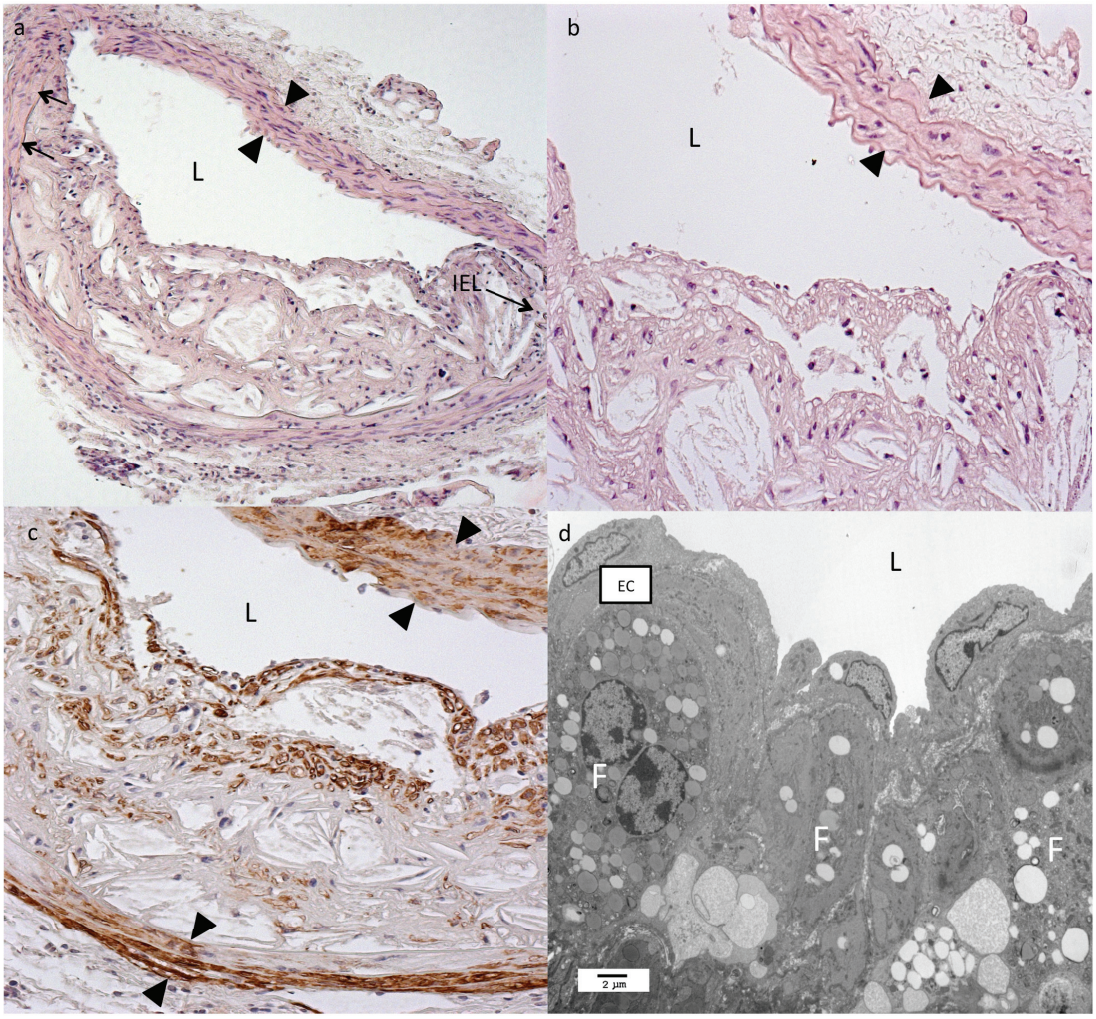

Figure 3.10. Representative cross sections of ApoEKO mice bearing an atherosclerotic lesion before transplant. Panel a and b show histological examination at low and high magnification, respectively. Infiltrating cells, cholesterol clefts, foam cells, intracellular and extracellular lipid, and ECM all comprise the atherosclerotic lesion. Panel c shows distribution of alpha-smooth muscle actin (alpha-SMA) positive cells. Panel d shows TEM micrograph of lesion. Arrowheads demarcate the media. Arrows indicate IEL. EC=endothelial cell. F= foam cell. L=lumen.

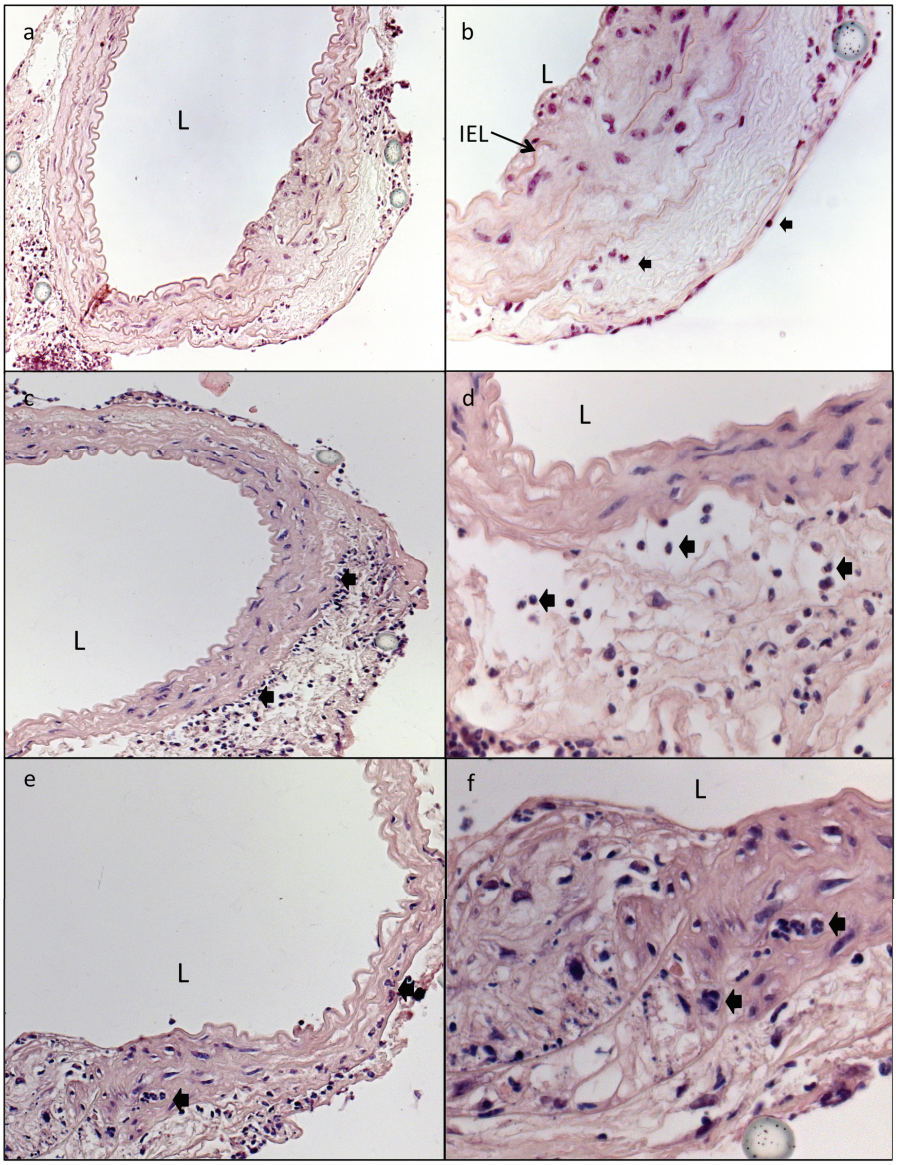

Figure 3.11. Histology micrographs showing aorta with lesion at 1d post-transplant. (a-b) shows loss of endothelium due to IRI (low and high magnification). Fractures in the IEL are characteristic of the established atherosclerotic plaque. (c-d) neutrophil influx due to IRI. (e-f) neutrophils penetrating the media and corresponding SMC loss. An otherwise intact lesion is observed. Neutrophils are demarcated by block arrows. L= lumen.

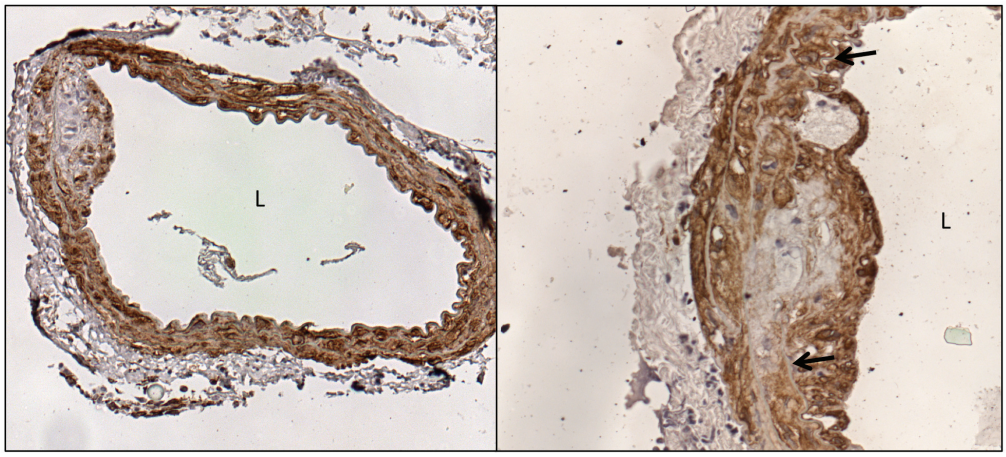

Figure 3.12. Alpha-SMA staining 1d post-transplant. Panels a and b show low and high magnification, respectively. Positive staining is evident in the media in the areas not affected by the lesion and in the region that comprises the fibrous cap. IEL is demarcated by arrows. L= lumen.

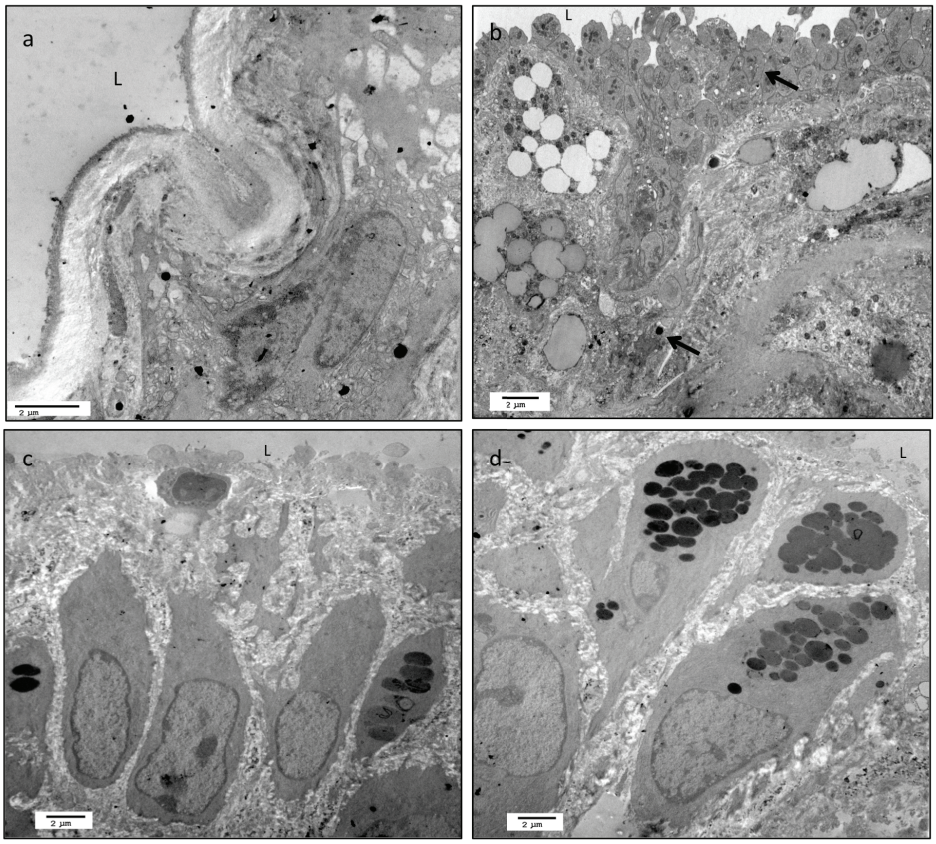

Figure 3.13. TEM of aorta 1d post-transplant. Panel a shows complete loss of endothelium (uninvolved area) immediately post-transplant. Panel b shows massive influx of platelets in the lesioned area upon loss of the endothelium. Lipid-bearing macrophages (foam cells) are tightly packed and arranged in similar orientation, and remain unchanged at 1d post-transplant (c-d). Platelets demarcated by arrows. L= lumen.

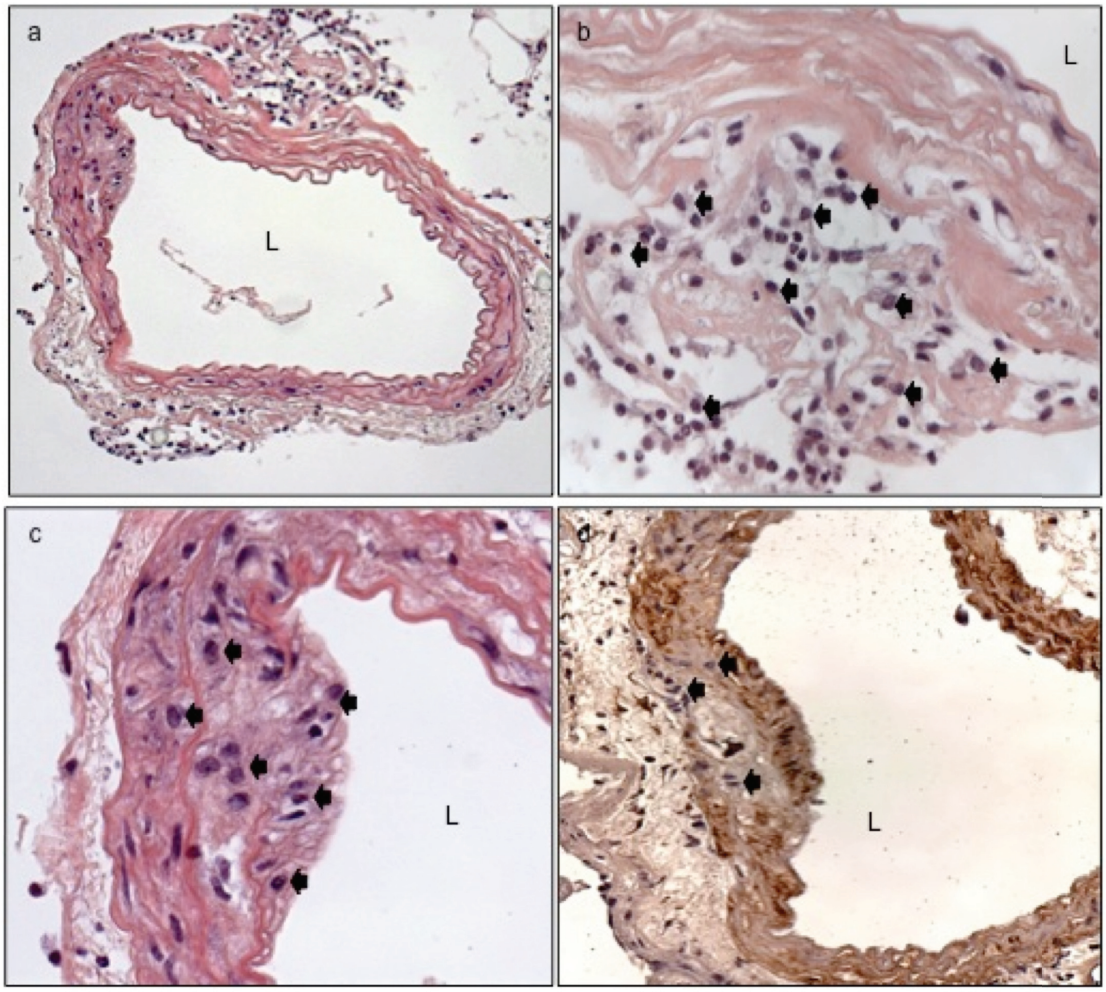

Figure 3.14. Composition of the atherosclerotic lesion 4d after transplantation. There is continued loss of smooth muscle cells from the media (panel a). There is an apparent transition from neutrophils to macrophages in the adventitia (b) but otherwise the lesion still remains macrophage-rich and intact (c). Alpha-SMA staining shows fibrous cap remains at 4d. L= lumen.

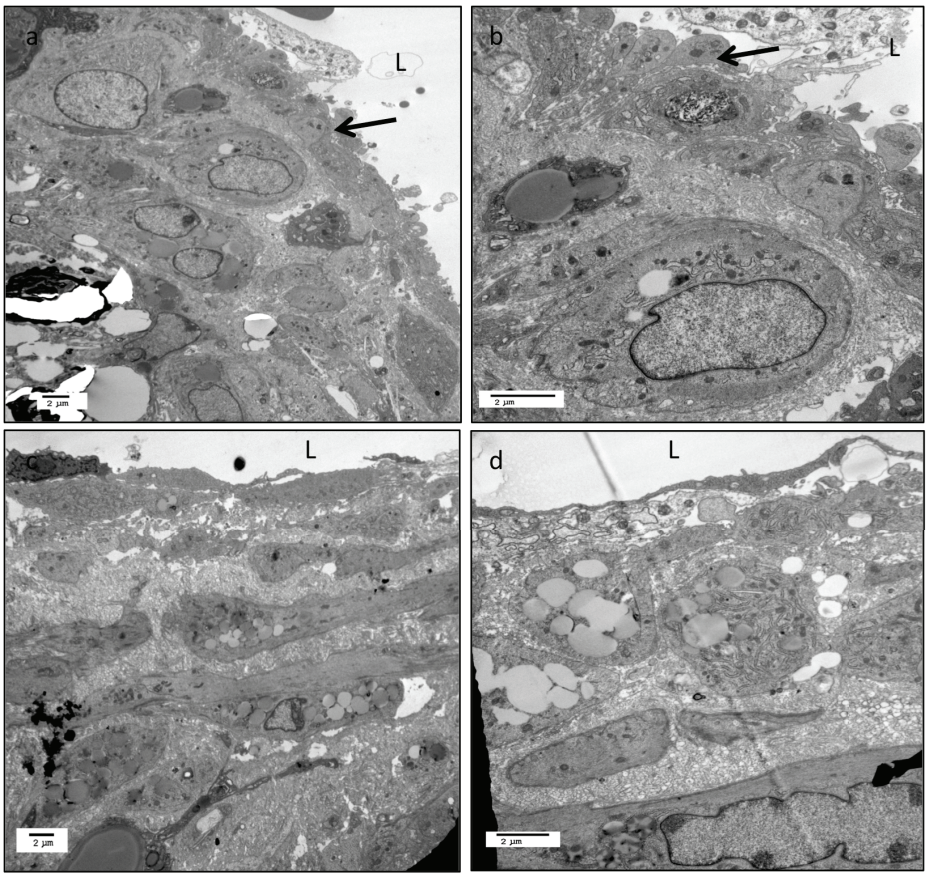

Figure 3.15. TEM micrographs at 4d post-transplant. Panel a and b show platelet deposition that is still present at 4d. Panel c and d show the presence of lipid-bearing macrophages with some change in orientation. Increased ground substance is also evident by 4d (d). Platelets are demarcated by arrows. L= lumen.

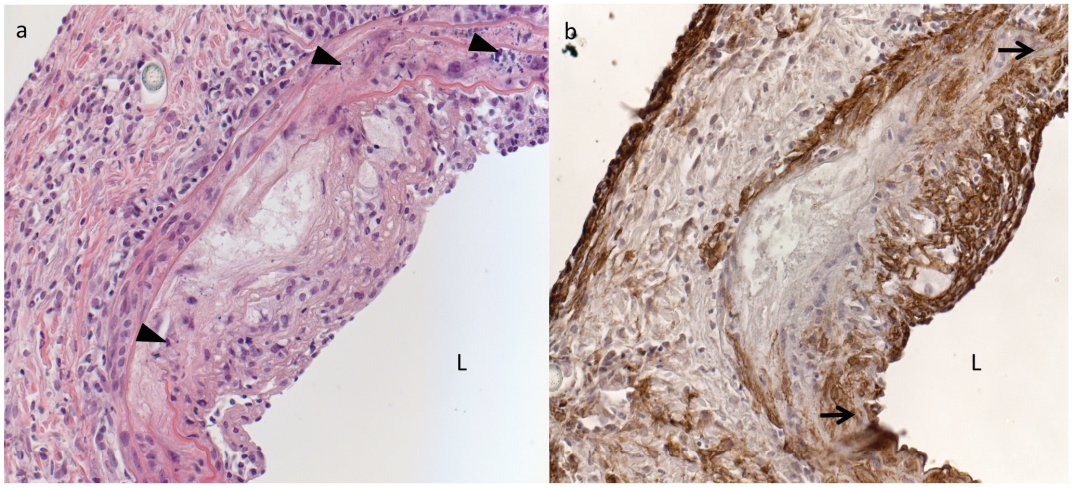

Figure 3.16. Composition of lesion 7d post-transplant. By 7d there is an inflammatory response evident in the adventitia and this cellular infiltration is migrating into the media by this time (a). The alpha-SMA staining shows that the fibrous cap in the lesion persists at 7d (b). IEL is demarcated by arrows and block arrowheads indicate presence of apoptotic cells. L= lumen.

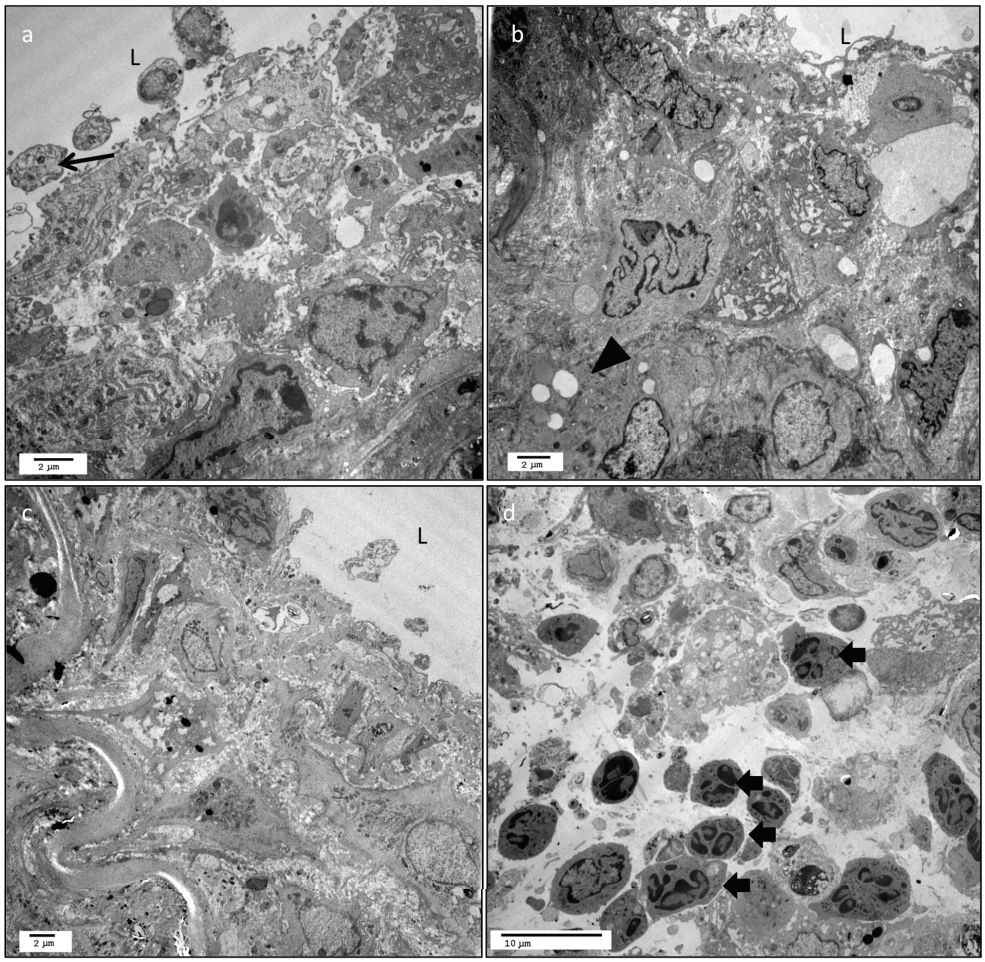

Figure 3.17. TEM micrographs at 7d post-transplant. Panel a shows that re-endothelialization has not taken place, and that there is still evidence of platelets. Panel b shows the reduced presence of lipid. There are large areas of ground substance, loss of cell-to-cell contact, and cellular changes evident in (c). Cellular infiltration in adventitia with high presence of neutrophils is shown in panel d. L= lumen.

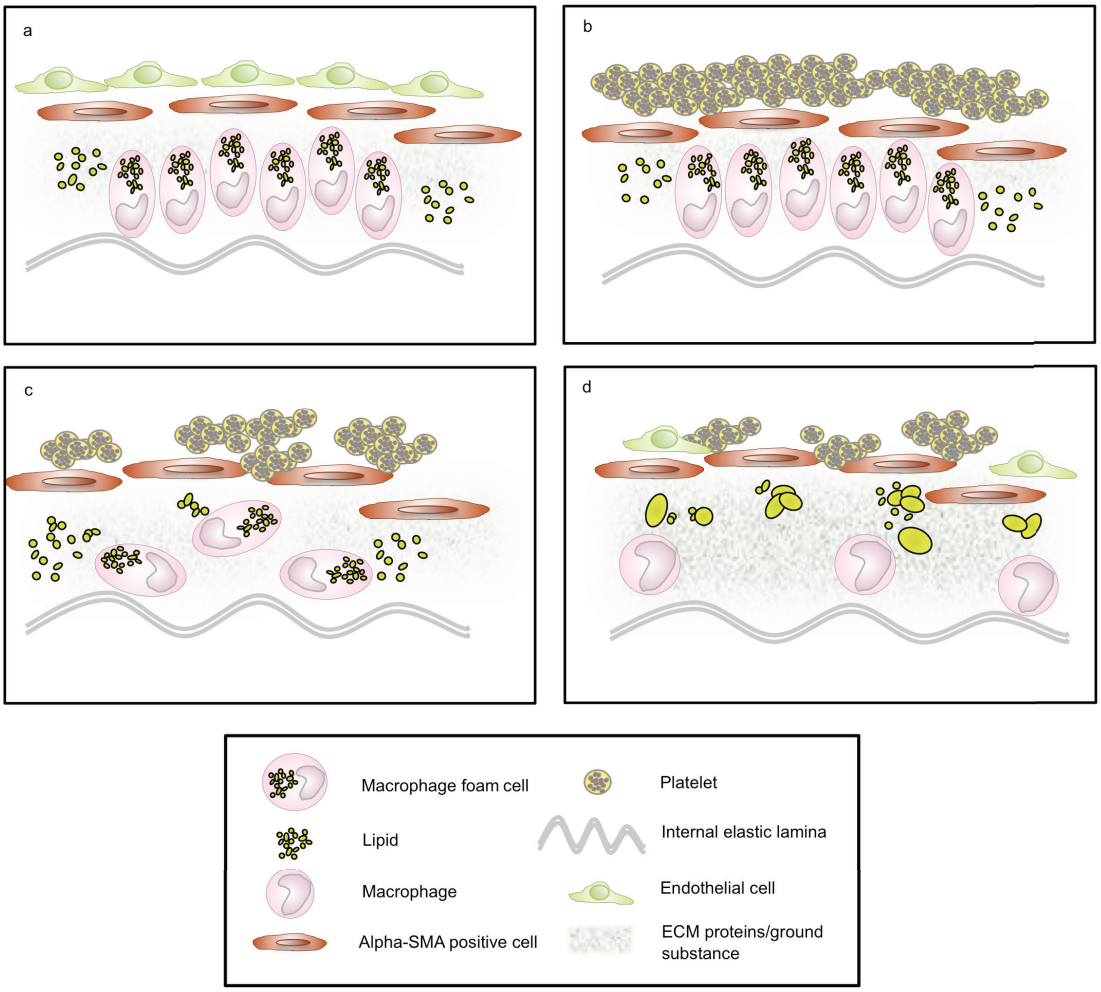

Figure 3.18. Summary diagram of the changes in the atherosclerotic lesion after transplantation. Panel a shows the lesion composition pre-transplant. Panel b-d demonstrate the changes in lesion structure that were observed at 1d, 4d, and 7d, respectively.

CHAPTER 4. DISCUSSION

4.1. *Echinacea purpurea, Cordyceps sinensis*, and *Heracleum maximum* as potential immunotherapeutics against *Mtb* infection (Project 1)

Tuberculosis is a deadly, rapidly progressing epidemic, especially in those regions of the world with widespread poverty, HIV/TB co-infection, and antibiotic resistance.[33] In areas like Sub-Saharan Africa, people face high drug costs and poor sanitation, and the population as a whole struggles with non-compliance while treating TB disease.[48] Despite the fact that TB is curable, it continues to expand with our exploding population, and drug-resistance strains of *Mtb* are more deadly than ever before.[2] Expanding the current TB treatments with the addition of natural immune-boosting agents could be an important finding in changing the course of TB disease.

The recent popularity of natural remedies has brought many laboratory studies to the forefront when investigating novel anti-mycobacterial agents.[104] Despite this, there is still a lack of evidence at the clinical trial level to make these therapies reliable alternatives to current mainstream treatments. Our laboratory has had a long-standing interest in studying alternative therapies that stimulate an individual's immune system to fight infection. The most recent work conducted in our laboratory using extracts from medicinal plants gave us evidence that *Ep*, *Cs*, and *Hm* had potential as immunostimulatory agents in our *ex vivo* TB model, as all have been proven to stimulate macrophages under a variety of conditions *in vitro* or *ex vivo*. Sullivan (2008) and demonstrated the ability of *Ep* to stimulate macrophages *in vitro* to produce pro-inflammatory cytokines and ROS, but most importantly, TNF and NO, and that neither of

these extracts were contaminated by LPS. Webster et al (2008) showed strong antimycobacterial activity with *Hm in vitro* using the colormetric microplate resazurin assay. His subsequent study showed significant cell viability in three separate human cell cultures against a DMSO control after the addition of varying dilutions of *Hm* aqueous extract.[143] Jordan (2008) demonstrated that an aqueous extract from the fungal mycelium of *Cs* could stimulate macrophages *in vitro* and *ex vivo*.[134] This work was worth expanding in this *ex vivo* model of TB infection to test similar aqueous extracts of these treatment agents.

Peripheral blood human monocytes were isolated and transitioned into macrophages in culture, then infected with either an avirulent or virulent strain of *Mtb.* Together with our collaborator, I created a model for the *ex vivo* infection of the freshly isolated human macrophages. The *Mtb* inoculum was prepared by the Level III laboratory staff in advance of the infection date. There were a series of "trial" experiments to achieve an MOI that would be high enough for intracellular growth, but not so concentrated that the macrophages would be overwhelmed and killed. Due to the natural robustness of *Mtb*, working with it in liquid culture is challenging. There is a high incidence of cording and settling out of suspension. It also grows very slowly, doubling every 22h in liquid culture.[146] When I saw colony formation in our isolated macrophage lysates, I proceeded to the next step of the experimentation and treated the inoculated cells with our extracts.

Macrophage activation by a variety of agents is enhanced in the presence of IFNγ. In these experiments we tested the ability of *Ep*, *Cs*, or *Hm* to act in conjunction with IFN-γ to increase macrophage pro-inflammatory responses. In this model, there was evidence to believe that treating the infected cells with our extracts would create a synergistic effect

with low level IFN-γ to reduce colony counts, if not ablate *Mtb* growth all together. In the case of *Ep*, it was the same product that was used in clinical trials for rhinovirus.[147]

There was one complete experiment with results for each treatment agent tested. However, my pilot data with each of these treatment groups did not show evidence of synergy compared to an IFN-γ control. In the case of *Ep*, there was no significant difference in CFU between the media control and *Ep* (+ low level IFN-γ) at either 5.6 or 2.8mg/ml. Not only is this a negative result, but it may be indicative that *Ep* is interfering with the IFN-γ and limiting its ability to stimulate macrophages.

With the *Cs* aqueous extract as our treatment agent, the data suggest that *Cs* did not synergize with IFN-γ to enhance macrophage activation to reduce CFU. Based on limited cell number, I chose not to include a media control, and instead used IFN-γ as the internal control. As above, if *Cs* + IFN-γ had a reduction in CFU, I would know there was some synergy between them. Because of the variability in CFU, It is possible that the addition of a low concentration of *Cs* was also interfering with the effects of IFN-γ.

An aqueous extract of *Hm* was the third agent I tested on our infected cells. *Hm* at 1:20 + IFN-γ shows best reduction of colony counts versus the lower concentrations. Therefore it is doing something similar to *Cs*. It is possible that the lower concentrations are interfering with IFN-γ, which alone contains the *Mtb* growth. Again, with limited cell counts, I chose to do IFN-γ as our internal control, and excluded a media alone group. *Hm* in this preliminary data at both concentrations appears to be making *Mtb* growth worse. This was a more rudimentary preparation than *Ep* or *Cs*. *Hm* comes from a family of plants that contain high amounts of coumarins.[136] It is possible that this preparation

was cytotoxic to the cells at every concentration we tested, creating a more susceptible host to *Mtb*.

Each agent in this experimentation failed to synergize with low-level IFN-γ to stimulate macrophages to control *Mtb* growth. The reasons seem multifactorial, but in each case, it would appear that the extracts are interfering with the effects of IFN-γ. They may be reducing IFN-γ binding to its receptor, which might reduce overall TLR expression at the cell membrane. It is possible that in the cytosol *Ep* is disrupting a signaling pathway that blocks downstream iNOS expression (e.g. a JAK antagonist). The *Ep* was purified to create a polysaccharide-enriched extract from a commercial preparation. There may be additional activity via other components in the extract we prepared. One component may enhance macrophage activity at a specific concentration, and one may hinder it. With increased concentrations, an active agent could block IFN-γ and another could reach a threshold effect in its ability to activate the macrophage. The other possibility is that *Ep* is directly enhancing *Mtb* growth. The extract may have a level of cytotoxicity that renders the macrophage more susceptible to *Mtb* entering the cell membrane, by inadvertently increasing the expression of *Mtb*-co-receptors, including TLR4 via potential LPS contamination, aiding in *Mtb*-binding capacity.[148]

It is important to note that in these experiments, IFN-γ alone ablates *Mtb* growth. For future experimentation, it would be critical to determine an appropriate dose of IFN-γ that would control *Mtb* growth, but not ablate it. For example, I could test for a minimum inhibitory concentration of 50% (MIC_{50}) for the IFN-γ treatment versus a media control. Once this was established the treatment groups at doubling dilutions could be tested with the addition of IFN-γ at MIC_{50}. Then, to further confirm the effect of the extracts, we

could add an experiment to test them at their optimal concentration, and titer the IFN-γ from 2U/ml, 1U/ml, 0.5U/ml, etc., until we started to see the CFU increase beyond MIC_{50}.

This proposed work would be contingent on the potential result of seeing similar CFU in the treatment groups compared to IFN-γ in the original experimentation. For any future experimentation, there would have to be a number of repeats to determine if the wide distribution of CFU in the treatment groups was a true finding or experimental artifact. If it were a true result, there would be no avenue to pursue further effects on enhanced macrophage responses. If it were artifact, the time and cost associated with doing any future work would have to be taken into account for practical reasons.

4.2. Summary (Project 1)

There have been many experimental models of human tuberculosis. Given its host specificity, it is important that the models have a high degree of applicability to human disease. Most models are *in vitro* based and study *Mtb* in isolation.[149] Others include the use of faster growing, non-pathogenic organisms, and thus are limited in their ability to closely represent pathogenic *Mtb*.[149] This was a complicated project for several reasons. The direct study of virulent *Mtb* is vital to understanding the effects of novel anti-TB therapeutics in humans. Due to the fact that *Mtb* H37Rv is a Level III human pathogen, I was required to receive substantial training before handling *Mtb* organisms and obtaining access to the Level III laboratory. This was the case at both the QEII Hospital in Halifax and the Saint John Regional Hospital. Dr. Webster was providing access to the Level III laboratory in Halifax on a regular basis while the model was being developed. His

practice was transferred to the Saint John Regional Hospital in Saint John, New Brunswick and working alongside Dr. Webster required travel between Halifax and Saint John. The project continued in New Brunswick temporarily, but proved to be costly and time-consuming, which tested its feasibility in continuing. The final set (3) of experiments was performed at the Level III laboratory at the QEII in Halifax on a conditional, short-term basis, after which access was denied. Even though it was early in the experimentation, I did not see positive results from *Ep* or the other extracts in this model. The data show the importance of getting the concentration of extract correct, because if it is to be used in combination with IFN-γ and the dose is wrong (i.e. IFN-γ is rendered inactive), the containment of the bacilli may be lost. The preliminary data, alongside practical difficulties, didn't suggest a fruitful avenue for further research. However, the establishment of this infection model is novel in Canada, and deserves to be revisited and fine-tuned until reproducible results are achieved.

In summary, this *ex vivo* model of human TB infection has promise to serve as a template for the development of a model for novel therapies in TB. Treatments using herbal preparations from *Echinacea purpurea*, *Cordyceps sinensis,* and *Heracleum maximum,* alongside low-dose IFN-γ provide a potential avenue of study for the development of urgently needed novel anti-TB therapeutics.

4.3. Early changes in the atherosclerotic lesion after transplantation (Project 2)

There is increasing evidence that the large epicardial coronary arteries of potential cardiac donors show a high prevalence of at least mild to moderate atherosclerosis, and in

some cases severe atherosclerosis.[248] In our experience, as noted above, we found that random samples of coronary arteries from ten potential donors revealed that 80% (8/10) of the patients had moderate to severe stenosis in at least one major epicardial artery (LAD, RCA or Circumflex). This prevalence of pre-existing atherosclerotic disease in the epicardial coronary arteries of donors has been confirmed by studies that have attempted to establish "baseline disease" by IVUS examination in recipients shortly after transplantation. At one month post- transplant a significant prevalence of donor-derived atherosclerotic disease in the donor epicardial arteries has been shown.[251,252] This situation has been exacerbated by the fact that the shortage of donor hearts has recently driven the use of hearts from increasingly older donors. Since donor age is the single-most influential, independent risk factor in the development of naturally occurring atherosclerosis,[265] it is obvious that this problem will continue to get worse.

What remains unclear is fate of the pre-existing atherosclerotic plaques and the contribution they may make to the development of CAV. While others continue to determine the extent of donor-derived atherosclerosis being transmitted to the recipient, I have concentrated on the fate of the pre-existing disease after transplant, and on how the presence of donor atherosclerosis could impact the longevity of the heart after it is transplanted.

The contribution of pre-existing donor lesions to the developing pathology of CAV has been very difficult to ascertain. CAV research is dominated by animal models, and in our laboratory these models have yielded valuable insights into the immunological mechanisms involved in CAV development,[167,197,266] but they are not capable of providing data on the role of pre-existing disease. These models have no pre-existing

atherosclerosis in the donor vessels, thus it is necessary to use a genetically modified animal that spontaneously exhibits atherosclerosis.

The ApoEKO mouse model presents an opportunity to address this in the laboratory. As noted earlier ApoE is a critical factor in lipoprotein metabolism, and the lack of this protein results in hyperlipidemia and development of atherosclerosis. The ApoEKO mouse model of atherosclerosis is well documented and used by a large number of researchers in the cardiovascular research community.[259] By using the well-established aortic interposition model of transplantation with ApoEKO donors, fully disparate C3H recipients, and CNI immunosuppression, the human transplant environment could be mimicked as closely as possible, where almost certainly some atherosclerosis will be transferred with the graft. The hope was that these studies would help us to understand the contribution of pre-existing atherosclerotic lesions to *de novo* CAV lesion generation.

It is important to note that many studies have demonstrated that ApoEKO mice develop naturally occurring atherosclerotic lesions that very closely resemble human atherosclerosis, both in morphology and predilection of site. The age of the mice used in this model was controlled to allow for development of advanced lesions in the abdominal aorta. One advantage of this is that the internal lesions are visible from the external surface of the aorta can be assessed for specific size and location before they are transplanted. For these experiments, small to moderate lesions (between 100 and 500μm in diameter) were used as donor lesions. Large lesions (>500μm long diameter) were not used for transplantation, as they were thought to exhibit sufficient luminal narrowing to initiate post-transplant clotting and transplant failure.

4.3.1. Analysis of changes in lesion volume

The ability to determine changes in lesion volume would be a valuable tool in the study of atherosclerosis in a transplantation setting. My first objective was to characterize changes in lesion volume to ascertain what these changes would mean to the development of AV. My interest was in one of three scenarios after the atherosclerotic lesion was transplanted: (1) the donor lesion would expand after transplant due to post-ischemic events and neutrophil influx, (2) the donor lesion would remain the same, and post-transplant, becoming a combination of donor atherosclerosis and recipient AV elements, contributing equally to overall luminal narrowing or (3) the donor lesion would regress as the allo-immune response replaced the lesion with *de novo* AV lesion.

It has been shown that the atherosclerotic lesion will regress on its own if transplanted from an ApoEKO mouse (C57BL/6 background) to a wild type C57BL/6 mouse, as the lipid profile transitions from hyperlipidemic to normal.[267,268] But in an allogeneic setting the fate of the lesion is less clear. Our laboratory has shown that the lesion persists, in some form, for at least 10wk post- transplant.[269] But in these studies mentioned above, no attempt was made to measure the initial size of the lesion and the examination of the lesion morphology itself was superficial. Others have attempted to chart the changes in lesion size of transplanted lesions.[270] In these studies luminal narrowing was measured by either stereological techniques or *in vivo* MRI, but neither took into consideration what occurs in a three-dimensional context.

To be able to accurately assess the fate of the transplanted lesion we would need to assess the initial lesion volume and the final lesion volume at harvest. The final lesion volume is

not a problem to assess, but this cannot be done on a fresh lesion for obvious reasons and thus obtaining an initial volume is problematic. To circumvent this I tested the feasibility of looking at whether the outer lesion area would be a sufficient predictor of volume (i.e. a surrogate marker of lesion volume). The outer lesion area from a group of lesions from ApoEKO mice was measured with a micro-ruler. After ruler measurements they were harvested and processed for histology, and internal volume for these lesions was assessed. The first parameter I calculated was the outer lesion area of each of a group of 10 lesions prior to transplant, and this represented the potential surrogate marker for internal lesion volume. I then performed serial sections through the entire lesion and calculated an **actual volume** from the sum of individual section volumes (area x 5μm thickness of each section).

Using the outer lesion area I calculated a **predicted volume** by assuming an elliptical shape of the internal lesion. In this experiment an exact correlation between outer lesion area and internal volume was not necessary. I was prepared to accept up to a 30% difference in these numbers. Unfortunately the data showed that measuring the outer lesion area prior to transplant could not be used as a surrogate marker for internal lesion size and thus we could not establish an initial internal lesion volume (and therefore not follow any change in that volume). The reason for this is the large variation in lesion shape that was clearly seen in Figure 7.3. This variation meant that a correlate was not possible to calculate internal lesion size based on outer lesion area.

4.3.2. Analysis of changes in lesion composition

My second objective for this project was to characterize changes in lesion composition. My original hypothesis was that early immune events in the graft post-transplant due to ischemia reperfusion injury would be sufficient to initiate changes in the lesion, and these changes would set the stage for post-transplant vasculopathy. The innate response after IRI is quick and robust, and our laboratory has shown that as early as 1d, neutrophils come flooding into the graft and there is a corresponding loss of medial SMC.[176] This loss of SMC would presumably cause architectural changes in the lesion, as well as degeneration of lesion components once the neutrophils were present. Originally it was believed that the donor atherosclerosis would be, at least in part, broken down by neutrophils internalizing allogeneic macrophage foam cells. This response would result in expelled lipid from the digested macrophages that would be taken up by recipient macrophages, perpetuating and expanding the lesion. This would ultimately lead to enhanced AV.

The data would suggest this is not completely the case (Figure 7.4-7.12). Between 1d and 7d, there was endothelial cell and medial SMC loss due to IRI as expected. The surprising observation was that the lesion seemed to be protected against the worst of the tissue damage. The distribution of neutrophils very early post-transplant was relegated to the adventitia. There appeared to be no neutrophil influx from the luminal side of the graft, only from the small vessels in the adventitia. This is perhaps not surprising with respect to neutrophil infiltration of the media, since there is such a robust elastic layer (the IEL) between the lumen and the media. But it is quite surprising that the intimal atherosclerotic lesion does not attract the attention of neutrophils. This is in the face of significant loss of endothelial cells and deposition of platelets on the surface of the lesion. In fact, in

contrast to our expectation, the lesion showed no significant changes until 7d post transplant. This is in the face of considerable tissue destruction around it. The reasons for this lack of reactivity of the lesion are unclear.

By 7d post-transplant it is evident that the lesion has begun to undergo changes. There are few recognizable large foamy macrophages, and the cells have lost their cell-to-cell contact. There is also a large amount of intercellular ground substance (loose connective tissue). Surprisingly, there is little in the way of immune cell infiltration. This is possibly due to the fact that acute rejection is being held at bay by CNI immunosuppression (as would be the case in humans).

4.4. Summary (Project 2)

The data above clarify, at least in this animal model of donor-derived atherosclerosis, that the atherosclerotic lesion survives transplantation and in the early stages is protected from extensive IRI injury. These data agree with earlier studies from our laboratory where it was demonstrated that the lesion is still present, in some form, at 10wk post-transplant. What these data show, especially the TEM data, is that significant changes are occurring to the lesion structure over the first 7d post-transplant. This suggests that the lesion is becoming biologically active and may thus contribute to the inflammatory response thought to be involved in the early stages of CAV. With this knowledge and that of carry-over intimal thickening that occurs in human coronary arteries post-transplant, donor-derived disease may set the stage for the inflammatory response that initiates CAV. The presence of atherosclerosis in donor vessels may accelerate this response. Further studies will take this examination to later time points to assess whether the initial stages are

followed by an expanded inflammatory response, or whether after IRI injury the lesion gradually resolves.

REFERENCES

1. World Health Organization. Global Tuberculosis Report (2012). www.who.int/tb/publications/factsheet_global.

2. Zumla, A., Raviglione, M., Hafner, R., Fordham von Reyn, C. Tuberculosis. *N. Engl. J. Med.* **368**, 745-755 (2013).

3. Halverson, J., Ellis, J., Gallant, V., Archibald, C. Canadian Tuberculosis Standards 7th Edition. Chapter 1: Epidemiology of Tuberculosis in Canada. 2-19 (2010).

4. Andrews, J. M. & Riley, R. L. Part IV. Bacterial Diseases. *Microbiol. Mol. Biol. Rev.* **25,** 243–248 (1961).

5. Nayak, S. Basanti, A. Mantoux test and its interpretation. *Indian Dermatol. Online J.* **3,** 2–6 (2012).

6. Farhat, M, Greenaway, C, Pai, M, Menzies, D. False-positive tuberculin skin tests: what is the absolute effect of BCG and non-tuberculous mycobacteria? *Int J Tuberc Lung Dis* **10,** 1192–204 (2006).

7. Singla, M., Sahai, V., Sodhi, S. & Gupta, R. P. BCG skin reaction in Mantoux-negative healthy children. *BMC Infect. Dis.* **5,** 19 (2005).

8. Kiwanuka, J. P. Interpretation of tuberculin skin-test results in the diagnosis of tuberculosis in children. *Afr. Health Sci.* **5,** 152–6 (2005).

9. Mancuso, J. D. *et al.* Discordance among commercially available diagnostics for latent tuberculosis infection. *Am. J. Respir. Crit. Care Med.* **185,** 427–34 (2012).

10. Dheda, K., van Zyl Smit, R., Badri, M. & Pai, M. T-cell interferon-gamma release assays for the rapid immunodiagnosis of tuberculosis: clinical utility in high-burden vs. low-burden settings. *Curr. Opin. Pulm. Med.* **15,** 188–200 (2009).

11. Pai, M., Kalantri, S. & Dheda, K. New tools and emerging technologies for the diagnosis of tuberculosis: Part I . 413–422 (2006).

12. Yew, W. W. & Leung, C. C. Update in tuberculosis 2006. *Am. J. Respir. Crit. Care Med.* **175,** 541–6 (2007).

13. Cattamanchi, A. *et al.* IGRA for the diagnosis of latent TB infection in HIV-infected individuals- a systematic review and meta-analysis. *J. Acquir. Immune Defic. Syndr.* **56,** 230–238 (2011).

14. Ahmad, S. Pathogenesis, immunology, and diagnosis of latent Mycobacterium tuberculosis infection. *Clin. Dev. Immunol.* **2011,** 814943 (2011).

15. Braun, J. F., King, L. & Ahuja, S. TB and HIV Coinfection: Current Trends , Diagnosis and Treatment Update. **11,** 17–23 (2006).

16. Pai, M., Minion, J., Steingart, K. & Ramsay, A. New and improved tuberculosis diagnostics: evidence, policy, practice, and impact. *Curr. Opin. Pulm. Med.* **16,** 271–84 (2010).

17. Frieden, T. R., Sterling, T. R., Munsiff, S. S., Watt, C. J. & Dye, C. Tuberculosis. *Lancet* **362,** 887–99 (2003).

18. Miller, W. T. Tuberculosis in the normal host: radiological findings. *Semin. Roentgenol.* **28,** 109–118 (1993).

19. Almeida Da Silva, P. E. A. & Palomino, J. C. Molecular basis and mechanisms of drug resistance in Mycobacterium tuberculosis: classical and new drugs. *J. Antimicrob. Chemother.* **66,** 1417–30 (2011).

20. Cohen, T., Sommers, B. & Murray, M. The effect of drug resistance on the fitness of Mycobacterium tuberculosis. *Lancet Infect. Dis.* **3,** 13–21 (2003).

21. Somoskovi, a, Parsons, L. M. & Salfinger, M. The molecular basis of resistance to isoniazid, rifampin, and pyrazinamide in Mycobacterium tuberculosis. *Respir. Res.* **2,** 164–8 (2001).

22. Alexander, P. E. & De, P. The emergence of extensively drug-resistant tuberculosis (TB): TB/HIV coinfection, multidrug-resistant TB and the resulting public health threat from extensively drug-resistant TB, globally and in Canada. *Can. J. Infect. Dis. Med. Microbiol.* **18,** 289–91 (2007).

23. Caminero, J. A, Sotgiu, G., Zumla, A. & Migliori, G. B. Best drug treatment for multidrug-resistant and extensively drug-resistant tuberculosis. *Lancet Infect. Dis.* **10,** 621–9 (2010).

24. World Health Organization. The DOTS Strategy. Building on and Enhancing DOTS to Meet the TB-Related Millennium Development Goals. 1–24 at <http://whqlibdoc.who.int/hq/2006/WHO_HTM_STB_2006.368_eng>

25. Murali, MS, Saijan, B. DOTS strategy for control of tuberculosis epidemic. *Indian J Med Sci* **56,** 16–18 (2002).

26. Gandhi, N. R. *et al.* Multidrug-resistant and extensively drug-resistant tuberculosis: a threat to global control of tuberculosis. *Lancet* **375,** 1830–43 (2010).

27. Jassal, M. & Bishai, W. R. Extensively drug-resistant tuberculosis. *Lancet Infect. Dis.* **9,** 19–30 (2009).

28. Chan, B., Khadem, T. M. & Brown, J. A review of tuberculosis: Focus on bedaquiline. *Am. J. Health. Syst. Pharm.* **70,** 1984–94 (2013).

29. Singh, H., Natt, N., Garewal, N. & T, P. Bedaquiline: a new weapon against MDR and XDR-TB. *Int. J. Basic Clin. Pharmacol.* **2,** 96 (2013).

30. Gler, M. T. *et al*. Delamanid for Multidrug-Resistant Pulmonary Tuberculosis. *N. Engl. J. Med.* **366,** 2151–2160 (2012).

31. Aaron, L. *et al*. Tuberculosis in HIV-infected patients: a comprehensive review. *Clin. Microbiol. Infect.* **10,** 388–98 (2004).

32. Harries, A. D. *et al*. The HIV-associated tuberculosis epidemic--when will we act? *Lancet* **375,** 1906–19 (2010).

33. Pawlowski, A., Jansson, M., Sköld, M., Rottenberg, M. E. & Källenius, G. Tuberculosis and HIV co-infection. *PLoS Pathog.* **8,** 1–7 (2012).

34. Corbett, E. L. *et al*. The Growing Burden of Tuberculosis. **163,** 1009–1021 (2011).

35. Kwara, A., Carter, E. J., Rich, J. D. & Flanigan, T. P. Development of opportunistic infections after diagnosis of active tuberculosis in HIV-infected patients. *AIDS Patient Care STDS* **18,** 341–7 (2004).

36. Diedrich, C. R. & Flynn, J. L. HIV-1/Mycobacterium tuberculosis coinfection immunology: how does HIV-1 exacerbate tuberculosis? *Infect. Immun.* **79,** 1407–17 (2011).

37. Shattock, RJ, Friedland, JS, and Griffin, G. Modulation of HIV transcription in monocytes and macrophages after phagocytosis of Mtb. *Res. Virol.* **144,** 7–12 (1993).

38. Goletti, D. *et al*. Effect of Mycobacterium tuberculosis on HIV replication. *J. Immunol.* **157,** 1271–1278 (1996).

39. Nakata, K. O. H. *et al*. Mycobacterium tuberculosis enhances human immunodeficiency virus-l replication in the lung. *Am. J. Respir. Crit. Care. Med.* **155**, 996-1003 (1997).

40. Rosas-Taraco, A. G., Arce-Mendoza, A. Y., Caballero-Olín, G. & Salinas-Carmona, M. C. Mycobacterium tuberculosis upregulates coreceptors CCR5 and CXCR4 while HIV modulates CD14 favoring concurrent infection. *AIDS Res. Hum. Retroviruses* **22,** 45–51 (2006).

41. Toossi, Z. Virological and immunological impact of tuberculosis on human immunodeficiency virus type 1 disease. *J. Infect. Dis.* **188,** 1146–55 (2003).

42. Jaryal, A., Raina, R., Sarkar, M. & Sharma, A. Manifestations of tuberculosis in HIV/AIDS patients and its relationship with CD4 counts. *Lung Ind.* **28,** 263-266 (2011).

43. Lawn, S. D., Butera, S. T. & Shinnick, T. M. Tuberculosis unleashed: the impact of human immunodeficiency virus infection on the host granulomatous response to Mycobacterium tuberculosis. *Microbes Infect.* **4,** 635–46 (2002).

44. Tufariello, J. M., Chan, J. & Flynn, J. L. Latent tuberculosis: mechanisms of host and bacillus that contribute to persistent infection. *Lancet Infect. Dis.* **3,** 578–90 (2003).

45. Patel, N. R. *et al.* HIV impairs TNF-alpha mediated macrophage apoptotic response to Mycobacterium tuberculosis. *J. Immunol.* **179,** 6973–80 (2007).

46. Onyebujoh, P, Ribeiro, I, Whalen, C. Treatment options for HIV-associated tuberculosis. *J. Infect Dis.* **15,** S35–45 (2007).

47. Pantaleo, G., Graziosi, C., Fauci, A. The immunopathogenesis of human immunodeficiency virus infection. *N. Engl. J. Med.* **328,** 327–335 (1993).

48. McShane, H. Co-infection with HIV and TB: double trouble. *Int. J. STD AIDS* **16,** 95–101 (2005).

49. World Health Organization. Consolidated Guidelines on the Use of Anti-Retroviral Therapy. 91–113 (2013). at <www.who.int/hiv/pub/guidelines/arv2013/en>

50. Akira, S., Uematsu, S. & Takeuchi, O. Pathogen recognition and innate immunity. *Cell* **124,** 783–801 (2006).

51. Takeuchi, O. & Akira, S. Pattern recognition receptors and inflammation. *Cell* **140,** 805–20 (2010).

52. Janeway, C. A. Pillars article: approaching the asymptote? Evolution and revolution in immunology. Cold spring harb symp quant biol. 1989. 54: 1-13. *J. Immunol.* **191,** 4475–87 (2013).

53. Medzhitov, R. Pattern recognition theory and the launch of modern innate immunity. *J. Immunol.* **191,** 4473–4 (2013).

54. Akira, S., Takeda, K. & Kaisho, T. Toll-like receptors: critical proteins linking innate and acquired immunity. *Nat. Immunol.* **2,** 675–80 (2001).

55. Kleinnijenhuis, J., Oosting, M., Joosten, L. B., Netea, M. G. & Van Crevel, R. Innate immune recognition of Mycobacterium tuberculosis. *Clin. Dev. Immunol.* **2011,** 405310 (2011).

56. Kawai, T. & Akira, S. Toll-like receptors and their crosstalk with other innate receptors in infection and immunity. *Immunity* **34,** 637–50 (2011).

57. Jo, E.-K. Mycobacterial interaction with innate receptors: TLRs, C-type lectins, and NLRs. *Curr. Opin. Infect. Dis.* **21,** 279–86 (2008).

58. Blasius, A. L. & Beutler, B. Intracellular toll-like receptors. *Immunity* **32,** 305–15 (2010).

59. Underhill, D. M., Ozinsky, A., Smith, K. D. & Aderem, A. Toll-like receptor-2 mediates mycobacteria-induced proinflammatory signaling in macrophages. *Proc. Natl. Acad. Sci. U. S. A.* **96,** 14459–63 (1999).

60. Crevel, R. Van, Ottenhoff, T. H. M., Van, J. W. M. & Meer, J. W. M. Van Der. Innate Immunity to Mycobacterium tuberculosis. *Clin. Microbiol. Rev.* **15,** 294–309 (2002).

61. Kaufmann, S. H. E. Protection against tuberculosis: cytokines, T cells, and macrophages. *Ann. Rheum. Dis.* **61 Suppl 2,** ii54–8 (2002).

62. Yoshida, A., Inagawa, H., Kohchi, C., Nishizawa, T. & Soma, G.-I. The role of toll-like receptor 2 in survival strategies of Mycobacterium tuberculosis in macrophage phagosomes. *Anticancer Res.* **29,** 907–10 (2009).

63. Geijtenbeek, T. B. H., Engering, A. & Van Kooyk, Y. DC-SIGN, a C-type lectin on dendritic cells that unveils many aspects of dendritic cell biology. *J. Leukoc. Biol.* **71,** 921–31 (2002).

64. Welin, A. & Lerm, M. Inside or outside the phagosome? The controversy of the intracellular localization of Mycobacterium tuberculosis. *Tuberculosis (Edinb).* **92,** 113–20 (2012).

65. Philpott, D. J. & Girardin, S. E. The role of Toll-like receptors and Nod proteins in bacterial infection. *Mol. Immunol.* **41,** 1099–108 (2004).

66. Athman, R. & Philpott, D. Innate immunity via Toll-like receptors and Nod proteins. *Curr. Opin. Microbiol.* **7,** 25–32 (2004).

67. Yang, Y. *et al.* NOD2 pathway activation by MDP or Mycobacterium tuberculosis infection involves the stable polyubiquitination of Rip2. *J. Biol. Chem.* **282,** 36223–9 (2007).

68. Cooper, A. M. Cell-mediated immune responses in tuberculosis. *Annu. Rev. Immunol.* **27,** 393–422 (2009).

69. Kawai, T. & Akira, S. Signaling to NF-kappaB by Toll-like receptors. *Trends Mol. Med.* **13,** 460–9 (2007).

70. Li, Q. & Verma, I. M. NF-kappaB regulation in the immune system. *Nat. Rev. Immunol.* **2,** 725–34 (2002).

71. Dunne, A. & O'Neill, L. a J. The interleukin-1 receptor/Toll-like receptor superfamily: signal transduction during inflammation and host defense. *Sci. STKE* **2003,** re3 (2003).

72. Sakamoto, K. The pathology of Mycobacterium tuberculosis infection. *Vet. Pathol.* **49,** 423–39 (2012).

73. Raupach, B. & Kaufmann, S. H. Immune responses to intracellular bacteria. *Curr. Opin. Immunol.* **13,** 417–28 (2001).

74. Lee, J., Remold, H. G., Ieong, M. H. & Kornfeld, H. Macrophage apoptosis in response to high intracellular burden of Mycobacterium tuberculosis is mediated by a novel caspase-independent pathway. *J. Immunol.* **176,** 4267–74 (2006).

75. Yang, C.-S., Yuk, J.-M. & Jo, E.-K. The role of nitric oxide in mycobacterial infections. *Immune Netw.* **9,** 46–52 (2009).

76. Clemens, D. L. Characterization of the Mycobacterium tuberculosis phagosome. *Trends Microbiol.* **4,** 113–8 (1996).

77. Rohde, K., Yates, R. M., Purdy, G. E. & Russell, D. G. Mycobacterium tuberculosis and the environment within the phagosome. *Immunol. Rev.* **219,** 37–54 (2007).

78. Rajni, Rao, N. & Meena, L. S. Biosynthesis and Virulent Behavior of Lipids Produced by Mycobacterium tuberculosis: LAM and Cord Factor: An Overview. *Biotechnol. Res. Int.* **2011,** 7 (2011).

79. Puissegur, M.-P. *et al.* Mycobacterial lipomannan induces granuloma macrophage fusion via a TLR2-dependent, ADAM9- and beta1 integrin-mediated pathway. *J. Immunol.* **178,** 3161–9 (2007).

80. Salgame, P. Host innate and Th1 responses and the bacterial factors that control Mycobacterium tuberculosis infection. *Curr. Opin. Immunol.* **17,** 374–80 (2005).

81. Wojtas, B. *et al*. Mannosylated lipoarabinomannan balances apoptosis and inflammatory state in mycobacteria-infected and uninfected bystander macrophages. *Microb. Pathog.* **51,** 9–21 (2011).

82. Sly, L. M., Hingley-Wilson, S. M., Reiner, N. E. & McMaster, W. R. Survival of Mycobacterium tuberculosis in host macrophages involves resistance to apoptosis dependent upon induction of antiapoptotic Bcl-2 family member Mcl-1. *J. Immunol.* **170,** 430–7 (2003).

83. Yoshida, A., Inagawa, H., Kohchi, C., Nishizawa, T. & Soma, G.-I. The role of toll-like receptor 2 in survival strategies of Mycobacterium tuberculosis in macrophage phagosomes. *Anticancer Res.* **29,** 907–10 (2009).

84. Fortune, S. M. *et al*. Mycobacterium tuberculosis inhibits macrophage responses to IFN-gamma through myeloid differentiation factor 88-dependent and -independent mechanisms. *J. Immunol.* **172,** 6272–80 (2004).

85. Herbst, S., Schaible, U. E. & Schneider, B. E. Interferon gamma activated macrophages kill mycobacteria by nitric oxide induced apoptosis. *PLoS One* **6,** e19105 (2011).

86. Wolf, A. J. *et al*. Initiation of the adaptive immune response to Mycobacterium tuberculosis depends on antigen production in the local lymph node, not the lungs. *J. Exp. Med.* **205,** 105–15 (2008).

87. Yu, C.-C. *et al*. Factors associated with in vitro interferon-gamma production in tuberculosis. *J. Formos. Med. Assoc.* **110,** 239–46 (2011).

88. Winslow, G. M., Cooper, A., Reiley, W., Chatterjee, M. & Woodland, D. L. Early T-cell responses in tuberculosis immunity. *Immunol. Rev.* **225,** 284–99 (2008).

89. Berger, A. Th1 and Th2 responses: what are they? *BMJ* **321,** 424 (2000).

90. Green, A. M., Difazio, R. & Flynn, J. L. IFN-γ from CD4 T cells is essential for host survival and enhances CD8 T cell function during Mycobacterium tuberculosis infection. *J. Immunol.* **190,** 270–7 (2013).

91. Flynn, J. L. *et al*. An essential role for interferon gamma in resistance to Mycobacterium tuberculosis infection. *J. Exp. Med.* **178,** 2249–54 (1993).

92. Schroder, K., Sweet, M. J. & Hume, D. A. Signal integration between IFNgamma and TLR signalling pathways in macrophages. *Immunobiology* **211,** 511–24 (2006).

93. Decker, T, and Muller, M. JAK-STAT signalling: from basics to disease. 133–151 (2012).

94. Schroder, K., Hertzog, P. J., Ravasi, T. & Hume, D. A. Interferon-gamma: an overview of signals, mechanisms and functions. *J. Leuk. Biol.* **75,** 163-189 (2004).

95. Wallis, R. S. Reactivation of latent tuberculosis by TNF blockade: the role of interferon gamma. *J. Investig. Dermatol. Symp. Proc.* **12,** 16–21 (2007).

96. Ehlers, S. Role of tumour necrosis factor (TNF) in host defence against tuberculosis: implications for immunotherapies targeting TNF. *Ann. Rheum. Dis.* **62** Suppl 2**,** ii37–42 (2003).

97. Tsai, M. C. *et al.* Characterization of the tuberculous granuloma in murine and human lungs: cellular composition and relative tissue oxygen tension. *Cell. Microbiol.* **8,** 218–32 (2006).

98. Russell, D. G., Cardona, P., Kim, M. & Allain, S. Foamy macrophages and the progression of the human TB granuloma. *Nat. Immunol.* **10,** 943–948 (2010).

99. Grosset, J. Mycobacterium tuberculosis in the Extracellular Compartment: an Underestimated Adversary. **47,** 833–836 (2003).

100. Boom, W. Human immunity to Myocbacterium tuberculosis: T cell subsets and antigen processing. *Tuberculosis* **83,** 98–106 (2003).

101. Saunders, B. M. & Britton, W. J. Life and death in the granuloma: immunopathology of tuberculosis. *Immunol. Cell Biol.* **85,** 103–11 (2007).

102. Ramakrishnan, L. Revisiting the role of the granuloma in tuberculosis. *Nat. Rev. Immunol.* **12,** 352–66 (2012).

103. Alexander, P. E. & De, P. The emergence of extensively drug-resistant tuberculosis (TB): TB/HIV coinfection, multidrug-resistant TB and the resulting public health threat from extensively drug-resistant TB, globally and in Canada. *Can. J. Infect. Dis. Med. Microbiol.* **18,** 289–91 (2007).

104. Mitscher, L. A. & Baker, W. Tuberculosis: A Search for Novel Therapy starting with Natural Products. *Med Res Rev* **18,** 363–374 (1998).

105. Patience, S. *et al.* Activity against Mycobacterium smegmatis and M . tuberculosis by Extract of South African Medicinal Plants. *Phyther. Res.* **845,** 841–845 (2008).

106. Zaidan, M. R. S. *et al.* In vitro screening of five local medicinal plants for antibacterial activity using disc diffusion method. *Trop. Biomed.* **22,** 165–70 (2005).

107. Palombo, E. A. Traditional Medicinal Plant Extracts and Natural Products with Activity against Oral Bacteria: Potential Application in the Prevention and

Treatment of Oral Diseases. *Evid. Based. Complement. Alternat. Med.* **2011,** 680354 (2011).

108. Barrett, B. Medicinal properties of Echinacea: a critical review. *Phytomedicine* **10,** 66–86 (2003).

109. Shah, S. A, Sander, S., White, C. M., Rinaldi, M. & Coleman, C. I. Evaluation of echinacea for the prevention and treatment of the common cold: a meta-analysis. *Lancet Infect. Dis.* **7,** 473–80 (2007).

110. Zhai, Z. *et al.* Enhancement of innate and adaptive immune functions by multiple echinacea species. *J Med Food* **10,** 423–434 (2007).

111. Jawad, M., Schoop, R., Suter, A., Klein, P. & Eccles, R. Safety and Efficacy Profile of Echinacea purpurea to Prevent Common Cold Episodes: A Randomized, Double-Blind, Placebo-Controlled Trial. *Evidence-based Complement. Altern. Med.* **2012,** 7 (2012).

112. Caruso, T. J. & Gwaltney, J. M. Treatment of the common cold with Echinacea: a structured review. *Clin. Infect. Dis.* **40,** 807–10 (2005).

113. Balan, B. Immunotropic activity of Echinacea . Part I . History and chemical structure. *Cent. Eur J Immunol* **37,** 45–50 (2012).

114. Percival, S. S. Use of echinacea in medicine. *Biochem. Pharmacol.* **60,** 155–8 (2000).

115. Goel, V. *et al.* Efficacy of a standardized echinacea preparation (Echinilin) for the treatment of the common cold: a randomized, double-blind, placebo-controlled trial. *J. Clin. Pharm. Ther.* **29,** 75–83 (2004).

116. Pugh, N. D. *et al.* The majority of in vitro macrophage activation exhibited by extracts of some immune enhancing botanicals is due to bacterial lipoproteins and lipopolysaccharides. *Int. Immunopharmacol.* **8,** 1023–32 (2008).

117. Sullivan, A. M., Laba, J. G., Moore, J. A. & Lee, T. D. G. Echinacea-induced macrophage activation. *Immunopharmacol. Immunotoxicol.* **30,** 553–574 (2008).

118. Goel, V. Echinacea stimulates macrophage function in the lung and spleen of normal rats. *J. Nutr. Biochem.* **13,** 487 (2002).

119. Rininger, J. A., Kickner, S., Chigurupati, P., Mclean, A. & Franck, Z. Immunopharmacological activity of Echinacea preparations following simulated digestion on murine macrophages and human peripheral blood mononuclear cells. *J. Leukoc. Biol.* **68,** 503–510 (2000).

120. Stimpel, M., Proksch, A, Wagner, H. & Lohmann-Matthes, M. L. Macrophage activation and induction of macrophage cytotoxicity by purified polysaccharide fractions from the plant Echinacea purpurea. *Infect. Immun.* **46,** 845–9 (1984).

121. Roesler, J. & Steinmoller, C. Application of purified polysaccharides from cell cultures of the plant Echinacea purpurea to test subjects mediates activation of the phagocyte system. *Int J Immunopharmac* **13,** 931–941 (1991).

122. Burger, R. A., Torres, A. R., Warren, R. P., Caldwell, V. D. & Hughes, B. G. Echinacea-induced cytokine production by human macrophages. *Int. J. Immunopharmacol.* **19,** 371–9 (1997).

123. Yue, K., Ye, M., Zhou, Z., Sun, W. & Lin, X. The genus Cordyceps : a chemical and pharmacological review. *J. Pharm. Pharmacol.* **65,** 474–493 (2013).

124. Zhou, X., Gong, Z., Su, Y., Lin, J. & Tang, K. Cordyceps fungi: natural products, pharmacological functions and developmental products. *J. Pharm. Pharmacol.* **61,** 279–91 (2009).

125. Li, S. P., Yang, F. Q. & Tsim, K. W. K. Quality control of Cordyceps sinensis, a valued traditional Chinese medicine. *J. Pharm. Biomed. Anal.* **41,** 1571–84 (2006).

126. Halliday, J. Medicinal value of the catepillar fungi species of the genus Cordyceps. A review. *Int. J. Med. Mushrooms* **10,** 219–234 (2008).

127. Guo, D., Lu, A. & Liu, L. Modernization of traditional Chinese medicine. *J. Ethnopharmacol.* **141,** 547–8 (2012).

128. Tuli, H. S., Sandhu, S. S. & Sharma, a. K. Pharmacological and therapeutic potential of Cordyceps with special reference to Cordycepin. *3 Biotech* **4,** 1–12 (2013).

129. Lo, H., Hsieh, C., Lin, F. & Hsu, T. A Systematic Review of the Mysterious Caterpillar Fungus Ophiocordyceps sinensis and Related Bioactive Ingredients. *J. Trad. Comp. Med.* 16–32 (2013).

130. Koh, J.-H., Yu, K.-W., Suh, H.-J., Choi, Y.-M. & Ahn, T.-S. Activation of macrophages and the intestinal immune system by an orally administered decoction from cultured mycelia of Cordyceps sinensis. *Biosci. Biotechnol. Biochem.* **66,** 407–11 (2002).

131. Cheung, J. K. H. *et al.* Cordysinocan, a polysaccharide isolated from cultured Cordyceps, activates immune responses in cultured T-lymphocytes and macrophages: signaling cascade and induction of cytokines. *J. Ethnopharmacol.* **124,** 61–8 (2009).

132. Meng, L.-Z. *et al*. Mycelia extracts of fungal strains isolated from Cordyceps sinensis differently enhance the function of RAW 264.7 macrophages. *J. Ethnopharmacol*. 1–8 (2013).

133. Zhang, W., Yang, J., Chen, J., Hou, Y. & Han, X. Immunomodulatory and antitumour effects of an exopolysaccharide fraction from cultivated Cordyceps sinensis (Chinese caterpillar fungus) on tumour-bearing mice. *Biotechnol. Appl. Biochem*. **42,** 9–15 (2005).

134. Jordan, J. L., Sullivan, A M. & Lee, T. D. G. Immune activation by a sterile aqueous extract of Cordyceps sinensis: mechanism of action. *Immunopharmacol. Immunotoxicol*. **30,** 53–70 (2008).

135. Page, N. A., Wall, R. E., Darbyshire, S. J. & Mulligan, G. A. The Biology of Invasive Alien Plants in Canada (4). Heracleum mantegazzianum. *Can J. Plant Sci*. **3,** (2006).

136. Firuzi, O., Asadollahi, M., Gholami, M. & Javidnia, K. Composition and biological activities of essential oils from four Heracleum species. *Food Chem*. **122,** 117–122 (2010).

137. Bogucka-Kocka, A, Smolarz, H. D. & Kocki, J. Apoptotic activities of ethanol extracts from some Apiaceae on human leukaemia cell lines. *Fitoterapia* **79,** 487–97 (2008).

138. Jones, N. P. *et al*. Antifungal activity of extracts from medicinal plants used by First Nations Peoples of eastern Canada. *J. Ethnopharmacol*. **73,** 191–8 (2000).

139. Webster, D., Taschereau, P., Belland, R. J., Sand, C. & Rennie, R. P. Antifungal activity of medicinal plant extracts; preliminary screening studies. *J. Ethnopharmacol*. **115,** 140–6 (2008).

140. Webster, D., Taschereau, P., Lee, T. D. G. & Jurgens, T. Immunostimulant properties of Heracleum maximum Bartr. *J. Ethnopharmacol*. **106,** 360–3 (2006).

141. McCutcheon, A. R. *et al*. Anti-Mycobacterial Screening of British Columbian Medicinal Plants. *Pharm. Biol*. **35,** 77–83 (1997).

142. O'Neill, T., Johnson, J. A., Webster, D. & Gray, C. A. The Canadian medicinal plant Heracleum maximum contains antimycobacterial diynes and furanocoumarins. *J. Ethnopharmacol*. **147,** 232–7 (2013).

143. Webster, D., Lee, T., Moore, J., Manning, T., Kunimoto, D., LeBlanc, D., Johnson, J., Gray, C. Antimycobacterial screening of traditional medicinal plants using the microplate resazurin assay. *Can. J. Microbiol*. **56,** 487–94 (2010).

144. Mehta, P. K., King, C. H., White, E. H., Murtagh, J. J. & Quinn, F. D. Comparison of in vitro models for the study of Mycobacterium tuberculosis invasion and intracellular replication. *Infect. Immun.* **64,** 2673–9 (1996).

145. Mehta, P. K., Karls, R. K., White, E. H., Ades, E. W. & Quinn, F. D. Entry and intracellular replication of Mycobacterium tuberculosis in cultured human microvascular endothelial cells. *Microb. Pathog.* **41,** 119–24 (2006).

146. Shiloh, M. U. & DiGiuseppe Champion, P. a. To catch a killer. What can mycobacterial models teach us about Mycobacterium tuberculosis pathogenesis? *Curr. Opin. Microbiol.* **13,** 86–92 (2010).

147. Goel, V. *et al.* A proprietary extract from the echinacea plant (Echinacea purpurea) enhances systemic immune response during a common cold. *Phytother. Res.* **19,** 689–94 (2005).

148. Sánchez, D. *et al.* Role of TLR2- and TLR4-mediated signaling in Mycobacterium tuberculosis-induced macrophage death. *Cell. Immunol.* **260,** 128–36 (2010).

149. O'Toole, R. Experimental models used to study human tuberculosis. *Adv. Appl. Microbiol.* **71,** 75–89 (2010).

150. Canadian Institute of Health Information. *Canadian Organ Replacement Register Annual Report. Treatment of End-Stage Organ Failure in Canada 2001-2010.* **142** (2010).

151. Wang, Z. & Nakayama, T. Inflammation, a link between obesity and cardiovascular disease. *Mediators Inflamm.* **2010,** 535918 (2010).

152. Butler, J. Primary prevention of heart failure. *ISRN Cardiol.* **2012,** 982417 (2012).

153. Kittleson, M. M. & Kobashigawa, J. A. Management of advanced heart failure: the role of heart transplantation. *Circulation* **123,** 1569–74 (2011).

154. Smith, L., Farroni, J., Baillie, B. R. & Haynes, H. Heart transplantation. *Crit. Care Nurs. Clin. North Am.* **15,** 489–494 (2003).

155. Cooper, D. K. C. & Cooley, D. A. Christiaan Neethling Barnard: 1922-2001. *Circulation* **104,** 2756–2757 (2001).

156. Keon, W. J. Heart transplantation in perspective. *J. Card. Surg.* **14,** 147–51 (1998).

157. Opelz, G., Wujciak, T., Dohler, B., Scherer, S., Mytilineos, J. HLA compatibility and organ transplant survival. *Rev. Immunogenet.* **1,** 334–342 (1999).

158. Takemoto, S., Port, F. K., Claas, F. H. J. & Duquesnoy, R. J. HLA matching for kidney transplantation. *Hum. Immunol.* **65,** 1489–505 (2004).

159. Sheldon, S. & Poulton, K. HLA typing and its influence on organ transplantation. *Methods Mol. Biol.* **333,** 157–74 (2006).

160. Vasilescu, E. R. *et al.* Anti-HLA antibodies in heart transplantation. *Transpl. Immunol.* **12,** 177–83 (2004).

161. Stavropoulos-Giokas, C. HLA compatibility in organ transplantation. *Nephrol. Dial. Transplant* **16 Suppl 6,** 147–9 (2001).

162. Angaswamy, N. *et al.* Interplay between immune responses to HLA and non-HLA self-antigens in allograft rejection. *Hum. Immunol.* **74,** 1478–85 (2013).

163. Carvajal, T. *et al.* Human Leukocyte Antigen Mismatch in Heart Transplants Continues To Predict Outcomes in Modern Era of Immunosuppression. *J. Hear. Lung Transplant.* **32,** S213 (2013).

164. LaRosa, D. F., Rahman, A. H. & Turka, L. A. The innate immune system in allograft rejection and tolerance. *J. Immunol.* **178,** 7503–9 (2007).

165. Patel, J. K. & Kobashigawa, J. A. Should we be doing routine biopsy after heart transplantation in a new era of anti-rejection? *Curr. Opin. Cardiol.* **21,** 127–31 (2006).

166. Michaels, P. J. *et al.* Humoral rejection in cardiac transplantation: risk factors, hemodynamic consequences and relationship to transplant coronary artery disease. *J. Heart Lung Transplant.* **22,** 58–69 (2003).

167. Gareau, A. J., Nashan, B., Hirsch, G. M. & Lee, T. D. G. Cyclosporine immunosuppression does not prevent the production of donor-specific antibody capable of mediating allograft vasculopathy. *J. Heart Lung Transplant.* **31,** 874–80 (2012).

168. Bayliss, J. *et al.* Late onset antibody-mediated rejection and endothelial localization of vascular endothelial growth factor are associated with development of cardiac allograft vasculopathy. *Transplantation* **86,** 991–7 (2008).

169. Ho, E. K. *et al.* Alloantibodies in heart transplantation. *Hum. Immunol.* **70,** 825–9 (2009).

170. McManigle, W., Pavlisko, E. N. & Martinu, T. Acute cellular and antibody-mediated allograft rejection. *Semin. Respir. Crit. Care Med.* **34,** 320–35 (2013).

171. Farrar, C. a, Kupiec-Weglinski, J. W. & Sacks, S. H. The innate immune system and transplantation. *Cold Spring Harb. Perspect. Med.* **3,** a015479 (2013).

172. Millington, T. M. & Madsen, J. C. Innate immunity in heart transplantation. *Curr. Opin. Organ Transplant.* **14,** 571–6 (2009).

173. Wood, K. J., Zaitsu, M. & Goto, R. Transplantation Immunology. **1034,** 71–83 (2013).

174. Herrero-Fresneda, I. *et al.* Role of cold ischemia in acute rejection: characterization of a humoral-like acute rejection in experimental renal transplantation. *Transplant. Proc.* **37,** 3712–5 (2005).

175. Jordan, J. E., Zhao, Z. Q. & Vinten-Johansen, J. The role of neutrophils in myocardial ischemia-reperfusion injury. *Cardiovasc. Res.* **43,** 860–78 (1999).

176. King, C. L., Devitt, J. J., Lee, T. D. G. & Hancock Friesen, C. L. Neutrophil mediated smooth muscle cell loss precedes allograft vasculopathy. *J. Cardiothorac. Surg.* **5,** 52 (2010).

177. Murphy, S. P., Porrett, P. M. & Turka, L. a. Innate immunity in transplant tolerance and rejection. *Immunol. Rev.* **241,** 39–48 (2011).

178. Benichou, G. Direct versus indirect alorecognition pathways: on the right track. *Am J Transpl.* **9,** 655–656 (2009).

179. Van Besouw, N. M. *et al.* The direct and indirect allogeneic presentation pathway during acute rejection after human cardiac transplantation. *Clin. Exp. Immunol.* **141,** 534–40 (2005).

180. Rogers, N. J. & Lechler, R. I. Allorecognition. *Am. J. Transplant* **1,** 97–102 (2001).

181. Li, L. & Okusa, M. D. Macrophages, dendritic cells, and kidney ischemia-reperfusion injury. *Semin. Nephrol.* **30,** 268–77 (2010).

182. Yamada, A., Salama, A. D. & Sayegh, M. H. The role of novel T cell costimulatory pathways in autoimmunity and transplantation. *J. Am. Soc. Nephrol.* **13,** 559–75 (2002).

183. Lewis, R. S. Calcium signaling mechanisms in T lymphocytes. *Annu. Rev. Immunol.* **19,** 497–521 (2001).

184. Joseph, N., Reicher, B. & Barda-Saad, M. The calcium feedback loop and T cell activation: how cytoskeleton networks control intracellular calcium flux. *Biochim. Biophys. Acta* **1838,** 557–68 (2014).

185. Tedesco, D. & Haragsim, L. Cyclosporine: a review. *J. Transplant*. **2012,** 230386 (2012).

186. Bayer, A. L., Pugliese, A. & Malek, T. R. The IL-2/IL-2R system: from basic science to therapeutic applications to enhance immune regulation. *Immunol. Res*. **57,** 197–209 (2013).

187. Macdonald, A. S. Use of mTOR inhibitors in human organ transplantation. *Expert Rev. Clin. Immunol*. **3,** 423–36 (2007).

188. Keogh, A. *et al*. Sirolimus in de novo heart transplant recipients reduces acute rejection and prevents coronary artery disease at 2 years: a randomized clinical trial. *Circulation* **110,** 2694–700 (2004).

189. Reiner, S. L. Development in motion: helper T cells at work. *Cell* **129,** 33–6 (2007).

190. Lindenfeld, J. *et al*. Drug therapy in the heart transplant recipient: part I: cardiac rejection and immunosuppressive drugs. *Circulation* **110,** 3734–40 (2004).

191. Lindenfeld, J. *et al*. Drug therapy in the heart transplant recipient: part II: immunosuppressive drugs. *Circulation* **110,** 3858–65 (2004).

192. Keogh, A. Calcineurin inhibitors in heart transplantation. *J. Heart Lung Transplant*. **23,** S202–6 (2004).

193. Takeuchi, K., Roehrl, M. H. A., Sun, Z.-Y. J. & Wagner, G. Structure of the calcineurin-NFAT complex: defining a T cell activation switch using solution NMR and crystal coordinates. *Structure* **15,** 587–97 (2007).

194. Barbarino, J. M., Staatz, C. E., Venkataramanan, R., Klein, T. E. & Altman, R. B. PharmGKB summary: cyclosporine and tacrolimus pathways. *Pharmacogenet. Genomics* **23,** 563–85 (2013).

195. Macian, F. NFAT proteins: key regulators of T-cell development and function. *Nat. Rev. Immunol*. **5,** 472–84 (2005).

196. Kobashigawa, J. A. Strategies in immunosuppression after heart transplantation: is less better? *Circ. Heart Fail*. **4,** 111–3 (2011).

197. Hart-Matyas, M., Nejat, S., Jordan, J. L., Hirsch, G. M. & Lee, T. D. G. IFN-gamma and Fas/FasL pathways cooperate to induce medial cell loss and neointimal lesion formation in allograft vasculopathy. *Transpl. Immunol*. **22,** 157–64 (2010).

198. Nejat, S., Zaki, A., Hirsch, G. M. & Lee, T. D. G. Transplant Immunology CD8 T cells mediate aortic allograft vasculopathy under conditions of calcineurin immunosuppression: Role of IFN-7 and CTL mediators. **19,** 103–111 (2008).

199. Choy, J. C., Kerjner, A., Wong, B. W., McManus, B. M. & Granville, D. J. Perforin mediates endothelial cell death and resultant transplant vascular disease in cardiac allografts. *Am. J. Pathol.* **165,** 127–33 (2004).

200. Vessie, E. L., Hirsch, G. M. & Lee, T. D. G. Aortic allograft vasculopathy is mediated by CD8(+) T cells in Cyclosporin A immunosuppressed mice. *Transpl. Immunol.* **15,** 35–44 (2005).

201. Lund, L. The registry of the international society for heart and lung transplantation: thirtieth official adult heart transplant report. *J Hear. Lung Transpl.* **32,** 951–964 (2013).

202. Ramzy, D. *et al.* Cardiac allograft vasculopathy: a review. *Can. J. Surg.* **48,** 319–27 (2005).

203. Valantine, H. Cardiac allograft vasculopathy after heart transplantation: risk factors and management. *J. Heart Lung Transplant.* **23,** S187–93 (2004).

204. Kapadia, S. R. *et al.* Development of Transplantation Vasculopathy and Progression of Donor-Transmitted Atherosclerosis : Comparison by Serial Intravascular Ultrasound Imaging. *Circulation* **98,** 2672–2678 (1998).

205. Mitchell, R. N. Graft Vascular Disease: Immune Response Meets the Vessel Wall. *Annu. Rev. Pathol. Mech. Dis.* **4**, 19–47 (2009).

206. Rahmani, M., Cruz, R. P., Granville, D. J. & McManus, B. M. Allograft vasculopathy versus atherosclerosis. *Circ. Res.* **99,** 801–15 (2006).

207. Stary, H. C. Natural History and Histological Classification of Atherosclerotic Lesions: An Update. *Arterioscler. Thromb. Vasc. Biol.* **20,** 1177–78 (2000).

208. Nakashima, Y., Wight, T. N. & Sueishi, K. Early atherosclerosis in humans: role of diffuse intimal thickening and extracellular matrix proteoglycans. *Cardiovasc. Res.* **79,** 14–23 (2008).

209. Subbotin, V. M. Theoretical Biology and Medical Analysis of arterial intimal hyperplasia: review and hypothesis. *Theor. Biol. Med. Mod.* **20,** 1–20 (2007).

210. Houser, S., Muniappan, A., Allan, J., Sachs, D. & Madsen, J. Cardiac allograft vasculopathy: real or a normal morphologic variant? *J. Heart Lung Transplant.* **26,** 167–73 (2007).

211. Mennander, A., Tiisala, S., Paavonen, T., Halttunen, J., Hayry, P. Chronic rejection of rat aortic allograft. Administration of cyclosporine induces accelerated allograft arteriosclerosis. *Transpl. Int.* **4,** 173–179 (1991).

212. Isik, FF, McDonald TO, Ferguson, M, Yamanaka, E, Gordon, D. Transplant arteriosclerosis in a rat aortic model. *Am. J. Pathol.* **141,** 1139–1149 (1992).

213. Li, J., Han, X.Z., Jiang, J.F., Zhong, R., Williams, G.M., Pickering, J. G. Vascular smooth muscle cells of recipient origin mediate intimal expansion after aortic allotransplantation in mice. *Am. J. Pathol.* **158,** 1943–1947 (2001).

214. Johnson, P., Carpenter, M., Hirsch, G., Lee, T. Recipient cells form the intimal proliferative lesion in the rat aortic model of allograft arteriosclerosis. *Am. J. Transplant.* **2,** 207–214 (2002).

215. Mitchell, R. N. Allograft arteriopathy: pathogenesis update. *Cardiovasc. Pathol.* **13,** 33–40 (2004).

216. Atkinson, C., Horsley, J., Rhind-Tutt, S., Charman, S., Philpotts, C., Wallwork, J., Goddard, M. Neointimal smooth muscle cells in human cardiac allograft coronary artery vasculopathy are of donor origin. *J Hear. Lung Transpl.* **23,** 427–435 (2004).

217. Quaini, F. *et al.* Chimerism of the transplanted heart. *N. Engl. J. Med.* **346,** 5–15 (2002).

218. Huibers, M. *et al.* Intimal fibrosis in human cardiac allograft vasculopathy. *Transpl. Immunol.* **25,** 124–32 (2011).

219. Libby, P., Ridker, P. M. & Hansson, G. K. Progress and challenges in translating the biology of atherosclerosis. *Nature* **473,** 317–25 (2011).

220. Devitt, J. J. *et al.* Impact of donor benign intimal thickening on cardiac allograft vasculopathy. *J. Heart Lung Transplant.* **32,** 454–60 (2013).

221. Wight, T. N. & Merrilees, M. J. Proteoglycans in atherosclerosis and restenosis: key roles for versican. *Circ. Res.* **94,** 1158–67 (2004).

222. Nakashima, Y., Fujii, H., Sumiyoshi, S., Wight, T. N. & Sueishi, K. Early human atherosclerosis: accumulation of lipid and proteoglycans in intimal thickenings followed by macrophage infiltration. *Arterioscler. Thromb. Vasc. Biol.* **27,** 1159–65 (2007).

223. Dandel, M. & Hetzer, R. Impact of immunosuppressive drugs on the development of cardiac allograft vasculopathy. *Curr. Vasc. Pharmacol.* **8,** 706–19 (2010).

224. Milei, J. *et al*. Coronary intimal thickening in newborn babies and <or=1-year-old infants. *Angiology* **61,** 350–6 (2010).

225. Williams, K. J. & Tabas, I. The response-to-retention hypothesis of early atherogenesis. *Arterioscler. Thromb. Vasc. Biol.* **15,** 551–61 (1995).

226. Fukuchi, M. *et al*. Normal and Oxidized Low Density Lipoproteins Accumulate Deep in Physiologically Thickened Intima of Human Coronary Arteries. *Lab. Investig.* **82,** 1437–1447 (2002).

227. Napoli, C., Armiento, F. P. D., Mancini, F. P., Postiglione, A. & Witztum, J. L. Fatty Streak Formation Occurs in Human Fetal Aortas and is Greatly Enhanced by Maternal Hypercholesterolemia. *J. Clin. Invest.* **100,** 2680–2690 (2005).

228. Foteinos, G. & Xu, Q. Immune-mediated mechanisms of endothelial damage in atherosclerosis. **42,** 627–633 (2009).

229. Bobryshev, Y. V *et al*. Correlation between lipid deposition, immune-inflammatory cell content and MHC class II expression in diffuse intimal thickening of the human aorta. *Atherosclerosis* **219,** 171–83 (2011).

230. Libby, P. Inflammation and Atherosclerosis. *Circulation* **105,** 1135–1143 (2002).

231. Hansson, G. K. & Hermansson, A. The immune system in atherosclerosis. *Nat. Immunol.* **12,** 204–12 (2011).

232. Rahmani, M., Cruz, R. P., Granville, D. J. & McManus, B. M. Allograft vasculopathy versus atherosclerosis. *Circ. Res.* **99,** 801–15 (2006).

233. Ketelhuth, D. F. J. & Hansson, G. K. Cellular immunity, low-density lipoprotein and atherosclerosis: break of tolerance in the artery wall. *Thromb. Haemost.* **106,** 779–86 (2011).

234. Bursill, C. A., Channon, K. M. & Greaves, D. R. The role of chemokines in atherosclerosis : recent evidence from experimental models and population genetics. *Curr. Opin. Lipidol.* **15,** 145–149 (2004).

235. Lundberg, A. M. & Hansson, G. K. Innate immune signals in atherosclerosis. *Clin. Immunol.* **134,** 5–24 (2010).

236. Greaves, D. R. & Channon, K. M. Inflammation and immune responses in atherosclerosis. *Trends Immunol.* **23,** 535–41 (2002).

237. Reis, E. D. *et al*. Dramatic remodeling of advanced atherosclerotic plaques of the apolipoprotein E-deficient mouse in a novel transplantation model. *J. Vasc. Surg.* **34,** 541–7 (2001).

238. Kruth, H. S. Macrophage foam cells and atherosclerosis. *Front. Biosci.* **6,** D429–55 (2001).

239. Takahashi, K., Takeya, M. & Sakashita, N. Multifunctional roles of macrophages in the development and progression of atherosclerosis in humans and experimental animals. *Med. Electron Microsc.* **35,** 179–203 (2002).

240. Watanabe, N. & Ikeda, U. Matrix metalloproteinases and atherosclerosis. *Curr. Atheroscler. Rep.* **6,** 112–20 (2004).

241. Gui, T., Shimokado, A., Sun, Y., Akasaka, T. & Muragaki, Y. Diverse roles of macrophages in atherosclerosis: from inflammatory biology to biomarker discovery. *Mediators Inflamm.* **2012,** 693083 (2012).

242. Rekhter, M. D. Collagen synthesis in atherosclerosis: too much and not enough. *Cardiovasc. Res.* **41,** 376–84 (1999).

243. Gomez, D. & Owens, G. K. Smooth muscle cell phenotypic switching in atherosclerosis. *Cardiovasc. Res.* **95,** 156–64 (2012).

244. Tao, Z., Smart, F. W., Figueroa, J. E., Glancy, D. L. & Vijayagopal, P. Elevated expression of proteoglycans in proliferating vascular smooth muscle cells. *Atherosclerosis* **135,** 171–9 (1997).

245. Rudijanto, A. The role of vascular smooth muscle cells on the pathogenesis of atherosclerosis. *Acta Med. Indones.* **39,** 86–93

246. Stary, H. C. Natural history and histological classification of atherosclerotic lesions: an update. *Arterioscler. Thromb. Vasc. Biol.* **20,** 1177–8 (2000).

247. Grauhan, O. *et al.* Coronary atherosclerosis of the donor heart--impact on early graft failure. *Eur. J. Cardiothorac. Surg.* **32,** 634–8 (2007).

248. Li, H. *et al.* Influence of pre-existing donor atherosclerosis on the development of cardiac allograft vasculopathy and outcomes in heart transplant recipients. *J. Am. Coll. Cardiol.* **47,** 2470–6 (2006).

249. Costanzo, M.R., et al. The international society of heart and lung transplantation guidelines for the care of heart transplant recipients. *J. Heart. Lung Transplant.* **29,** 914–956 (2010).

250. Wick, G., Schett, G., Amberger, a, Kleindienst, R. & Xu, Q. Is atherosclerosis an immunologically mediated disease? *Immunol. Today* **16,** 27–33 (1995).

251. Yamasaki, M. *et al*. Impact of donor-transmitted atherosclerosis on early cardiac allograft vasculopathy: new findings by three-dimensional intravascular ultrasound analysis. *Transplantation* **91,** 1406–11 (2011).

252. Tuczu, E.M., DeFranco, A.C., et al. Dichotomous pattern of coronary atherosclerosis 1 to 9 years after transplantation: insights from systematic intravascular ultrasound imaging. *Coll. Cardiol.* **27,** 839–846 (1996).

253. Gao, S. Z., Alderman, E. L., Schroeder, J. S., Silverman, J. F. & Hunt, S. A. Accelerated coronary vascular disease in the heart transplant patient: coronary arteriographic findings. *J. Am. Coll. Cardiol.* **12,** 334–40 (1988).

254. Breslow, J. L. Mouse models of atherosclerosis. *Science* **272,** 685–8 (1996).

255. Coleman, R., Hayek, T., Keidar, S. & Aviram, M. A mouse model for human atherosclerosis: long-term histopathological study of lesion development in the aortic arch of apolipoprotein E-deficient (E0) mice. *Acta Histochem.* **108,** 415–24 (2006).

256. Kolovou, G., et al. Apolipoprotein E KO models.pdf. *Curr. Pharm. Des.* **14,** 338–351 (2008).

257. Ohashi, R., Mu, H., Yao, Q. & Chen, C. Cellular and molecular mechanisms of atherosclerosis with mouse models. *Trends Cardiovasc. Med.* **14,** 187–90 (2004).

258. Maganto-Garcia, E., Tarrio, M. & Lichtman, A. H. Mouse models of atherosclerosis. *Curr. Protoc. Immunol.* **Chapter 15,** Unit 15.24.1–23 (2012).

259. Meir, K. S. & Leitersdorf, E. Atherosclerosis in the apolipoprotein-E-deficient mouse: a decade of progress. *Arterioscler. Thromb. Vasc. Biol.* **24,** 1006–14 (2004).

260. Horejsí, B. & Ceska, R. Apolipoproteins and atherosclerosis. Apolipoprotein E and apolipoprotein(a) as candidate genes of premature development of atherosclerosis. *Physiol. Res.* **49 Suppl 1,** S63–9 (2000).

261. Pendse, A. a, Arbones-Mainar, J. M., Johnson, L. a, Altenburg, M. K. & Maeda, N. Apolipoprotein E knock-out and knock-in mice: atherosclerosis, metabolic syndrome, and beyond. *J. Lipid Res.* **50 Suppl,** S178–82 (2009).

262. Daugherty, A. Mouse models of atherosclerosis. *Am. J. Med. Sci.* **323,** 3–10 (2002).

263. Nakashima, Y., Plump, A. S., Raines, E. W., Breslow, J. L. & Ross, R. ApoE-deficient mice develop lesions of all phases of atherosclerosis throughout the arterial tree. *Arterioscler. Thromb. Vasc. Biol.* **14,** 133–140 (1994).

264. Koulack, J., McAlister, V., Giacomantonio, C.A., Bitter-Suermann, H., MacDonald, A.S., Lee, T. D. G. Development of a mouse aortic transplant model of chronic rejection. *Microsurgery* **16,** 110–113 (1995).

265. Botas, J. *et al*. Influence of preexistent donor coronary artery disease on the progression of transplant vasculopathy. An intravascular ultrasound study. *Circulation* **92,** 1126–32 (1995).

266. Currie, M., Zaki, A. M., Nejat, S., Hirsch, G. M. & Lee, T. D. G. Immunologic targets in the etiology of allograft vasculopathy: Endothelium versus media. *Transpl. Immunol*. **19,** 120–126 (2008).

267. Reis, E. D. *et al*. Dramatic remodeling of advanced atherosclerotic plaques of the apolipoprotein E-deficient mouse in a novel transplantation model. *J. Vasc. Surg*. **34,** 541–7 (2001).

268. Trogan, E. *et al*. Gene expression changes in foam cells and the role of chemokine receptor CCR7 during atherosclerosis regression in ApoE-deficient mice. *Proc. Natl. Acad. Sci. U. S. A*. **103,** 3781–6 (2006).

269. Zaki, A. M., Hirsch, G. M. & Lee, T. D. G. Contribution of pre-existing vascular disease to allograft vasculopathy in a murine model. *Transpl. Immunol*. **22,** 93–8 (2009).

270. Tonar, Z. *et al*. Aorta transplantation in young apolipoprotein E-deficient mice: possible model for studies on regression of atherosclerotic lesions? *Cent. Eur. J. Med*. **5**, 280-291 (2010).